Spring 1-1-2015

Contaminant Source Identification in Building Hvac Systems Using Adjoint Probability Method

Qi Jin
University of Colorado at Boulder, Qi.Jin@Colorado.edu

CONTAMINANT SOURCE IDENTIFICATION IN BUILDING HVAC SYSTEMS USING ADJOINT PROBABILITY METHOD

by

QI JIN

B.S., Tongji University, 2013

A thesis submitted to the

Faculty of the Graduate School of the

University of Colorado in partial fulfillment

of the requirement for the degree of

Master of Science

Department of Civil, Environmental and Architectural Engineering

2015

This thesis entitled:

Contaminant Source Identification in Building HVAC Systems Using Adjoint Probability Method

written by Qi Jin

has been approved for the Department of Civil, Environmental and Architectural Engineering

_____

(Chair: Dr. John Zhai)

_____

(Dr. Michael Brandemuehl)

_____

(Dr. Moncef Krarti)

Date_____

The final copy of this thesis has been examined by the signatories, and we Find that both the content and the form meet acceptable presentation standards Of scholarly work in the above mentioned discipline.

Abstract

Jin, Qi (M.S., Civil, Environmental and Architectural Engineering)

Contaminant Source Identification in Building HVAC Systems Using Adjoint Probability Method

Thesis directed by Professor John Zhai, Department of Civil, Environmental and Architectural Engineering, University of Colorado at Boulder

Although high efficiency filter is one critical component in the Air Handler Unit (AHU), HVAC system is potential contaminant emission source. Released contaminants can be transported through HVAC system and impacts the indoor air quality (IAQ). Effective control and improvement measures are required to remove the contaminant source located in HVAC systems in order to eliminate its influence on the IAQ. Accurate and fast identification of contaminant sources in HVAC systems makes it. This thesis studies the application of adjoint backward probability model in identification of contaminant source in Building HVAC system. The adjoint backward probability model was mostly applied to identify contaminant source information in groundwater and inside building. According to the similar properties between water and air, and same contaminant transport fate in water and air, the adjoint probability model is applied to study the contaminant source identification in HVAC systems.

Sensors are used to detect contaminant concentration change in certain sampling locations of HVAC ductwork. Using sensor detection information, we can trace back and find the source information. In this research CONTAM is used to provide a steady state airflow field. A simple building model with three zones and detailed duct work is built. This

model is applied into later research in identification of contaminant source in HVAC system.

Four cases are analyzed in the research to study the application of adjoint backward probability method. The first case is identifying an instantaneous contaminant source location with known source release time and source release mass. The second case is identifying the location of a dynamic contaminant source with known release time and known release mass. The third case is identifying source release time and release location simultaneously for a decaying contaminant source with known source release mass. The fourth case is identifying the location of a dynamic contaminant source in a two-floor building with known release time and known release mass. The conclusions come to that a sensor network with two sensors reading historical concentrations can identify source information accurately. Further, in future research, contaminant source information will be recovered without knowing any source information in advance.

Acknowledgement

The thesis work was done under the profound and far-sighted guidance of my advisor, Dr. John Zhai. Without his supervision and encouragement, I cannot make it, which is for sure. According to Dr. Zhai's advice, I selected this topic last October and have been working on that nearly one year. In this whole process, Dr. Zhai always gave me valuable advice, and pointed out the problems in my research, from which I benefited a lot. I believe that this would be a great and memorable experience in my future whole life. Additionally, I would like to appreciate the thesis committee members' (Prof. Michael Brandemuehl and Prof. Moncef Krarti) help. Appreciate them for taking their valuable time serving in my committee and giving me feedback.

I would like to give my thanks to W. Stuart Dols in the National Institute of Standards and Technology (NIST) during my study of CONTAM. Although CONTAM is not hard to learn, there are still some components I don't know can be used to solve the problems in my CONTAM models. Additionally, I would like to show my appreciation to the PhD candidate from Tianjing University of Tianjin City China, Yu (Snow) Xue. He has been doing a good research on other topics using the Adjoint backward probability method. Talking with him about my research reduced much of my time exploring the mathematics and physics meaning of this method.

For my parents and little brother, I cannot use any word to express my feeling of gratitude. They are the most solid backing of me. Under their support and encouragement, I don't have to care about so many things and can focus on my study. Last but not least, I would like to appreciate my girlfriend's support. I always feel I'm so lucky having her as my girlfriend in my master study in the United States. Although she is pretty busy, she always listens to me and is so helpful!

Contents

List of Tables

List of Figures

Chapter 1 Introduction

Building indoor air quality (IAQ) has been being paid much attention to around the world in recent years because of the increasing concern on the health issue related to poor indoor air environment. US EPA (2009) reported that US individuals spend about an average of 90% or more of their time indoors, and that indoor levels of contaminant may be two or five times higher, and occasionally more than 100 times higher, than outdoor levels. Poor indoor air quality (IAQ) is a threat to people's health. It was studied poor indoor environment quality can cause a range of respiratory illness, allergy and asthma symptoms, and Sick Building Syndrome (SBS) (ASHRAE 2009a and 2009b). Jones (1999) indicated that indoor air contaminants emit from a range of sources, such as the fabric of buildings and the by-product of activities undertaken within buildings. Primary causes of this can be classified into several categories, including activities of occupants, chemical and biological sources, combustion of heating fuels, emissions from buildings, and infiltration from outside buildings. Additionally, Fisk estimated that, due to poor indoor environments in U.S. commercial buildings, the overall economic losses are about tens billion US dollars per year in lost wages and productivity, administrative expenses and health care costs (Fisk, 2000).

In order to eliminate the contaminant source within buildings and protect occupants from the unhealthy indoor environment, contaminant sources inside buildings need to be identified and removed fast and accurately. Before identifying the contaminant source, we need study and know the contaminant transport mechanic in different building circumstances. Indoor pollutant transport can be complex since it is case-dependent and

can be affected by critical factors, such as the Heating, Ventilation and Air-conditioning (HVAC) systems, layouts, and partitions. According to the literature review, both experimental and numerical methods have been applied to study indoor air pollutant transport mechanic. Experimental method takes much more time and cost than simulation method. However, with the rapid development of computer technology and numerical calculation, more and more engineering problems have been being solved using computer simulation methods. Additionally, computer simulation methods are helpful for predicting and optimizing the research topics and details. Therefore, many scholars have been trying to apply computer simulation methods to explore the indoor pollutant transport mechanic within buildings during past years.

Although several computer simulation models have been published, two of which are mostly widely used to study the indoor transport fate; multi-zone indoor air quality and ventilation analysis program, and the computational fluid dynamics program-CFD. Computational Fluid Dynamics (CFD) model has been being used to research airflow and contaminant concentration distribution within one certain zone. CFD model can give more detailed information by solving mass, momentum and energy equations in terms of spatial and temporal distribution of critical information, such as temperature, pressure, and airflow rate and contaminant concentration. Compared to the well-mixed zone model, one certain zone in CFD model will be divided into many small control volumes, which is a cost of tons of time during computation. CFD model is not practical for a building containing many zones because simulating so many zones will be greatly time-consuming.

Multi-zone simulation model divides a building into different zones connected with airflow paths, to study airflow and contaminant movement in buildings. The airflow paths include HVAC systems duct network, infiltration between building and ambient environment, doors, windows and orifices (Walton and Dols, 2013). Based on the law of

mass balance within one control volume and the flow path connections, the airflow rates and indoor pollutant concentrations can be calculated (Shaelin et al., 1993) by solving a set of non-linear equations. There have been two comprehensive literature reviews of multi-zone models (Feustel and Kendon 1985, Feustel and Dieris 1992), which introduced fifty models. Several multi-zone simulation programs were developed, of which the most well-known programs are CONTAM (Walton and Dols, 2013) developed by the U.S. National Institute of Standards and Technology (NIST) and COMIS (Pelletret and Keilholz, 1997) developed by the U.S. Lawrence Berkeley National Laboratory (LBNL). CONTAM and COMIS used similar algorithms to solve a set of non-linear flow equations and contaminant transport equations (Wang J. et al., 1998). This research focuses on contaminant source identification in HVAC duct network. A detailed HVAC duct network should be built in the building system model. CONTAM can provide the function, building a detailed HVAC duct component. Additionally, there have been many successful applications of CONTAM detailed duct work (Walton and Dols, 2013). The duct work's applicability in CONTAM has been validated by several experiment. Therefore, CONTAM duct network can be applied in the research to study the application of contaminant source identification in HVAC system.

CONTAM can be used to calculate the airflow field and contaminant concentration distribution within buildings. Three kinds of models can be selected for zones in CONTAM, including normal zone (well-mixed zone), one dimensional zone, computational fluid dynamics zone (Walton and Dols, 2013). CFD model is not practical since there are many zones in buildings which will take much more time than imagined. Well-mixed zone is defined as one zone in which contaminant can be distributed uniformly within one time step after releasing the contaminant source. One dimensional zone is kind of zone can be considered as one dimensional, in which a zone will be divided into many same cells along the one dimensional direction. In this research, detailed HVAC duct work is built in

CONTAM to provide a steady state airflow field. In CONTAM, two kinds of models can be used for detailed duct work, including well-mixed zonal duct and one dimensional duct. According to the user guide (Walton and Dols, 2013), in well-mixed zonal duct case, the volumes of the duct junctions are determined from the duct segments to which they are connected. This may not produce an accurate simulation of transient concentrations for duct because of the use of control volumes which are considered as well-mixed. It takes much longer time for contaminant transporting from one duct end to the other duct end, which produces a transport time delay of contaminant change in the two ends. The well-mixed zonal duct model may not display the transport time delay. Therefore, the one dimensional duct model is applied.

As mentioned above, no matter the experiment method or computer simulation technology, both of them are forward model. In the forward model, contaminant source is known or assumed to be known, and contaminant distribution is studied using experiment or simulation. However, the research's goal is identify contaminant source which is a backward model. Forward model and backward model are two opposite process. According to the problem-modeling characteristics, Friedr summarized the generic modeling process shown in the following figure 1-1 (Friedr, 1978).

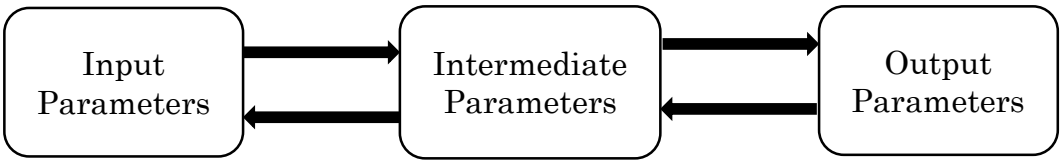

Figure 1-1 Flow Chart of the Generic Problem Modeling Process

According to the figure 1-1, there are three components in the generic problem modeling process, including input parameters, intermediate system, and output

parameters. In the forward problem, given input parameters and intermediate system, output parameters can be obtained. In the inverse problem, there are two cases. The first case is, given output parameters and intermediate system, input parameter can be identified. The other case is, given input parameters and output parameters, intermediate system can be traced. In the forward model, source locations, strength, release time, relative initial conditions and boundary conditions are known and specified. While in this research, contaminant source information should be identified based on information detected by sensors, which is the inverse problem-modeling process. Four kinds of information needs to be recovered in the HVAC duct work: contaminant source location, contaminant source release strength (release mass), contaminant source release time, and number of contaminant sources. The contaminant source may be eliminated to remove its influence on the indoor air quality (IAQ).

As we know, Heating, Ventilation and Air-conditioning system (HVAC) has been extensively applied to improve the indoor air quality (IAQ). However, according to a questionnaire-based survey of 43 British office buildings, Burge and his partners (Burge et al., 1987) found that complaints were given more frequently in buildings where HVAC systems provided cooling and humidification. In the analysis of emission contaminant sources that affect indoor air quality (IAQ), Fanger et al. (1988) and Molhave and Thorsen (1991) found that a large proportion of poor indoor air quality was due to the contaminant source located in HVAC systems (Fanger et al., 1988; Molhave and Thorsen, 1991). The contaminant can be transported through the duct systems and then is supplied into rooms within buildings, which is harmful for people's health. For example, a lot of fire cases in buildings have been reported that the fire was transported into other zones and around building through the duct system. The contaminant source in HVAC systems needs to be identified and removed to eliminate the air degrading issues, which is rarely studied.

Therefore, professional research on the contaminant source identification in building HVAC systems becomes necessary and needs to be paid much attention to.

This section mainly talked about the indoor air quality exacerbation, contaminant transport fate, associated computer programs, generic problem modeling process, and the research model. The research goal is study the contaminant source identification in HVAC system using the one dimensional duct model of CONTAM software tool. In following sections, methodology of contaminant source identification will be discussed.

Chapter 2 Literature Review

In this section, literature review is conducted to study and compare different models that can be used to solve inverse problems. Through the literature review analysis, the most effective model is used to identify the contaminant source information in the HVAC system.

Unlike the input and output forward problem solving process, pollutant source identification is an inverse problem. Actually the inverse identification problem has been widely researched in several fields, such as groundwater contamination (Atmadja et al., 2001), heat transfer (Huang and Wang, 1999), soil pollution (Zhang et al., 2008) and atmospheric constituent transport (Annunzio et al., 2012).

According to the literature review, it's found that research on the inverse transport model of groundwater system is more active than that of air transport in buildings and duct work system. Considering that contaminant transport in air and water has the same convection-diffusion mechanics, this section will review the existing inverse methods that have been applied to study the contaminant transport through air and water medium. Liu and Zhai (Liu and Zhai, 2008) divided the existing inverse models into three groups: forward model, backward model and probability model. In addition, there are also some other duct network models that are not belong to the three categories.

2.1. Forward Models and Backward Models

The forward model is a straightforward problem-modeling methodology, which identifies the contaminant source information through a "trial-error" process. Using sensor

detection information, the contaminant source information can be identified using the difference between simulated results (calculation results) and measured results. The simulated results are obtained with given source conditions and system parameters while the measured results are detected by the sensors. With an effective parameter-adjusting model, the contaminant source can be identified by an iterative "trail-error" process when it converges. Objective functions describe how well the measured results match with simulated results. Proper objective functions need to be studied to identify the contaminant source. The residual function is a straightforward optimization objective function, which reflects the difference between a simulated concentration C_s (p) and a measured value C_m (p), where, p is the contaminant source parameters. Once the residual function is solved to get the minimal value, the identification process converges and the best-fit source conditions can be acquired. According to Liu and Zhai (Liu and Zhai, 2008), the most common residual function is the Least Squares Function, as follows:

$$\mathrm{E}(p)=\sum_{k=1}^{N}\left[C_{k,s}(p)-C_{k,m}(p)\right]^2 \tag{2.1}$$

Where, p is the contaminant source parameters, k is the comparing points (sensor locations), and N is the total number of points (how many sensor locations) to be compared. $C_{k,s}(p)$ is the simulation results while $C_{k,m}(p)$ is the measured results. Once $\mathrm{E}(p)$ reaches its minimal value as required, the equation converges and then the contaminant source information can be acquired.

Above equation is only applicable to one-directional engineering areas. Additionally, in order to improve the accuracy of identifying the contaminant source information, several

other objective functions have been developed. Gorelick et al. (1983) identified groundwater pollutant source locations and release magnitudes in two-dimensional cases by optimizing normalized residuals with linear programming (Taylor, 1974) and multiple regressions (Draper and Smith, 1966).

$$\sum_{k=1}^{N}\left|\frac{C_{k,s}-C_{k,m}}{C_{k,m}}\right| \text{ and} \sum_{k=1}^{N}\left[\frac{C_{k,s}-C_{k,m}}{C_{k,m}}\right]^2 \tag{2.2}$$

This new objective function had successful applications to identify source locations in two dimensional cases. However, in this method, potential source locations have to be known in advance and the number of pollutant sources must be no more than the number of measuring points. These are limitations of this new objective function. Similar as previous methods, this equation was solved iteratively to get converged.

Further, Mahar and Datta (Mahar and Datta, 1997) developed an optimization-based methodology to identify source locations and fluxes for ground-water pollution with specified aquifer parameters. A normalized form of residual function was shown as following:

$$\sum_{m=1}^{M}\sum_{k=1}^{N}\left[\frac{C_{k,s}^{m}-C_{k,m}^{m}}{C_{k,m}^{m}+\alpha}\right]^2 \tag{2.3}$$

Compared to the above two objective functions, this objective function was developed by incorporating time domain and error suppression factor into the residual function. In this equation, M is the concentration observation time periods, and α is a constant that

prevents error domination at low concentrations. In the simulation process, potential source locations, activation period and contaminant transport time need to be specified for the simulation in advance.

In conclusion, the forward method of inverse modeling is good for cases where some previous source information can be obtained in advance and the forward simulation is not computing demanded. For complex engineering cases, scholars may have to face several issues: the forward method of inverse modeling may not be applicable; time-consuming; new objective functions may have to be proposed and verified. Additionally, in practical engineering, we don't know the source locations, release time and other source information. In this research, the iterative process may be much more time-consuming in some cases with complex duct work. Therefore, some effective measures need to be applied to identify these kinds of information.

For some conditions that contaminant source information are unknown, the forward model cannot be used effectively to identify the contaminant source information. Like mentioned in the previous chapter, the backward inverse modeling method starts from the output results and then traces back the source information. It's possible that sensor detection information are applied to identify the contaminant source information without knowing some prior source information in advance.

According to Skaggs and Kabala's research (1995), a quasi-reversible (QR) method was developed to solve the convection-dispersion equation (CDE) by applying a QR diffusion operator into a moving coordinate system. The solution was used to recover the history of a groundwater contaminant based on the sensor detection information. In the governing contaminant transport equation, there are four terms, transient term, convection term, diffusion term, and source term.

$$\frac{\partial C}{\partial t}+\frac{\partial u_j C}{\partial x_j}=\frac{\partial}{\partial x_j}\left[\beta_j \frac{\partial C}{\partial x_j}\right]+S \tag{2.4}$$

Where, C is contaminant resident concentration (volume-averaged concentration), u_j is the velocity in different directions, β_j is the diffusion coefficient, and S is the source term. Skaggs and Kabala replaced the diffusion operator $\frac{\partial}{\partial t}-\nabla^2$ in the above forward transport equation with the quasi-reversible (QR) as following:

$$\frac{\partial}{\partial t}-\nabla^2-\varepsilon\nabla^4 \tag{2.5}$$

In this equation, ϵ is a positive constant. After replacing the diffusion term, the new equation was solved with negative time step. Then the release history of the contaminant can be recovered by solving the revised governing equation.

Further, Zhang and Chen (2007a) applied the quasi-reversibility (QR) method and numerical scheme to locate indoor particular source locations and strength by reversing the time and replacing the second-order diffusion term with a fourth-order stabilization term. The QR method was successfully used to recover the contaminant source location and strength in a 2-D aircraft cabin while not good in its application of a 3-D office building. They concluded that in the application of 3-D office building, the contaminant strength becomes dispersive because the QR equation is not the transport equation for contaminants. Therefore, the QR method works better in convection dominating flows.

The governing contaminant transport equation of contaminant concentration without a source is described as follows:

$$\frac{\partial C(t)}{\partial t} = -\frac{\partial}{\partial x_i}\left[u_i C(t)\right] + \frac{\partial}{\partial x_i}\left[\frac{\Gamma}{\rho}\frac{\partial C(t)}{\partial x_i}\right] \tag{2.6}$$

After replacing the diffusion term, the new QR equation is defined as following:

$$\frac{\partial C(t)}{\partial t} = -\frac{\partial}{\partial x_i}\left[u_i C(t)\right] + \varepsilon\frac{\partial^2}{\partial x_i^2}\left[\frac{\partial^2 C(t)}{\partial x_i^2}\right] \tag{2.7}$$

It was found that the diffusion term change is shown in below equation:

$$\frac{\partial}{\partial x_i}\left[\frac{\Gamma}{\rho}\frac{\partial C(t)}{\partial x_i}\right] \to \varepsilon\frac{\partial^2}{\partial x_i^2}\left[\frac{\partial^2 C(t)}{\partial x_i^2}\right] \tag{2.8}$$

In equation (2.8), ε is the stabilization coefficient; the second-order diffusion term with a fourth-order stabilization term.

Then Zhang and Chen (Zhang and Chen, 2007b) studied the contaminant source locations and release strengths using the quasi-reversibility (QR) method and pseudo-reversibility (PR) methods in the same applications of 2-D aircraft cabin and 3-D office building. They proposed the backward probability density function (PDF) and adopted the QR and PR methods to solve the PDF. It was found that the QR method is slightly better than the PR method but more time-consuming. The QR method reverses the time step, instead of which, the Pseudo-reversibility (PR) method reverses the airflows. Similarly, in the PR method, the diffusion term was replaced with the fourth-order stabilization term. However, same with QR method, when the diffusion term is dominating in the contaminant transport, the result seems poor. The limitation of using PR method is that the sensor has to be placed in the downstream location of the contaminant source.

Instead of studying gaseous contaminant source identification within gaseous air, Zhang et al. (Zhang et al., 2012) researched the airborne particulate agents. The airborne particles are discrete within gaseous air. The transport mechanic of airborne particles is more complex than that of gaseous agents. The particle may deposit when they hit a solid surface in the duct network. Therefore, the gravitational deposition and inertia are among the most important characteristics for particle transport (Lai and Cheng, 2007).

In their research, the forward Eulerian model for particle dispersion is as following:

$$\frac{\partial C(t)}{\partial t} = -\frac{\partial}{\partial x_i}\left[\left(U_i + V_{s,i}\right)C(t)\right] + \frac{\partial}{\partial x_i}\left[\left(D + \varepsilon_p\right)\frac{\partial C(t)}{\partial x_i}\right] + S_c \qquad (2.9)$$

Where $C(t)$ is the particulate number concentration, m^{-3}; t is time, s; x_i is the position in Cartesian coordinates, m; U_i is the velocity component of air, m s^{-1}; $V_{s,i}$ is the particle settling velocity in the x_i direction, m s^{-1}; D is the Brownian diffusivity, m^2 s^{-1}; ε_p is the particle eddy diffusivity,m^2 s^{-1}; S_C is the source term, m^{-3} s^{-1}. Except the Brownian diffusion, turbulent, diffusion and gravitational settling, Zhao and Wu (2006) also considered the turbophoretic velocity. Turbophoretic is regarded as a particle transport mechanism different from Brownian diffusion, which is produced by the gradient in turbulent fluctuating velocity components when the turbulence is inhomogeneous. According to the research, Zhang et al. compared the quasi-reversibility (QR) model and the zone prescription of contaminant sources with the Lagrangian-reversibility (LR) model. Just like pseudo-reversibility (PR) method, the LR model reverses the flow field and recovers individual particulate motion in a Lagrangian reference.

Additionally, Atmadja and Bagtzoglou (Atmadja and Bagtzoglou, 2000) studied and optimized the Backward Beam Equation (BBE) method (Carasso, 1972) to solve the convection-dispersion equation with negative time steps. Based on their research conclusions, this method can recover the time history and spatial distribution of a groundwater contaminant from measurements for both homogeneous and heterogeneous problems.

Some scholars also studied the application of QR method and BBE method. Cornacchiulo et al. (2002) compared the applications of QR method and BBE method in certain cases. In their research, they included that the BBE method is able to handle highly heterogeneous parameters and is also able to preserve the salient features of the initial input data. However, the QR method is better in handling cases with homogeneous parameters and cases with initial data that are plagued by uncertainty while the QR method performs poorly in cases with heterogeneous media (Liu and Zhai, 2008, 2009).

As a sum, the backward method has two characteristics. It may not be time-consuming like the forward model since it just needs to solve the convection diffusion contaminant transport equation with negative time steps or reversing airflow field. Additionally, in order to solve the backward model, prior source information are still needs to be given, such as source locations and release time, which is also the limitation of the backward model.

2.2. Backward Probability Model

Scholars estimate the probability of contaminant source locations or source release time using probability models. In this section, the existing inverse probability methods are reviewed and discussed.

By reversing the flow field, Bagtzoglou et al. (1992) obtained backward location probabilities that were used for identifying contamination sources. Wilson and Liu (1994 and 1997) proposed a method to obtain a backward probabilistic continuum model from the forward advection-dispersion equation using a single detection of contamination. Neupauer and Wilson (1999 and 2001) developed an adjoint method of the forward contaminant transport equation, to predict groundwater contaminant source location and release time. They first studied the application of this method in one dimensional cases and found that they can predict the groundwater contaminant source information (source locations and release time) well. In addition, the adjoint method can be used to successfully identify the historical characteristics of contaminant in a multidimensional aquifer with complex domain geometries. In the adjoint method, the forward location probability represents the probability that contaminant from a source will reach an arbitrary location in the domain after releasing a given time. In the first step, they studied the forward model of the groundwater air flow and contaminant distribution based on the forward contaminant transport model. In the second step, they deduced the adjoint probability model equations and solved the adjoint probability of the contaminant source locations, result of which is the backward location probability. Similarly, they deduced the adjoint backward equation to solve the adjoint probability of the contaminant release time.

The adjoint backward probability-based inverse model was given an extensive study by Liu and Zhai (2007, 2008, and 2009) on the building indoor contaminant source

identification. This probability-based inverse model was derived from the adjoint probability method initially proposed by Neupauer and Wilson (2002 and 2003) in their research of identifying contaminant source in the groundwater system. Liu and Zhai deduced the forward contaminant distribution equations for both CFD and multi-zone models. Then they derived the adjoint probability equation for CFD and multi-zone models in order to track the contaminant source location in the enclosed environment. Two cases were used successfully to test the application of the two adjoint models: a two dimensional office building and a three dimensional aircraft cabin.

As a sum, it was found that only the adjoint probability method developed by Neupauer and Wilson (1999, 2000, and 2001) for identifying groundwater pollution can find contaminant source locations, release strength and release time without prior source information. For most building indoor environment incidents, source conditions, such as source locations, release intensity and activation time may be unknown. Additionally, contaminant transport in groundwater follows the same advection-dispersion law as that in the air, indicating the feasibility of applying the adjoint probability model in building indoor air quality study. Adjoint backward probability modeling may be used to identify the gaseous contamination source in HVAC duct network.

2.3. Inverse Network Models

Except the above types of inverse models, there are also some other models developed to solve the issue of contaminant source information identification. These models applied different inverse methodology to identify contaminant source information.

Sohn et al. (2002) adopted Bayesian statistics model to identify the contaminant source in a building with five rooms. This Bayesian approach was divided into two stages. In the first stage, a multi-zone model (COMIS model) was used to calculate the airflow and contaminant transport. This stage produces a big enough database which is much time-consuming. In the second stage, when a pollutant is detected, the Bayesian updating was applied to optimize the agreement between each of the model simulation and sensor data. The second stage is faster compared to the first stage since a good enough database needs to be built in advance in the first stage.

The artificial neural network (ANN) was applied to detect the contaminant source in buildings by Vukovic et al. (2007 and 2010) and Bastani et al. (2012). Vukovic et al. (2007 and 2010) proposed the artificial neural networks trained with multi-zone models. The model was divided into two steps. First, multi-zone model (CONTAM model) was used to develop a forward database with known source inputs, which is faster than the CFD model. The database was used for the neural network training in next step. Second, the neural network (ANN) model was built and trained to predict the unknown contaminant source locations with the real-time sensor data. An office space with six cubicles was used to test the accuracy of the artificial neural network and was found that the accuracy can be acceptable. This model was shown in the following figure 2-1. In the figure 2-1, in the first step, parameters were input into CONTAM model, the CONTAM model was simulated many times to build a database. In the second step, the database, namely the output of CONTAM models was input into ANN network. The outputs of the ANN was contaminant source.

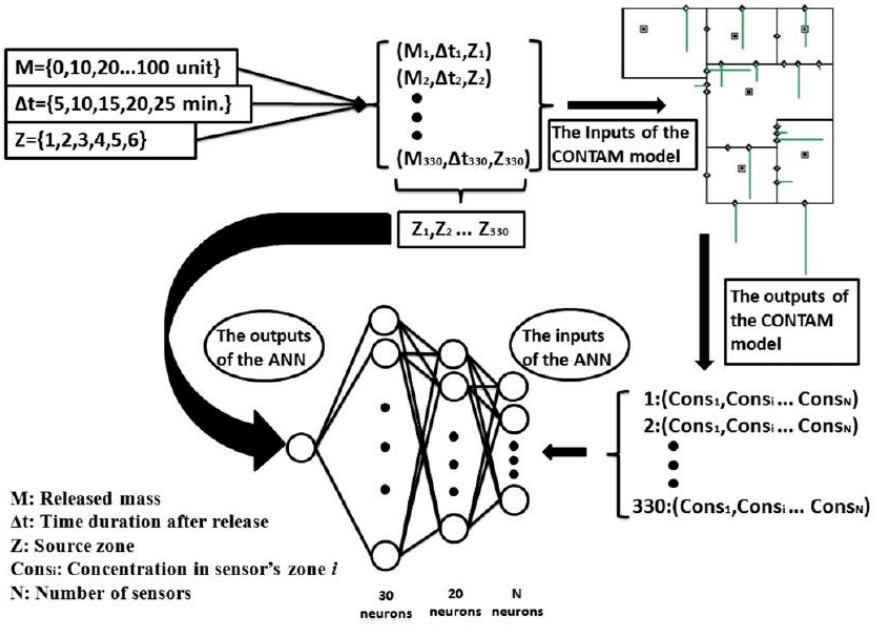

Figure 2-1 Artificial Neural Network Flow Chart

Allen et al. (2007) coupled a forward dispersion model with a backward model which uses the genetic algorithm (GA). They incorporated the sophisticated dispersion model, the Second-Order Closure Integrated Puff (SCIPUFF) model into a GA system. SCIPUFF was adopted to compute the contaminant concentrations from each source in the first step. Then the GA method was used to optimize the contaminant source information based on the sensor data from real data runs. It was found that the GA-coupled model has a high degree of accuracy.

A method based on the characteristics matrix derived from the governing transport equation was developed by Wang et al. (2013) in their research of identifying the point source of indoor gaseous contaminant. CFD model was used to calculate the contaminant concentration distributions under a steady point source is presumed at a certain point. Then based on the characteristics matrix method, the concentration data at the specified

sampling points were applied to trace the source position. A 2-D room as the demonstration case was selected. They found that sampling points have to be increased if concentration measurement errors are considered.

Cai et al. (2012 and 2014) proposed a model combing a linear programming model with an analytical expression of indoor contaminant dispersion. Similarly, this model is like the optimization method which has two stages. In the first stage, before a contaminant source is released, a limited number of time-consuming CFD simulations, which equal to the number of predefined potential source locations in the buildings, was completed to determine the transport of each contaminant source. In the second stage, the linear programming model was solved to identify the contaminant source information. However, in buildings especially a lot of spaces in building, it's impossible to use CFD simulations in the first step, which is this method's limitation to a certain extent.

In this section, some other models instead of the above three types of inverse models are described to identify contaminant source information. There are two characteristics in this method. First, two steps need to be conducted to identify the contaminant source information. Second, the database producing process is very time-consuming in the first stage since a good enough database is the basic to improve the accuracy of identification.

Although several research has been done on the contaminant source identification in buildings, few people are focusing on the contaminant source identification in building duct work. As we know, the heating, ventilation and air conditioning (HVAC) system could be contaminant source. The contaminant in the building duct work will be transported through the duct and distributed inside the whole building. The contaminant source identification in HVAC system is necessary to be researched.

Moreover, although CFD model can provide more details and accuracy for the contaminant distribution, it's in the expense of simulation time. Our goal is identify the contaminant source quickly and eliminate their influence on the indoor air quality. Simulation time is an important concern in the inverse model. Several scholars have selected the multi-zone model to solve the forward model, which takes much less time. Multi-zone uses well-mixed zone model which considers the contaminant distributes uniformly in the zone within just one time step, which, however, is not practical for duct work. In duct work system, when the air velocity is small and duct is long, we cannot regard the duct as a well-mixed zone since it takes time for contaminant transporting from one point to the other terminal point. To compromise the CFD model and mixed zonal model, the one dimensional convection dispersion model for the duct work is proposed in multi-zone model.

Additionally, according to the existing major method for contaminant source identification, the adjoint probability method can find source locations, release mass and release time and multiple sources without knowing source information in advance. The adjoint probability method may be an ideal choice to identify the contaminant source information.

In conclusion, in the research of contaminant source identification in building duct work, the one dimensional convection dispersion model for duct work in CONTAM is used as the forward model and the adjoint backward probability method is applied in the inverse model.

Chapter 3 Methodology Analysis

3.1. Principles of Adjoint Backward Probability Method

Before deriving the adjoint backward probability equation, principles of adjoint probability method needs to be understood. Figure 3-1 gives the contaminant distribution after releasing an instantaneous contaminant source for some time. An instantaneous contaminant source is released with a mass of M_0 at location $\vec{x} = \vec{x}_0$ and at time t=0. After a given time t=T, the contaminant reaches some area in the domain. Figure 3-1 shows that a very small finite volume (ΔV_1) of pollutant is trapped in the red rectangle at location $\vec{x} = \vec{x}_1$ and time t=T. The mass in the trapped volume ΔV_1 is M_1. Then the forward location probability at the volume ΔV_1 can be defined in the following equation:

$$P\left(\Delta V_1 \mid \vec{x} = \vec{x_1}; t = T, \vec{x_0}\right) = \frac{M_1}{M_0} \tag{3.1}$$

The forward location probability is defined as the probability that the contaminant reaches some area in the domain after a release time of given time t=T. This equation defines the probability that the contaminant ($M_0, \vec{x} = \vec{x}_0$) reaches the area with a small volume of ΔV_1 in the domain after a release time of T.

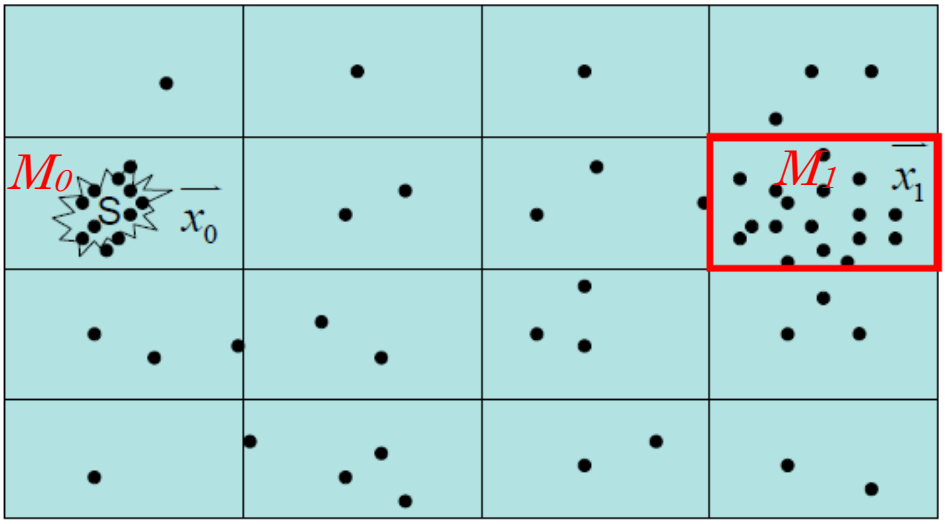

Figure 3-1 Illustration of Forward Location Probability

According to the forward location probability in the small finite volume ΔV_1, the location probability density function at time t=T, is expressed as following equation (Liu, 2008):

$$f_x\left(\vec{x}_1; t=T, \vec{x}_0\right) = \frac{P\left(\Delta V_1 \mid \vec{x}=\vec{x}_1; t=T, \vec{x}_0\right)}{\Delta V_1} = \frac{M_1}{M_0 * \Delta V_1} = \frac{C_1}{M_0} \tag{3.2}$$

Where C_1 is the contaminant resident concentration at location $\vec{x}=\vec{x}_1$, which is a volume-averaged concentration. This equation indicates the relationship between the contaminant resident concentration and the source release mass. Generalizing the definition of location probability density function to all the areas in the domain, the generalized equation can be shown as follows:

$$f_x\left(\vec{x}; t=T, \vec{x}_0\right) = \frac{C\left(\vec{x}, T\right)}{M_0} \tag{3.3}$$

This equation gives the relationship of resident contaminant concentration and source mass M_0. As we know, for cases with steady-state airflow filed, the relationship between source release mass and resident concentration is linear, expressed in following equation:

$$f_x\left(\vec{x};t=T,\overrightarrow{x_0}\right)=\frac{dC\left(\vec{x},T\right)}{dM_0}=\psi_x\left(\vec{x};t=T,\overrightarrow{x_0}\right) \tag{3.4}$$

In this equation, $\psi_x\left(\vec{x};t=T,\overrightarrow{x_0}\right)$ is the state sensitivity of resident concentration at location $\vec{x}$ to the source mass M_0 at source location $\overrightarrow{x_0}$ .The location probability density function, $f_x\left(\vec{x};t=T,\overrightarrow{x_0}\right)$ defines that the resident concentration at location $\vec{x}$ varies with the change of source release mass. This makes sense under a steady-state airflow field. With a newly defined time sing $\tau=T-t$, it was proved that the backward location probability can be determined by applying the following equation (Liu, 2008):

$$f_x\left(\vec{x}=\vec{x}_0;\tau=T,\vec{x}\right)=\psi_x^*\left(\overrightarrow{x_0};\tau=T,\vec{x}\right) \tag{3.5}$$

Where, $\psi_x^*\left(\overrightarrow{x_0};\tau=T,\vec{x}\right)$ is defined as the adjoint backward location probability, which is the solution of an adjoint location probability equation. The backward location probability $f_x\left(\vec{x}=\vec{x}_0;\tau=T,\vec{x}\right)$ defines the backward location probability with known release time and measurement location. Through solving the adjoint backward location probability equation, the adjoint location probability can be obtained, which is also the backward location probability. Similarly, the adjoint probability of backward release time also can be expressed using this equation, except a little difference of the sign for the equation.

3.2. CONTAM Model

CONTAM is a multi-zone indoor air quality (IAQ) and ventilation analysis computer tool, which is used to determine airflows in buildings, contaminant concentration distribution, and personal exposure influence on the indoor air quality. CONTAM has been successfully applied to study the indoor air quality (IAQ) improvement measures in many applications. As mentioned above, CONTAM is adopted to provide a steady state airflow field and solve the adjoint backward probability equation. According to the user guide, there are five basic steps to build the building model and run simulation using CONTAM, then the forward airflow field and forward contaminant concentration distribution can be obtained (Walton and Dols, 2013). The five steps are documented as follows:

(1) Building Idealization. The real building is too complex to be built into a simulation model in CONTAM. It normally can be simplified and idealized, and then was developed into a simulation model in CONTAM. The whole modeling process was documented in figure 3-2. This CONTAM model includes several other components to conduct different research topics.

(2) Building Leakage Characteristics and Airflow Paths. The building leakage characteristics have two categories: doors and windows, and envelope leakages, which were created in the form of airflow paths. There are various types of models for building leakage airflow paths in CONTAM.

(3) Building HVAC Systems. Various existing HVAC system models in CONTAM can be applied to study the airflow and contaminant distribution in HVAC duct work. In the HVAC duct work, there are several components, including air handling unit (AHU), supply air duct, return air duct, exhaust air duct and outdoor air duct.

(4) Contaminant Source and Sinks. In CONTAM, several contaminant source and sink models can be selected to reflect the real contaminant source characteristics. Specific types of contaminant source are added into the zones or HVAC duct work, then the contaminant distribution in the building and HVAC duct work can be acquired.

(5) Simulation. After the above steps, the building model with several components is done using CONTAM. Then various types of analysis can be conducted to run the simulation.

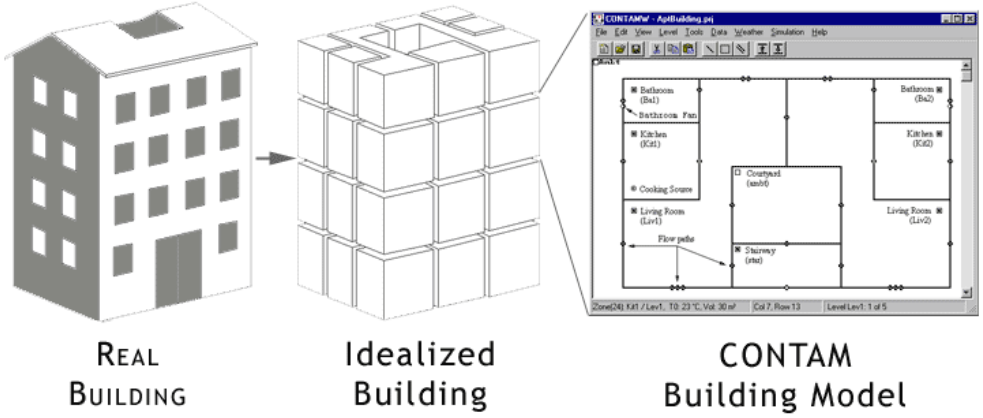

Figure 3-2 CONTAM Modeling Process (Walton and Dols, 2013)

Figure 3-2 documents the process of a real building idealization. A real building is idealized, and then built into a CONTAM simulation model. Based on the above five steps, a building simulation model can be developed in CONTAM. In this research, a simple CONTAM model with detailed HVAC duct work is developed as following figure 3-3.

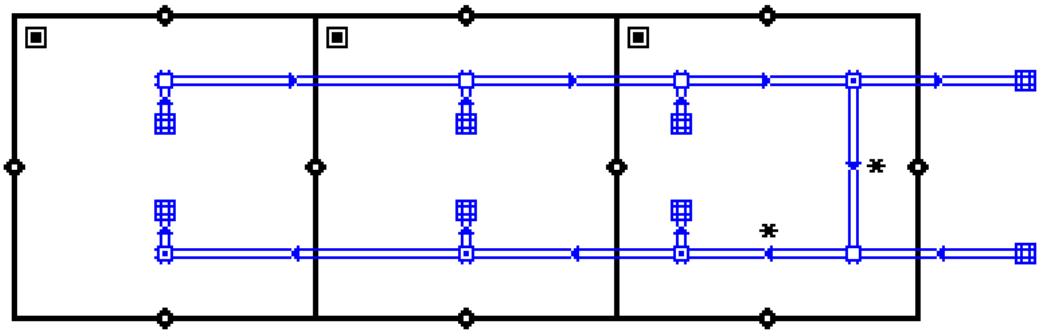

Figure 3-3 Building CONTAM Simulation Model

This building simulation model initially has two floors. However, in order to simplify the building model, the second model is removed with the first floor remained. In the CONTAM simulation model, several components are incorporated, including three zones, a detailed duct work, and airflow paths. In the detailed duct work that has been designed in advance in the mechanical system design, there are air handling unit (AHU), supply duct, return duct, exhaust air duct, and outdoor air duct. Like mentioned in previous chapters, the duct work is considered as the one dimensional convection dispersion duct while the zone is defined as the well-mixed zone.

It was proved that the adjoint backward probability equation is adjoint of the forward contaminant transport equation (Neupauer, 2000). According to the forward contaminant transport equation, the adjoint backward probability equation can be deduced both for one dimensional convection dispersion duct and well-mixed zone.

3.3. Adjoint Equation of the One Dimensional Convection Dispersion Equation

According to the literature review, Dr. Neupauer developed the adjoint backward probability method to identify the contaminant location and contaminant release time in

the groundwater system (Neupauer, 1999, 2000 and 2001). In her research, the adjoint backward probability method was demonstrated to identify the contaminant source information effectively. Based on the same contaminant transport fate of water and air, and their similar properties, Dr. Liu applied the adjoint backward probability-based method to study contaminant source identification in buildings (Liu, 2008). In this research, the adjoint equation of one dimensional convection dispersion equation is derived referring to their research work.

The forward contaminant transport equation for one dimensional convection dispersion duct is defined as following:

$$\begin{aligned}
&\frac{\partial(C)}{\partial t}+\frac{\partial(\mathrm{uC})}{\partial x}=\frac{\partial}{\partial x}\left(\beta\frac{\partial C}{\partial x}\right)+Q_{\text{source}}\\
&C\left(\vec{x},0\right)=C_0\left(\vec{x}\right)\\
&C\left(\vec{x},\ \mathrm{t}\right)=g_1(t)\\
&\beta\frac{\partial C}{\partial x}=g_2(t)\\
&\mathrm{uC}-\beta\frac{\partial \mathrm{C}}{\partial x}=g_3(t)
\end{aligned} \tag{3.6}$$

Where, $\frac{\partial C}{\partial t}$ is the transient term; $\frac{\partial(uC)}{\partial x}$ is convection term; $\frac{\partial}{\partial x}\left(\beta\frac{\partial C}{\partial x}\right)$ is the dispersion term; Q_{source} is the source term. C is the contaminant resident concentration (volume-averaged); u is the velocity of airflow; ß is the dispersion coefficient; $g_1(t), g_2(t), g_3(t)$ are three types of boundaries. Initial condition and boundary conditions are required to solve the governing contaminant transport equation (convection dispersion equation).

In the forward governing contaminant transport equation, it's necessary to introduce the dispersion term. Convection term indicates that contaminant transport with the same velocity as the airflow velocity while dispersion term is different. Dispersion term is used to describe the influence of contaminant concentration gradient on the transport of contaminant in the duct. Dispersion results from the molecular diffusion and convective diffusion.

According to the forward contaminant transport equation for the one dimensional convection dispersion duct, the adjoint backward probability equation is derived as following. The detailed deducing procedures were given in the appendix A which are not shown in here again.

$$\begin{aligned}
&\frac{\partial \psi^*}{\partial t} = \frac{\partial}{\partial x}\left(\beta \frac{\partial \psi^*}{\partial x}\right) + u\frac{\partial}{\partial x}\left(\psi^*\right) + \frac{\partial h}{\partial C} \\
&\psi^*\left(\vec{x}, 0\right) = 0 \\
&\psi^*\left(\vec{x}, \tau\right) = 0 \\
&\beta \frac{\partial \psi^*}{\partial x} + u\psi^* = 0 \\
&\beta \frac{\partial \psi^*}{\partial x} = 0 \\
&\frac{\partial h}{\partial C} = \delta\left(\vec{x} - \vec{x}_m\right) \bullet \delta\left(\tau\right)
\end{aligned} \tag{3.7}$$

Where, $\frac{\partial h}{\partial C}$ can be defined as the load term (Neupauer, 2000); ψ^* is the adjoint probability; τ is the defined backward time; $\vec{x}_m$ is the measurement locations; m is a sign means measurement of sensor. In the inverse model, the load term can be considered as a unit source. Other parameters are same with those of forward transport equation.

Compared the forward equation and backward equation, several differences can be found as following:

(1) In the forward equation, the convection term is located in the left side while it's in the right side in the adjoint equation. It means that the airflow field has been reversed, and that the adjoint backward probability equation will be solved with a reverse airflow field.
(2) The first-type boundary condition of adjoint equation is still the first-type boundary condition in the forward equation.
(3) The second-type boundary condition of adjoint equation becomes the third-type boundary condition in the forward equation.
(4) The third-type boundary condition of adjoint equation becomes the second-type boundary condition in the forward equation.

Therefore, it can be considered that the backward probability equation is adjoint of the forward contaminant transport equation. Through solving the above adjoint backward probability equation with initial condition and boundary conditions, the adjoint backward probability can be solved to obtain the backward location probability and backward release time probability.

3.4. Adjoint Equation of the Well-mixed Zone

The zones in the building model were considered as well-mixed zones. In this section, the adjoint equation of the well-mixed zone is derived referring to previous work (Liu, 2008). The detailed process is given in the appendix.

CONTAM calculates air flow rate and contaminant concentration in each zone based on the mass balance. According to the mass balance, the forward contaminant transport equation for the well-mixed zone is defined as following (Walton and Dols, 2013):

$$\frac{dC_{k,i}}{dt} = \left[\sum_{j=0,\neq i}^{n} \frac{\left(1-\eta_{k,j,i}\right)F_{j,i}}{Q_i} C_{k,j} - \sum_{j=0,\neq i}^{n} \frac{F_{i,j}}{Q_i} C_{k,i} \right] + \left[\sum_{l} k_{k,l} C_{l,i} + \frac{G_{k,i}}{Q_i} - C_{k,i} \frac{R_{k,i}}{Q_i} \right] = \sum_{m=1}^{n} A_{k,i,m} C_{k,m} + B_{k,i}$$

$$C_{k,i}\left(0\right) = C_{k,initial}$$

(3.8)

In this equation, all of these terms are described in following according to the airflow path, contaminant source, and reactions.

(1) Outward airflows from zone i at the rate of $\sum_{j=0,\neq i}^{n} F_{i,j} \cdot C_{k,i}$,

$F_{i,j}$ is the air flow rate from zone i to adjacent zone j;

(2) Inward airflows to zone i at the rate of $\sum_{j=0,\neq i}^{n} \left(1-\eta_{k,j,i}\right) F_{j,i} \cdot C_{k,j}$, where $\eta_{k,j,i}$ is the filter efficiency in the path from zone j to zone i;

(3) Removal at the rate of $C_{k,i} \cdot R_{k,i}$ where $R_{k,i}$ is a removal coefficient;

(4) Generation at the rate of $G_{k,i}$;

(5) First order chemical reactions with other contaminants $C_{l,i}$ at the rate of $Q_i \sum_{l} k_{k,l} \cdot C_{l,i}$ where $K_{k,l}$ is the kinetic reaction coefficient in zone i between species k and l (positive $K_{k,l}$ for generation and negative $K_{k,l}$ for removal).

The coefficients in above equation is defined in below:

$$A_{k,i,m}=\begin{cases}\dfrac{-R_{m,i}-\sum_{j=0,\neq i}^{n}F_{i,j}}{Q_i}, & (m=i,m\neq 0)\\ \dfrac{F_{m,i}\left(1-\eta_{k,m,i}\right)}{Q_i}, & (m\neq i,m\neq 0)\end{cases} \tag{3.9}$$

Following similar procedures as deducing the one dimensional convection dispersion equation, the adjoint equation for the well-mixed zone is shown as follows:

$$\begin{aligned}&\frac{\partial\psi^*}{\partial\tau}=\mathrm{A}^{\mathrm{T}}\psi^*+\frac{\partial\mathrm{h}}{\partial\mathrm{C}}\\&\psi^*\left(\vec{\mathrm{x}},\tau=0\right)=0\end{aligned} \tag{3.10}$$

Where, $\frac{\partial h}{\partial C}$ is defined as the load term, which can be considered as a unit source in the inverse model; ψ^* is the adjoint probability; τ is the backward time; A^{T} is the transpose matrix of A. Other parameters are same with those of forward transport equation.

3.5. Sensor Networks Description

Sensor networks are critical to identify the contaminant source information. In practical engineering, there are three types of sensor, including alarm sensor without contaminant concentration recording, sensor with current concentration recording, and sensor with historical concentration recording. Alarm sensor is that kind of sensor which will alarm once detecting a concentration larger than its threshold. It cannot record the contaminant concentration. Alarm sensors can be often seen, like fire alarm sensor. Another two kinds of sensors can record the current concentration and historical concentration, respectively. Recording contaminant concentration provides more information. Considering the combination of sensor types and sensor number, six analysis

were conducted for each case in this research. These six scenarios were shown in the table 3-1.

Table 3-1 Six Scenarios Based on Sensor Types and Sensor Numbers

Sensor Types	Sensor Number	
	Single Sensor	Two or more sensors
Alarm sensor without concentration recording	Scenario 1	Scenario 2
Sensor with current concentration recording	Scenario 3	Scenario 4
Sensor with historical concentration recording	Scenario 5	Scenario 6, 7, 8…

In table 3-1, scenario 1 and scenario 2 are the cases with a single alarm sensor and multiple alarm sensors respectively. Scenario 3 and scenario 4 includes sensor (s) with current concentration recording. Different from above two sensor types, scenario 5 and scenario 6 are studied using sensors with historical concentration recording.

According to the three types of sensor networks, different backward probability equations are deduced under the instantaneous contaminant source case. In the following section, the backward probability equations are reviewed and described in detail.

3.5.1. Adjoint Backward Probability Equation for a Single Alarm Sensor without Concentration Recording

Like mentioned above, under a single alarm sensor network, the adjoint backward probability can be calculated directly by solving the deduced adjoint backward probability equation. Single alarm sensor detection information can identify the contaminant source location or source release time. The adjoint backward probability has a sign

$f_x\left(\overrightarrow{x_0};\tau_0,\overrightarrow{x_{mk}},\tau_{mk}\right)$ according to Dr. Liu (Liu, 2008). In this sign, $\overrightarrow{x_{mk}}$ is sensor location; τ_{mk} is the sensor detection time; τ_0 is the source release time. $f_x\left(\overrightarrow{x_0};\tau_0,\overrightarrow{x_{mk}},\tau_{mk}\right)$ is defined as the probability of contaminant source location, given sensor locations, sensor detection time, and source release time. This is a simplified case because the release time is known. In the sensor network with only one alarm sensor, $f_x\left(\overrightarrow{x_0};\tau_0,\overrightarrow{x_{mk}},\tau_{mk}\right)$ can be calculated as the fundamental for later cases with much more complex sensor networks.

3.5.2. Backward Probability Equation for Multiple Sensors without Concentration Recording

According to table 3-1, for cases with multiple sensors, the backward probability equation can be defined as following (Neupauer, 2000; Liu, 2008):

$$f_x\left(\overrightarrow{x_0};\tau_0,\overrightarrow{x_{m1}},\overrightarrow{x_{m2}},\cdots,\overrightarrow{x_{mN}},\tau_{m1},\tau_{m2},\cdots,\tau_{mN}\right)=\frac{\prod_{k=1}^{N} f_x\left(\overrightarrow{x_0};\tau_0,\overrightarrow{x_{mk}},\tau_{mk}\right)}{\int_x \prod_{k=1}^{N} f_x\left(\overrightarrow{x_0};\tau_0,\overrightarrow{x_{mk}},\tau_{mk}\right)dx} \tag{3.11}$$

If there are multiple alarm sensors in the HVAC duct work, this equation can be used to calculate the backward probability. The adjoint backward probability equation for single alarm sensor without concentration recording is solved using equation (3.11), $f_x\left(\overrightarrow{x_0};\tau_0,\overrightarrow{x_{mk}},\tau_{mk}\right)$ is the fundamental for complex models with a sensor network of concentration recordings.

According to equation (3.11), the numerator is multiply of backward location probability densities of different inverse case. In each inverse case, an instantaneous contaminant source with a unit mass is released in a certain sensor location. Number of

inverse cases should equal to the number of sensors. Multiple sensors are assumed to be independent. So the multiple inverse cases can also be considered uncorrected and independent. According to the probability statistics, the probability of the event that source location is a certain point should be the multiply of probabilities for all independent cases. The integral in the denominator of that equation ensures that the total probability of all the cells is one.

3.5.3. Backward Probability Equation for Multiple Sensors with Concentration Recording

In this case, the sensors can detect the concentration recording, both for current concentration recording and historical concentration recording. According to Lin (2003), the sensor networks with contaminant concentration recording can improve the accuracy of identifying contaminant source information. The backward probability equation for multiple sensors with concentration recording can be expressed as follows (Liu, 2008):

$$f_x\left(\overrightarrow{x_0} \mid C_{m1}, C_{m2}, \cdots, C_{mN}; \tau_0, \overrightarrow{x_{m1}}, \overrightarrow{x_{m2}}, \cdots, \overrightarrow{x_{mN}}, \tau_{m1}, \tau_{m2}, \cdots, \tau_{mN}\right) = \frac{\int_{M_0} \prod_{k=1}^{N} P\left(C_k \mid M_0, \overrightarrow{x_0}; \tau_0, \overrightarrow{x_{mk}}, \tau_{mk}\right) f_x\left(\overrightarrow{x_0}; \tau_0, \overrightarrow{x_{mk}}, \tau_{mk}\right) dM_0}{\int_x \int_{M_0} \prod_{k=1}^{N} P\left(C_k \mid M_0, \overrightarrow{x_0}; \tau_0, \overrightarrow{x_{mk}}, \tau_{mk}\right) f_x\left(\overrightarrow{x_0}; \tau_0, \overrightarrow{x_{mk}}, \tau_{mk}\right) dx dM_0} \tag{3.12}$$

Where, N is the number of measurements; C_{mN} is the sensor measurement concentrations; $\overrightarrow{x_{mk}}$ and τ_{mk} are the sensor locations and sensor detection time, respectively; τ_0 is the contaminant source release time which is known to identify source location; M_0 is the instantaneous contaminant source release mass (release strength). $f_x\left(\overrightarrow{x_0}; \tau_0, \overrightarrow{x_{mk}}, \tau_{mk}\right)$ is still the adjoint backward probability under single alarm sensor.

$P\left(C_k \mid M_0, \overrightarrow{x_0}; \tau_0, \overrightarrow{x_{mk}}, \tau_{mk}\right)$ is the probability for measured concentration in terms of source release mass M_0 and source location $\overrightarrow{x_0}$. $P\left(C_k \mid M_0, \overrightarrow{x_0}; \tau_0, \overrightarrow{x_{mk}}, \tau_{mk}\right)$ follows a normal distribution (Neupauer, 2000 and 2002; Liu, 2008) as shown in below equation:

$$P\left(C_k \mid M_0, \overrightarrow{x_0}; \tau_0, \overrightarrow{x_{mk}}, \tau_{mk}\right) \sim N\left(M_0 \cdot f_x\left(\overrightarrow{x_0}; \tau_0, \overrightarrow{x_{mk}}, \tau_{mk}\right), \sigma_s^2\right) \tag{3.13}$$

Where, C_k is the measured concentration value; σ_s is the measurement variance of sensors. Therefore, under cases with multiple sensors recording contaminant concentrations, the backward location probability can be calculated using this equation. In the following applications, the backward location or release time probability can be calculated according to the three types of equations.

Equation (3.12) is a little bit different from equation (3.11) since contamination concentrations are recorded in the sampling locations. Sensor information (sensor location, release time and recorded concentration) are used to trace the source location. In practical situations, the sampled contamination concentration contains measurement error. Different from exact detecting, measurement error must be considered in practical data tracking process. Based on previous study, the measurement error distribution can be considered as a normal distribution, normally distributed with mean zero and variance σ^2. For a given source location, measured concentration is a normally distributed random variable with mean concentration and variance σ^2. Through Bayes' theorem, the numerator of equation (3.12) can be deduced. Likewise, the integral in the denominator of that equation ensures that the total probability of all the cells is one.

As a sum, in this methodology section, the primary methodology applied in this research is described in detail. First, CONTAM model is applied to study the airflow field and contaminant transport fate, and then is used to solve the adjoint backward probability equation. Second, the principles of adjoint backward probability equation is described in detail to show what the adjoint method does work. Third, according to previous work, both the adjoint equation of one dimensional convection dispersion duct and well-mixed zone are derived based on the forward transport equation. Through solving the adjoint backward probability equation, the adjoint backward location probability and adjoint backward release time probability can be calculated, which are also the possibility of backward contaminant source locations and backward source release time. Last but not least, three types of sensor networks are defined, which are critical for identifying contaminant source information. In following sections, these sensor networks are adopted to identify the source information.

Additionally, this research is conducted on the basis of previous study done by Neupauer R.M. and Liu X. Research of Neupauer R,M. provided theoretical fundamentals for the adjoint probability method. Liu X. applied the adjoint probability method into the application of indoor airborne contaminant sources. This research is an extensive study on the research of Liu X. and used the deduced equations of well-mixed zone from Dr. Liu and sensitivity analysis methods. The differences between this research and Liu X.'s work are described as follows:

1) The research focuses on identification of contaminant source in HVAC system using the adjoint probability method.
2) In this research, analytical solution of one-dimensional convection-diffusion equation is deduced and solved. The analytical solution is compared with

simulation results of CONTAM to validate the effectiveness of CONTAM duct network.

3) Several critical details of forward CONTAM model are studied in this research, like time step, laminar flow and turbulent flow.
4) In the COTNAM model, detailed duct networks are built and use a one-dimensional duct modeling. While in Dr. Liu's research, well-mixed zonal modeling was used for the airflow paths, which causes there is no time delay for the contaminant transport.
5) Like stated above, applications are different. This research focuses on HVAC system instead of indoor buildings. Because of limit of current CONTAM, several assumptions have to be proposed, including introduce contaminant to duct network through fake zone and consider limited points (junctions and terminals) in duct network as potential source locations.

Chapter 4 Forward Model Study

As we know, in the adjoint backward probability modeling, backward model is adjoint of forward transport model. In this section, several critical details of forward model are studied and discussed. The conclusion of forward model study will be fundamental for next step research.

4.1 Sensitivity Analysis of Time Step

Shorter time steps provide greater accuracy of simulation results but require more computing time. In CONTAM, 1 second is the smallest time step. This section mainly presents the sensitivity analysis on time step. Before the study, a forward CONTAM model should be developed first.

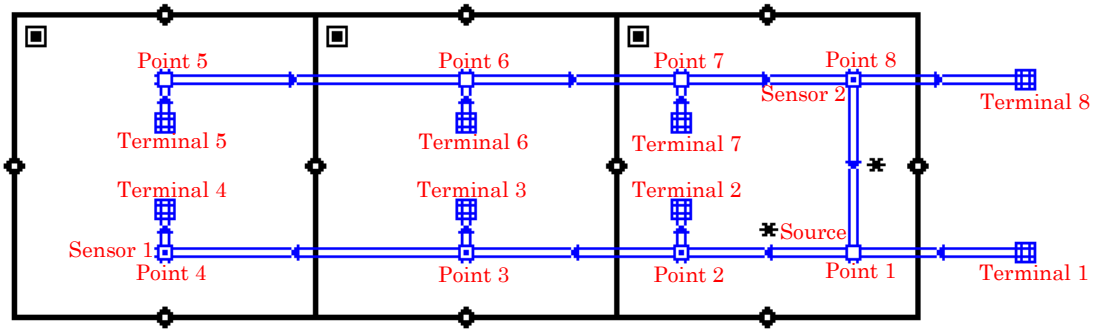

Figure 4-0-1 Forward CONTAM Building Model

In figure 4-1, there are three zones (named zone A1, zone B1 and zone C1 from left to right) connected with airflow paths and detailed duct work. In this duct work, eight junctions (from point 1 to point 8) and eight terminals (from terminal 1 to terminal 8) are

noted with red characters. In CONTAM model contaminant cannot be put into duct directly, which means duct cannot be contaminant source. A compromise is proposed to conduct this research. An assumed zone is created with a very short duct connected to point 1. Instantaneous contaminant source (Carbon Monoxide, CO) with a mass of 1000g is put into the assumed zone (called 'fake zone'). The fake zone has a space area of 3.33 square meters and a volume of 10 cubic meters. The duct connecting point 1 and the fake zone only has a length of 0.01 meters. To have an air flow balance for the fake zone, a boundary of 0.02 kg/s of air flow (infiltration) is set to the fake zone, direction of which is from ambient to the fake zone. After simulation, the velocity of connecting duct is 0.529 m/s. It takes 0.02 seconds for contaminant transporting from the fake zone to point 1, which is pretty fast and less than one second. In this way, point 1 can be assumed to be the contaminant source. The cell at the outlet end of the connecting duct segment will not necessarily have an edge at x = 0.01m (x means one-dimensional, 0.01m is duct length) in which case an interpolation is necessary to compute the concentration at x = 0.01m, which becomes the input concentration to the next duct segment downstream. When multiple duct segments merge at a junction the contaminant concentration at the junction is the flow-weighted average of the concentrations at the end of each incoming duct (Walton and Dols, 2013).

Two sensors (sensor 1 and sensor 2) are placed in point 4 and point 8 respectively to detect contaminant change in these two points. An instantaneous contaminant source (Carbon Monoxide, CO) with a mass of 1000 g is released in the fake zone at 1:00:00AM. Boundary conditions of the forward CONTAM model are listed in following table 4-1. The contaminant concentration change in the eight junctions were recorded to study the sensitivity analysis of time step. Four scenarios are studied, including scenario with time

step of 1 second, scenario with time step of 2 seconds, scenario with time step of 5 seconds, and scenario with time step of 10 seconds.

Table 4-0-1 Boundary Conditions of Forward Model

Airflow Paths	Airflow Rate	Velocity	Pressure Change	Airflow Direction	
	kg/s	m/s	Pa	From	To
Ventilation Duct	1.34	3.54	1.16	Ambient	Terminal 1
Exhaust Duct	0.5	1.32	0.16	Terminal 8	Ambient
Path 1	0.089	-	0.93	Zone C1	Ambient
Path 2	0.089	-	0.93	Zone C1	Ambient
Path 3	0.089	-	0.93	Zone B1	Ambient
Path 4	0.089	-	0.93	Zone A1	Ambient
Path 5	0.089	-	0.93	Zone A1	Ambient
Path 6	0.089	-	0.93	Zone A1	Ambient
Path 7	0.089	-	0.93	Zone B1	Ambient
Path 8	0.089	-	0.93	Zone C1	Ambient
Path 9	0.11	-	0.0033	Zone B1	Zone A1
Path 10	0.02	-	0.0001	Zone C1	Zone B1

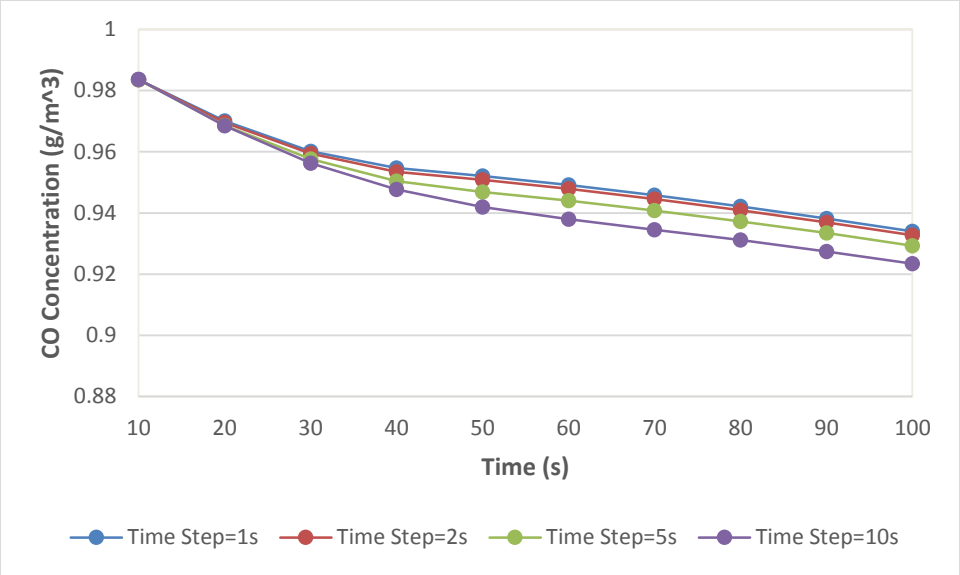

Figure 4-2 Contaminant Change in Point 1 under Different Time Steps

According to figure 4-2, carbon monoxide concentration has tiny difference between cases with 1 second of time step and 2 seconds of time step. However, with the increase of time step, concentration variations increase too. It can be found that smaller time step improves the concentration accuracy.

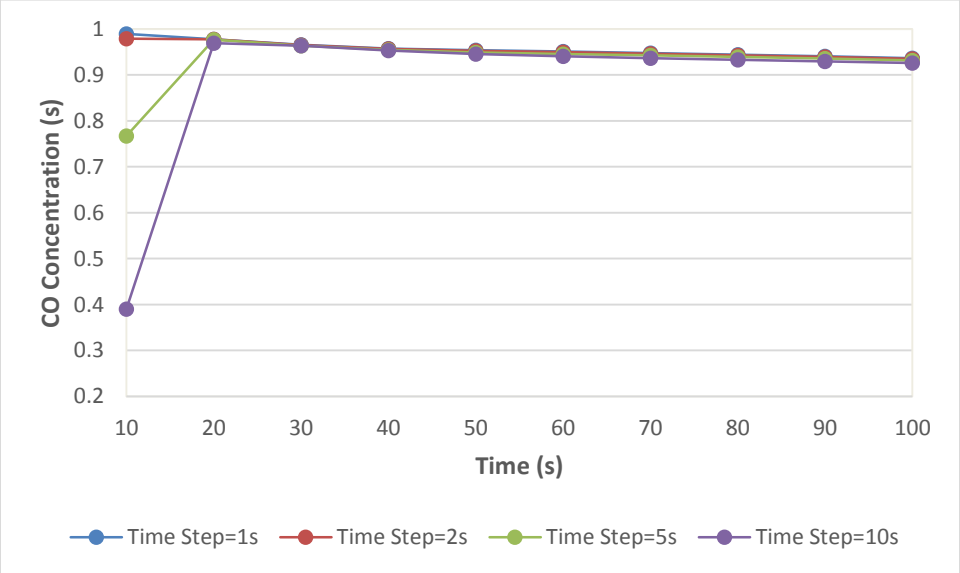

Figure 4-3 Contaminant Change in Point 2 under Different Time Steps

In figure 4-3, for the cases of 1 second time step and 2 seconds time step, contaminant concentration has very small difference. Within 20 seconds, contaminant concentration varies a lot with the increase of time step under different scenarios. Same conclusion can be drawn that the smaller the time step, the more accuracy the simulation can be improved.

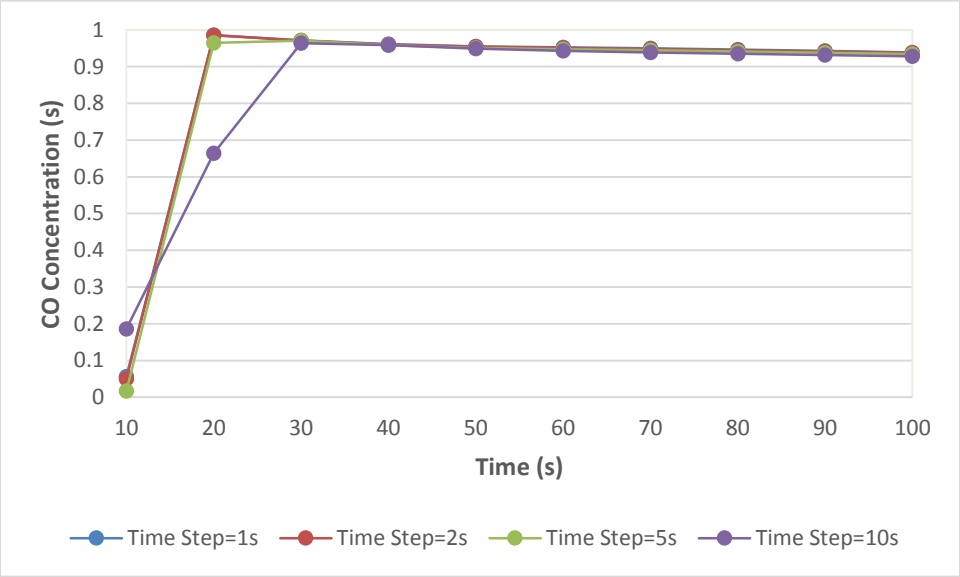

Figure 4-4 Contaminant Change in Point 3 under Different Time Steps

Figure 4-4 documents the contaminant change in point 3 under different time steps. Smaller time step improves accuracy of simulation result.

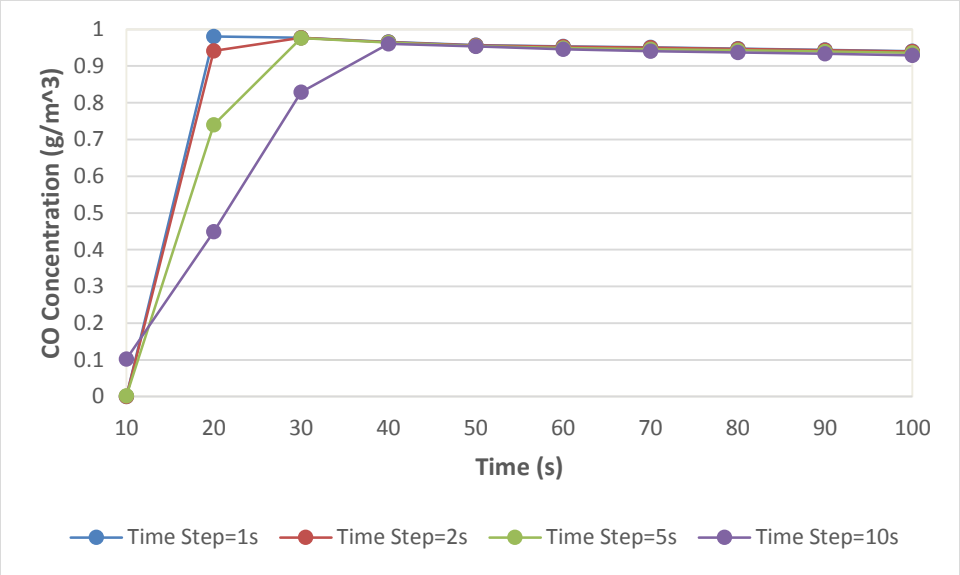

Figure 4-5 Contaminant Change in Point 4 under Different Time Steps

Figure 4-5 shows the contaminant concentration change in point 4 under different time steps after simulation starts on. With the increase of time step, simulation results under different scenarios varies. Considering small difference of simulation results between the scenario with 1 second time step and the scenario with 2 seconds time step, it can be found that smaller time step makes the simulation more accurate.

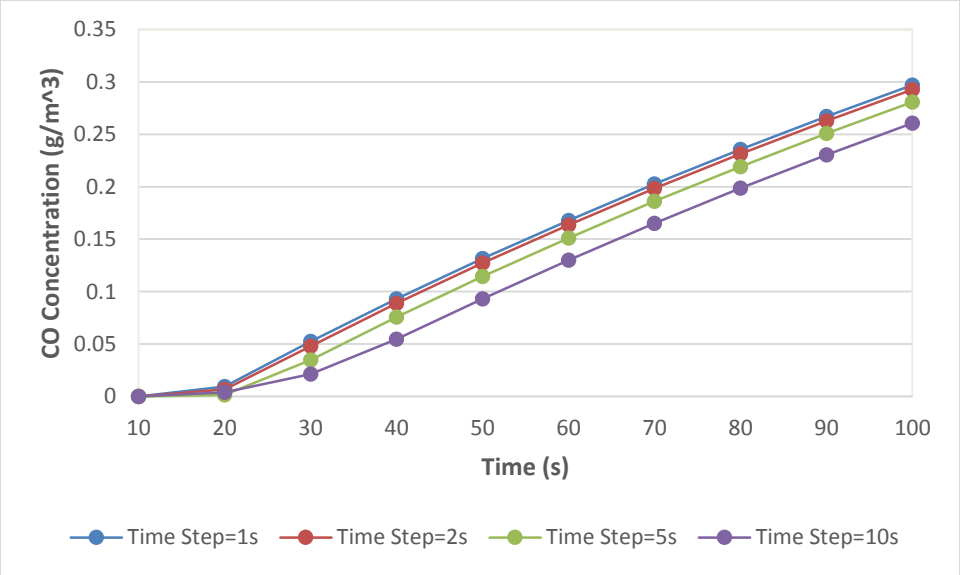

Figure 4-6 Contaminant Change in Point 5 under Different Time Steps

Figure 4-6 outlines the contaminant change in point 5 under different time steps. Figures from figure 6 to figure 9 look different from above figures. It's because point 5, point 6, point 7, and point 8 are located in return duct. It takes time for contaminant transports from contaminant source to these points and increases to a certain value. Likewise, smaller time step is also helpful for improving the accuracy.

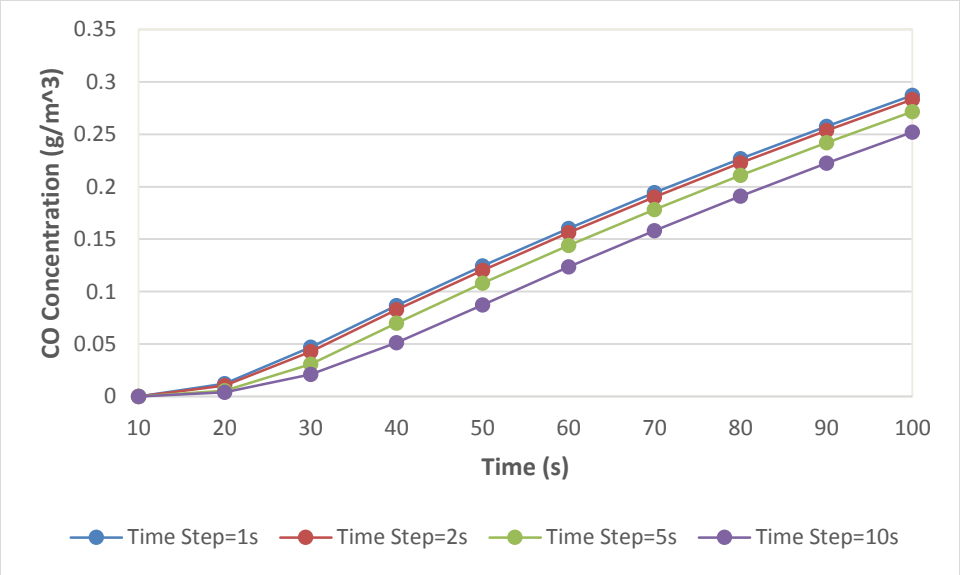

Figure 4-7 Contaminant Change in Point 6 under Different Time Steps

Figure 4-7 presents the contaminant change in point 6 under different time steps. There is tiny difference between the cases of one second time step and two seconds time step. One second time step is good enough.

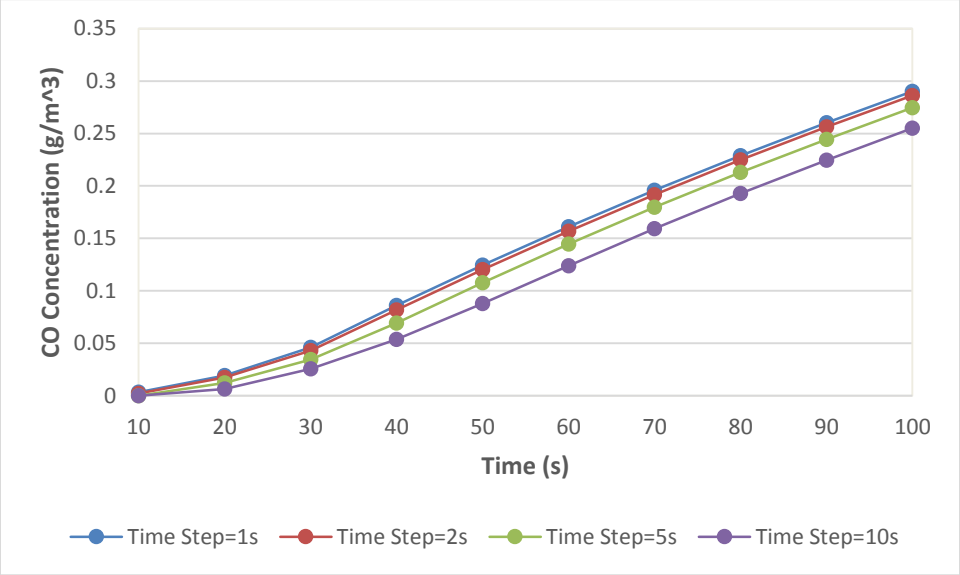

Figure 4-8 Contaminant Change in Point 7 under Different Time Steps

Figure 4-8 documents the contaminant change in point 7 under different time steps. It can be seen that smaller time step can improve the simulation accuracy.

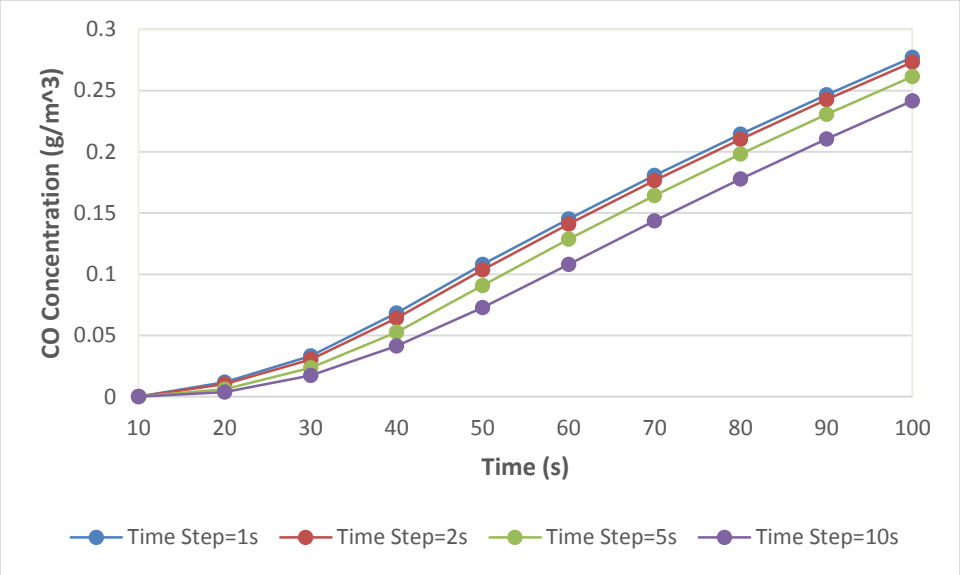

Figure 4-9 Contaminant Change in Point 8 under Different Time Steps

Figure 4-9 outlines the contaminant change in point 8 under different time steps. The contaminant concentration increases with time. Smaller time step improves the simulation accuracy.

From the above eight figures (figure 4-2 to figure 4-9), contaminant concentration under 1 second time step and 2 seconds time step have small difference. Simulation results vary a lot with the increase of time step. Smaller time step helps reduce the variations of simulation results. Using 1 second time step is good enough. Additionally, the simulation time for current CONTAM model is less than 30 seconds which is pretty fast. Even though it may take longer time for more complex CONTAM models, simulation time only has several minutes. It is much faster compared to CFD simulation. Therefore, in the later analysis of contaminant source identification, 1 second of time step was used.

4.2 Dispersion Coefficient Influence on the Contaminant Transport

As described above, the duct model is defined as one dimensional convection-diffusion model. Contaminant flow in one direction consists of a mixture of convection (the bulk movement of air), and diffusion (the mixing of the contaminant within the air). Carbon monoxide (CO), a kind of airborne contaminant, is used as an example in this research. CONTAM has the ability to simulate airborne contaminants within built structures. Algorithms of CONTAM are applicable to general airborne contaminants. Therefore, all the research results are applicable to general gas contaminants instead of only carbon monoxide.

CONTAM uses a Lagrangian model to handle high speed flows in ducts (Walton and Dols, 2013). In the Lagrangian model, air flowing at velocity of u will create a cell with a length of $u^*\Delta t$ at the inlet end of the duct segment and make the cell at x_j to move to ($x_j + u^*\Delta t$) during a time step of Δt. The length of the cell, Δx_j, namely $u^*\Delta t$, is unchanged. This process of adding cells at the inlet end of the duct and deleting cells at the outlet end handles convection process. At the same time, during that time step the contaminant will diffuse between adjacent cells due to molecular diffusion and turbulent mixing. That diffusion is solved by a standard implicit method using a tri-diagonal equation solver. When the duct velocity is low, more cells are required. One problem is if the velocity approaches zero, the number of cells approaches infinity. In order to prevent this issue happening, ContamX (CONTAM solver engine) automatically switches to the Eulerian finite volume model once $u^*\Delta t$ is less than the user specified minimum cell length (default value is 0.1 meter in the input settings).

CONTAM applies the axial dispersion coefficient in the one dimensional duct. Different equations are adopted to calculate the axial dispersion coefficient for duct with

laminar flow and turbulent flow. For laminar flow (Re<2000), the Taylor-Aris relation is adopted (Walton and Dols, 2013):

$$E = D_m + \frac{\bar{u}^2 d^2}{192 D_m}; \frac{L}{d} < 0.04 \frac{\bar{u} d}{D_m} \tag{4.1}$$

Where,

E= axial dispersion coefficient [m^2/s];

D_m= molecular diffusion coefficient [m^2/s];

u= average fluid velocity [m/s];

d= duct diameter [m];

L= length of duct [m].

While for turbulent flow, the axial dispersion coefficient E depends only on the Reynolds number:

$$\frac{E}{\bar{u} d} = \frac{3.0 \times 10^7}{\mathrm{Re}^{2.1}} + \frac{1.35}{\mathrm{Re}^{0.125}} \tag{4.2}$$

Where,

Re= Reynolds number.

A simple model with only one duct is built to study the impact of axial dispersion coefficient on the contaminant transport (see figure 4-10). The molecular diffusion coefficient (D_m) of carbon monoxide at temperature 20 ℃ and standard pressure is 2.08E-005 m^2/s. One assumption is considering the airflow temperature is 20 ℃ since temperature and pressure will affect the molecular diffusion coefficient. Based on the above equations, the molecular diffusion coefficient is used to calculate the axial dispersion coefficient in the laminar flow. However, when the molecular diffusion coefficient is set to be zero, the CONTAM model does not work. Additionally, in the turbulent flow, the axial dispersion coefficient only depends on the Reynolds number, and is calculated automatically by

CONTAM engine. Therefore, we cannot omit the axial dispersion coefficient in the CONTAM model if we study one dimensional convection diffusion duct.

Considering the above condition, I created a simple CONTAM model outlined in figure 4-10 with laminar flow, and simulated different cases by inputting different values of molecular diffusion coefficient. According to the simulation results of different cases, we can compare and analyze the impact of axial dispersion coefficient on the contaminant transport in the duct system.

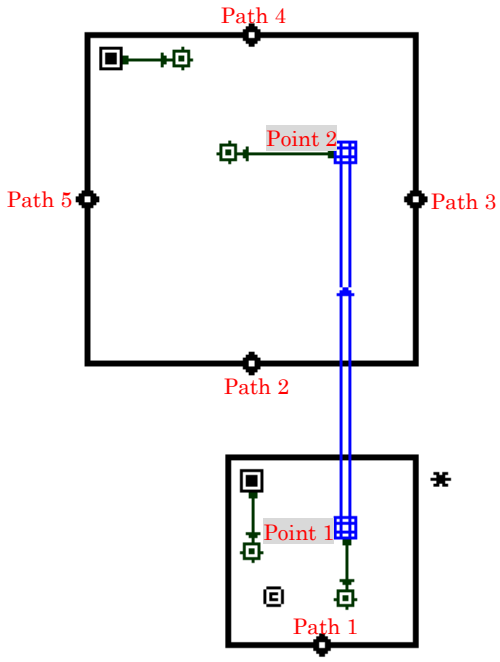

Figure 4-10 Simple Model to Study the Impact of Axial Dispersion Coefficient

In the CONTAM model of figure 4-10, the duct length is 10 meters, airflow rate in the duct is 0.0193 kg/s, duct diameter is 800mm, and airflow velocity is 0.0318 m/s. Calculated Reynolds number is 1683.7 (less than 2000). Simulation time step is the smallest one, namely 1 second. Other boundary conditions are 0.0193 kg/s and 0.0048 Pa, 0.0062 kg/s and 0.0045 Pa, 0.0062 kg/s and 0.0045 Pa, 0.0062 kg/s and 0.0045 Pa, and 0.0062 kg/s and 0.0045 Pa respectively from path 1 to path 5. Airflow paths from path 1 to

path 5 already are noted in figure 4-10. At 1:00:00AM, an instantaneous contaminant (Carbon Monoxide, CO) is released in the zone where point 1 is located. As the zone model is well-mixed zone model, contaminant concentrations in point 1 and in the source zone are same. Then the contaminant transported with the airflow and arrives at point 2. The laminar flow model is same for all cases only with difference on molecular diffusion coefficient. According to equation (1.23), various molecular diffusion coefficient (D_m) causes different axial dispersion coefficients. Simulation results are processed and documented in following figure 4-11.

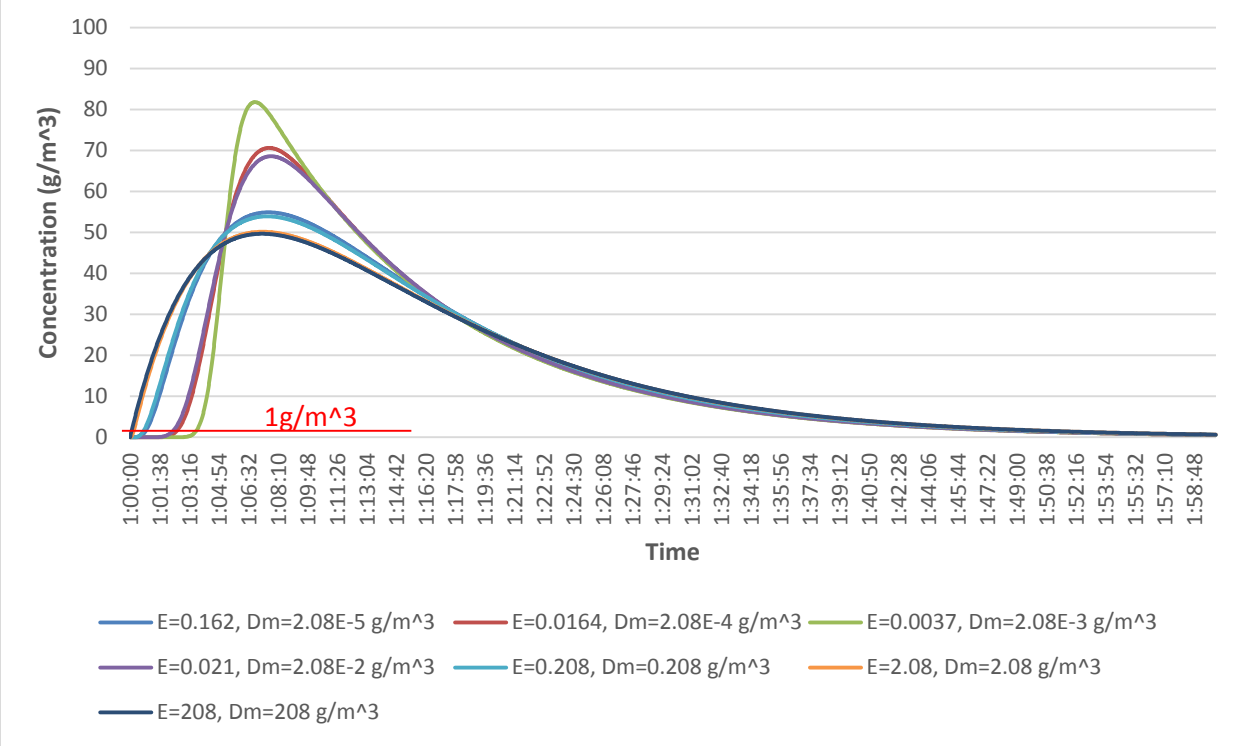

Figure 4-11 Impact of Axial Dispersion Coefficient on Contaminant Transport

Note: E is the axial dispersion coefficient while D_m is the molecular diffusion coefficient.

According to figure 4-11, contaminant will arrive at point 2 earlier as the duct axial dispersion coefficient increases. It's because diffusion contributes the mixing and spreading out of contaminant. Higher axial dispersion coefficient means higher concentration gradient

along the one direction duct which will speed the transport of contamination. The contaminant concentration in point 1 is 100 g/m^3 while the peaking contamination concentration is less than 100 g/m^3 in point 2. It's because axial dispersion coefficient contributes the contaminant transport, in which condition there are more contaminant in other area of domain. This can be also found from that the smaller the axial dispersion coefficient, the peaking concentration in point 2 is larger, and the peaking concentration point reaches more latter.

Assume that sensor in point 2 will alarm when the contamination concentration is larger than 1 g/m^3. The released time once alarming under different dispersion coefficients are shown as following table:

Table 4-0-2 Release Time Once Alarming under Different Dispersion Coefficients

E=0.0037 g/m^3	E=0.0164 g/m^3	E=0.021 g/m^3	E=0.162 g/m^3	E=0.208 g/m^3	E=2.08 g/m^3	E=208 g/m^3
214s	147s	135s	47s	40s	10s	4s

Based on this table, it can be seen that the release time once alarming reduces as the increase of duct axial dispersion coefficient. Additionally, the releasing time difference among these cases is significantly different from both the sensitivity time of contaminant sensors and time step. According to the above analysis, duct axial dispersion coefficient of contaminant transport in the duct cannot be neglected, needed to be considered instead. That's to say we need consider the duct axial dispersion coefficient in the analysis of contaminant source identification in duct network.

4.3 Verification of CONTAM Model Using Analytical Solution of One-D Advection-Dispersion Equation

In previous chapters, a simple building simulation model is built using CONTAM to study contaminant source identification in HVAC duct work. In the forward model, CONTAM is used to acquire a steady state airflow field and a forward contaminant distribution within the duct work. The forward contaminant concentration distribution within the duct work can be detected by sensor networks. Before CONTAM is applied to solve the adjoint backward probability equation in the inverse model, the forward contaminant transport equation in CONTAM needs to be verified. Like mentioned, the backward probability equation is adjoint of the forward contaminant transport equation. If CONTAM is solid to solve the forward contaminant transport equation, it can be also effective to get the solutions of the adjoint backward probability equation. In this section, the analytical solution of the forward contaminant transport equation (Advection-Dispersion Equation, ADE) and the simulation results obtained by CONTAM are compared and analyzed.

The governing forward contaminant transport equation with its initial condition and boundary conditions is given in following:

$$
\begin{aligned}
&\frac{\partial(C)}{\partial t}+\frac{\partial(\mathrm{uC})}{\partial x}=\frac{\partial}{\partial x}\left(\beta\frac{\partial C}{\partial x}\right)+Q_{\text{source}}\\
&C\left(\vec{x},0\right)=C_0\left(\vec{x}\right)\\
&C\left(\vec{x},\ \mathrm{t}\right)=g_1(t)\\
&\beta\frac{\partial C}{\partial x}=g_2(t)\\
&\mathrm{uC}-\beta\frac{\partial \mathrm{C}}{\partial x}=g_3(t)
\end{aligned}
\tag{4.3}
$$

Where, $\frac{\partial C}{\partial t}$ is the transient term; $\frac{\partial (uC)}{\partial x}$ is convection term; $\frac{\partial}{\partial x}\left(\beta \frac{\partial C}{\partial x}\right)$ is the dispersion term; Q_{source} is the source term. C is the contaminant concentration (volume-averaged); u is the velocity of airflow; ß is the dispersion coefficient; $C_0\left(\vec{x}\right)$ is the initial condition at arbitrary location $\vec{x}$; $g_1(t), g_2(t), g_3(t)$ are three types of boundaries, which in this thesis were called first-type boundary condition, second-type boundary condition, and third-type boundary condition, respectively.

In the first step, a simple CONTAM model is built to obtain the simulation result. A complex duct network is not selected to study the verification because it's very complicated to solve contaminant transport equations for a complex duct network. It makes sense that if this single duct can be verified to solve contaminant distribution, the solver engine of CONTAM should also work for the duct network. The simple CONTAM model is sketched in the following figure 4-12.

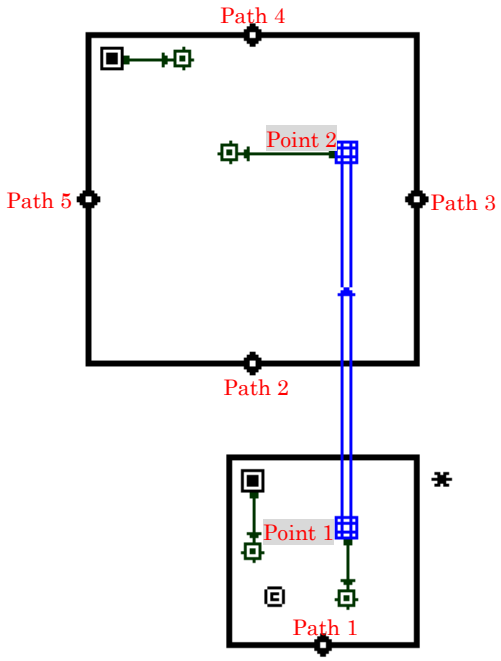

Figure 4-12 Simple CONTAM Comparison Model

In the CONTAM comparison model, there are two zones, and one duct with two terminal points (point 1 and point 2, shown in figure 4-12). A constantly released contaminant source (Carbon Monoxide, CO) with a mass of 1000 PPM is released in the zone where point 1 locates, and a sensor is put in point 2 to detect the contaminant concentration change in point 2. The length of this duct is 100 meters and duct airflow velocity is 1.56 m/s. Time step is 1 second. Airflow is turbulent flow and the calculated dispersion coefficient is 0.27 m^2/s. Other boundary conditions in path 1, path 2, path 3, path 4, and path 5 are 0.24 kg/s and 0.71 Pa, 0.008 kg/s and 0.67 Pa, 0.076 kg/s and 0.67 Pa, 0.076 kg/s and 0.67 Pa, 0.076 kg/s and 0.67 Pa, respectively. Airflow paths from path 1 to path 5 are noted in figure 4-12. After the model is set up, the simulation is run to get the contaminant change in point 2.

In the second step, the analytical solution of governing contaminant transport equation is deduced by hand. The deducing process is complex which is described and explained in detail in Appendix C. The analytical solution is obtained as follows:

$$C(x,t) = C_0 * A(x,t)$$
$$A(x,t) = 0.5 * erfc\left[\frac{x-ut}{2\sqrt{Et}}\right] + 0.5 * \exp\left(\frac{ux}{E}\right) erfc\left(\frac{x+ut}{2\sqrt{Et}}\right) + 0.5 * \left[2 + \frac{u(2L-x)}{E} + \frac{u^2 t}{E}\right] \quad (4.4)$$
$$\exp\left(\frac{uL}{E}\right) erfc\left(\frac{2L-x+ut}{2\sqrt{Et}}\right) - \sqrt{\frac{u^2 t}{\pi E}} \exp\left[\frac{uL}{E} - \frac{1}{4Et}(2L-x+ut)^2\right]$$

Where, u is airflow velocity in the duct, C_0 is the initial contaminant concentration; E is the dispersion coefficient; L is the length of duct; x is arbitrary location along the duct; t is time. All of the parameters have same value with those settings in CONTAM model to compare the simulation result and analytical solution. This equation can be solved to get the contaminant change with time in point 2.

In the above equation, erfc(x) is the complementary error function. When solving this equation, it's necessary to use the 1-erf(x) function to replace erfc(x) for greater accuracy when erfc(x) is close to 1. Likewise, 1-erf(x) function can be used to replace erfc(x) when erfc(x) is close to 0 (Mathworks, 2015). Except this method, erfc(x) can also be solved by using an approximation way. When $0 \leq x < \infty$, erfc(x) can be replaced using the following equation approximately (Abramowitz and Stegun, 1972):

$$
\begin{aligned}
&erfc(x) = \left(a_1 t + a_2 t^2 + a_3 t^3\right) e^{-x^2} + \varepsilon(x) \\
&\left|\varepsilon(x)\right| \le 2.5 \times 10^{-5} \\
&t = \frac{1}{1 + px} \\
&p = 0.47047 \\
&a_1 = 0.34802 \\
&a_2 = 0.09587 \\
&a_3 = 0.74785
\end{aligned}
\tag{4.5}
$$

In this research, erfc(x) is solved using the first approximation method. According to the above description, the analytical solutions can be solved using Matlab to get the contaminant change in point 2. Finally the analytical solution is compared with the simulation result which is documented in the following figure 4-13 in detail.

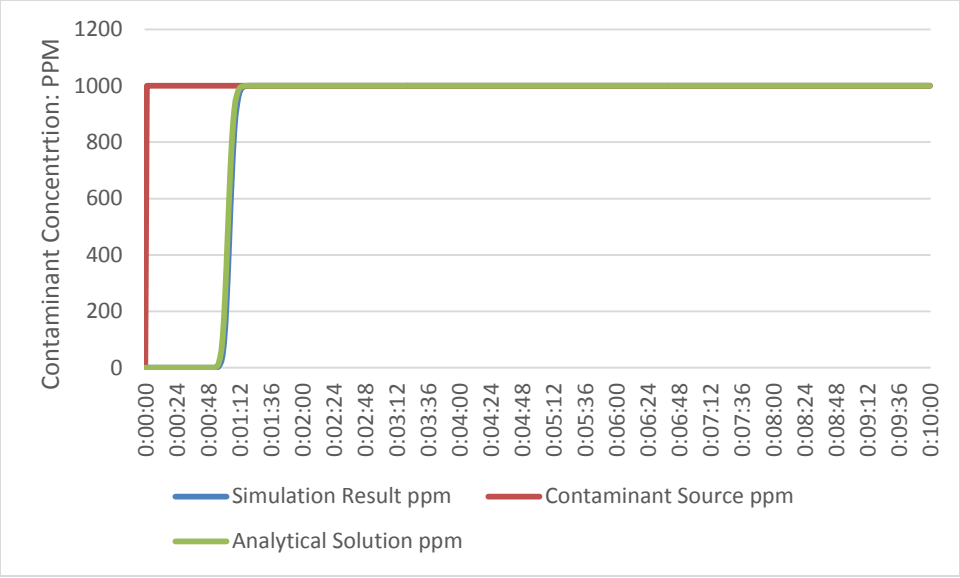

Figure 4-13 Comparison between Simulation Result and Analytical Solution

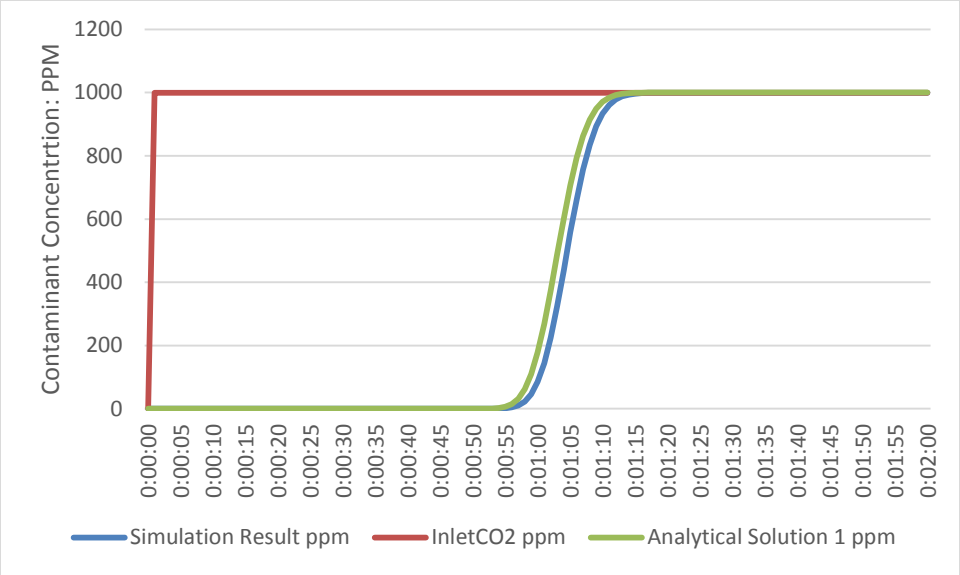

Figure 4-14 Comparison between Simulation Result and Analytical Solution (Zoomed Figure 4-13)

In figure 4-13 and figure 4-14, the time it takes for point 2 to getting a contaminant concentration larger than 1 PPM is 55 seconds and 54 sections in simulation result and analysis solution, respectively. The time difference is tiny, just one time step.

According to figure 4-13 and figure 4-14, the conclusions can be drawn as follows:

(1) Contaminant change in point 2 has a time delay. It's reasonable since it takes time for contaminant reaching point 2 after contaminant source was released at point 1. Contaminant concentration in point 2 will be same as concentration of source after releasing a given time. It is because the contaminant source at point 1 is constantly released.

(2) It is found that the simulation result and analytical solution are similar and have the same variation tendency along with time. It indicates that CONTAM is solid in solving the forward contaminant transport equation. On this basis, CONTAM model can be employed to solve the adjoint backward probability equation.

4.4 Assumptions of Forward Model

In the above equations (3.11) and (3.12), the integral in the denominator ensures that the total probability of all the cells is one. The numerator values for all the cells in the domain should be calculated and added together which is considered as the denominator. It is certified that the total probability in the whole network is one. But the problem is that in current version of CONTAM tool, we can only obtain the simulated contaminant concentrations in the junctions and terminals of duct while we cannot get the data inside the duct. In order to study the effectiveness of the adjoint probability methodology in the application of contaminant source identification in duct system, it's presumed that the contaminant source is located among the eight points (see figure 4-1). Additionally, note that the calculated results using the above two equations (equation 3.11 and equation 3.12) are backward location probability density. In order to get the backward location probability, the cell size in each point should be considered. Under the above assumption, the total probability of the eight points is one. Of course, in practice, the total probability of the eight points should be less than one since there are still contaminant concentration distribution in other areas of this domain. However, because of the limit of CONTAM, I only considered relative largeness of probability. It doesn't matter with what denominator is used since all numerators are divided or normalized by the same denominator. On the base of above assumption, contaminant source identification among the eight points is studied. Figure 4-1 gives a simple building model used to study the identification of contaminant source information.

The eight points are duct junctions where we can obtain contaminant concentration changes through control signals. It is assumed that the contaminant source is among the

eight points. In the forward model, contaminant source is in point 1 while sensor 1 and sensor 2 are where two sensors are located respectively. Contaminant source is released from point 1, and two sensors are adopted to track the contaminant change in the sampling locations. Additionally, in the inverse model, contaminant source with a unit mass is released in a certain sensor location.

On the other hand, in current version of CONTAM duct cannot be a contaminant source. To study the application of contaminant source in HVAC system, a fake zone is created to connect a certain point which is considered as contaminant source. Contaminant is put into the fake zone directly. In the proposed model, the point connected to fake zone is assumed as contaminant source.

Chapter 5 Contaminant Source Location Identification of an Instantaneous Point Source

Under the fundamental of above methodology description and assumptions, a simple example is started to identify an instantaneous point source location. In the first step of testing the application of adjoint backward probability method, an instantaneous point source transport fate in HVAC duct work is studied. An instantaneous contaminant is released in the HVAC duct work through the fake zone and then transported along the duct with airflow. This chapter focuses on the instantaneous point source location identification with given source release time and given source release mass.

After building the CONTAM model and verifying the effectiveness of CONTAM model, the CONTAM building model is used to study contaminant source identification using the adjoint backward probability methodology. In this research, a simple CONTAM model is applied as shown in figure 5-1.

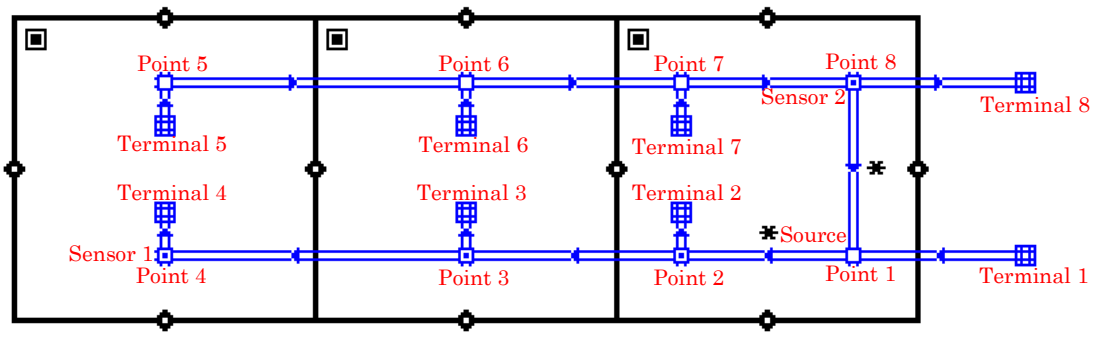

Figure 5-1 A Simple Building CONTAM Model Used to Identify the Contaminant Source Information

In figure 5-1, there are three zones (called zone A1, zone B1 and zone C1 from left to right) connected with airflow paths and detailed duct work. In this duct work, eight junctions (from point 1 to point 8) and eight terminals (from terminal 1 to terminal 8) are noted with red characters. Based on the assumption in the above chapter, potential source location will be identified in the eight points (point 1, point 2, … , point 8). The HVAC system (duct work) supplies air into zones and return air from zones to guarantee a good indoor air quality. A contaminant (carbon monoxide) is released in point 1 through the fake zone, which assumes point 1 is contaminant source location in the forward model. Two sensors (sensor 1 and sensor 2) are placed in point 4 and point 8 respectively to detect contaminant change in these two points. An instantaneous contaminant source with a mass of 1000 g was released in the fake zone connected to point 1 at 1:00:00AM. Boundary conditions of forward model for the three zones are shown in following table 5-1.

Table 5-0-1 Boundary Conditions of Forward Model

Airflow Paths	Airflow Rate	Velocity	Pressure Change	Airflow Direction	
	kg/s	m/s	Pa	From	To
Ventilation Duct	1.34	3.54	1.16	Ambient	Terminal 1
Exhaust Duct	0.5	1.32	0.16	Terminal 8	Ambient
Path 1	0.089	-	0.93	Zone C1	Ambient
Path 2	0.089	-	0.93	Zone C1	Ambient
Path 3	0.089	-	0.93	Zone B1	Ambient
Path 4	0.089	-	0.93	Zone A1	Ambient
Path 5	0.089	-	0.93	Zone A1	Ambient
Path 6	0.089	-	0.93	Zone A1	Ambient
Path 7	0.089	-	0.93	Zone B1	Ambient
Path 8	0.089	-	0.93	Zone C1	Ambient
Path 9	0.11	-	0.0033	Zone B1	Zone A1

Path 10	0.02	-	0.0001	Zone C1	Zone B1

According to the three types of sensor networks (alarm sensor network, current concentration recording sensor network, and historical concentration recording sensor network), the study flow chart is sketched to display how contaminant source location can be identified for an instantaneous point source.

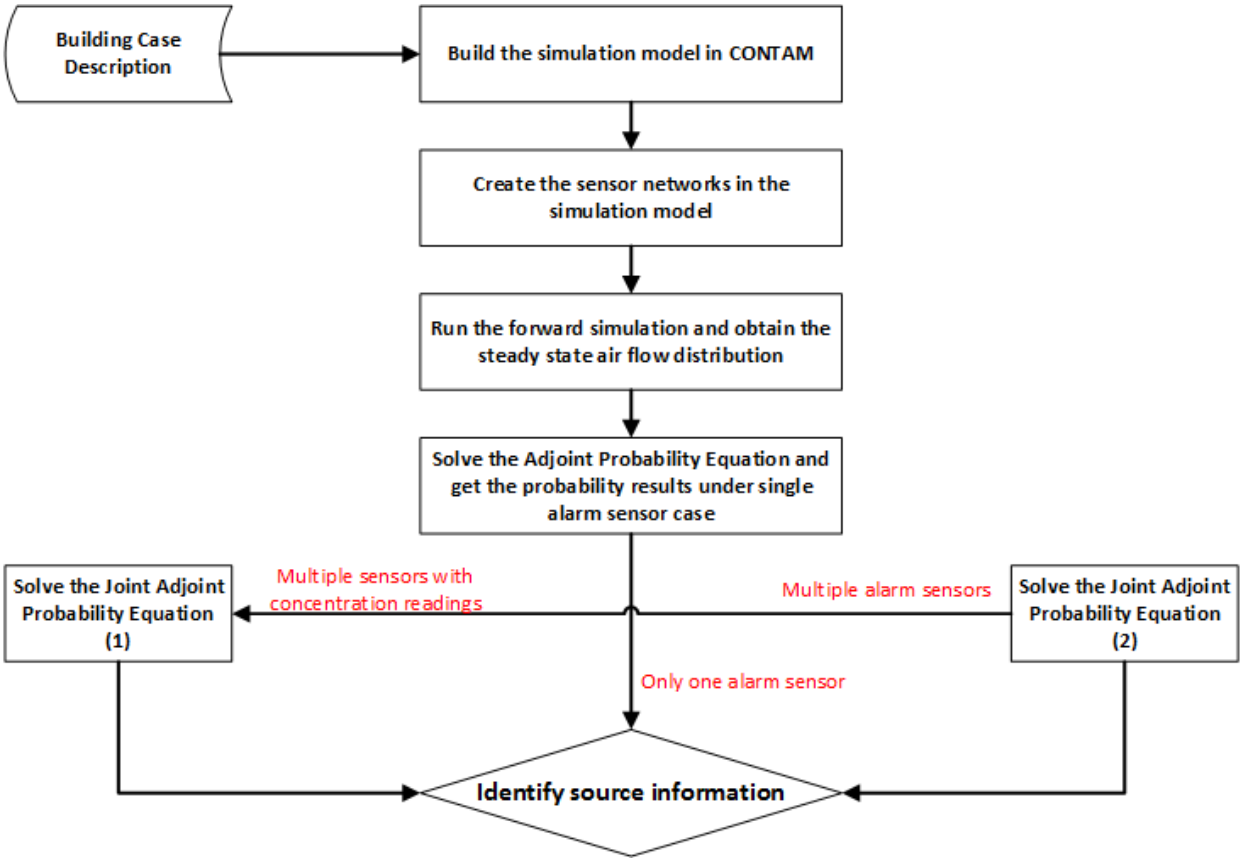

Figure 5-2 Flow Chart of Contaminant Source Identification under an Instantaneous Case

According to the figure 5-2, the whole process is described in detail in the following steps:

(1) Build simulation model. Based on the building case description, a real building can be idealized and developed into a CONTAM model.

(2) Sensor networks. Three types of sensor networks can be built to identify source location. It's necessary to study the effectiveness of sensor network and determine which kind of sensor network should be used.

(3) Run forward simulation. Forward simulation is run to get a steady state airflow field and forward contaminant concentration distribution.

(4) Solve adjoint backward probability equation to obtain the adjoint backward probability. The adjoint backward probability equation under a single alarm sensor case is solved to get the adjoint backward probability $f_x\left(\overrightarrow{x_0};\tau_0,\overrightarrow{x_{mk}},\tau_{mk}\right)$.

(5) Identifying source location based on sensor networks. All of the above four steps are basic for identifying contaminant source information. In this step, based on sensor networks specification, various backward probability equations are applied to calculate the backward probability. If there is only one alarm sensor, the adjoint backward location probability acquired in step (4) can be used directly to identify source location. If there are multiple alarm sensors, the backward location probability can be calculated using the equation (3.11). If there are multiple sensors with concentration recording, the backward location probability can be obtained using the equation (3.12).

In this case study, an instantaneous contaminant source (Carbon Monoxide, CO) is released in point 1 through the fake zone at time 1:00:00 AM. Then the contaminant is transported along the duct network. After releasing some time, sensor 1 and sensor 2 detecte the contaminant concentration in point 4 and point 8, respectively. Through

running the forward simulation, a forward airflow field is acquired which is shown in figure 5-3. In figure 5-3, green lines and red lines are the airflow and pressure for each airflow paths, respectively. Red lines are short because the pressure changes are small.

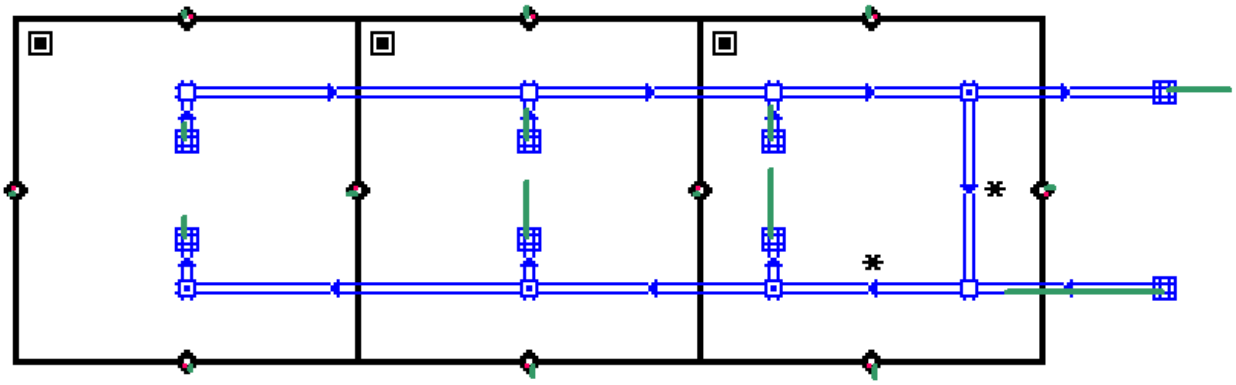

Figure 5-3 CONTAM Building Model and Predicted Airflow Field

On the base of steady state airflow field, the forward contaminant distribution is acquired. According to sensor 1 and sensor 2, contaminant change in point 4 and point 8 are documented in the following figure 5-4, which shows the contaminant change in point 4 and point 8 after the release of the instantaneous contaminant source at point 1 (CO). According to figure 5-4, the contaminant concentration detected by sensor 1 is higher than that detected by sensor 2. It makes sense since sensor 1 is located in the supply duct, which is closer to the contaminant source than sensor 2. Contaminant is transported to sensor 1 first and then to sensor 2. Comparing the contaminant change in the four points (source location, point 3, sensor 1, and sensor 2), there is a time delay. This is reasonable since contaminant transport with airflow takes time reaching from one point to another point.

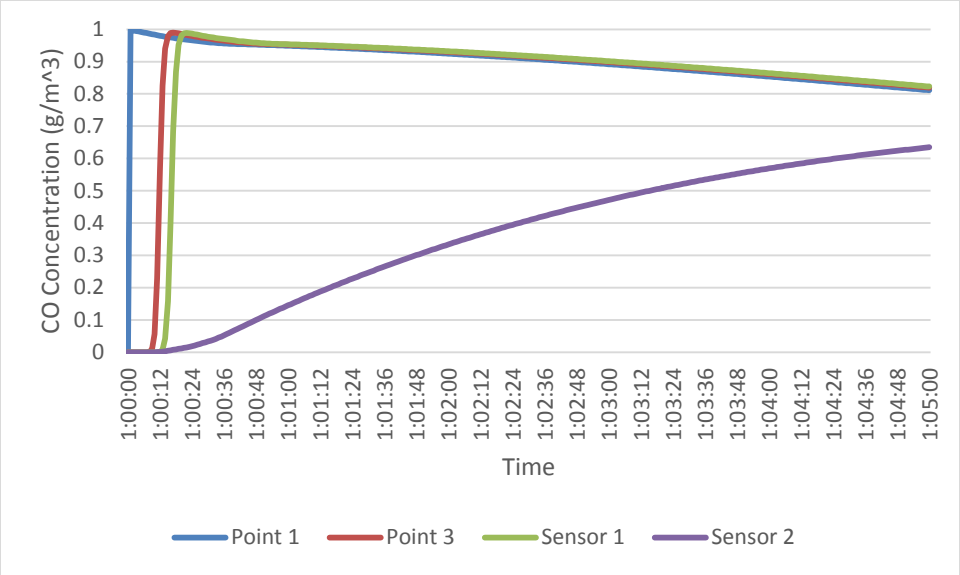

Figure 5-4 Predicted Contaminant Change in the Sensor Locations

After studying the contaminant transport fate in the forward model, the building CONTAM model is adopted to identify the contaminant source location with given source release time and given source release mass in the following section. According to the sensor networks, eight kinds of sensor detection information is shown in table 5-2.

Table 5-0-2 Scenarios Analysis of Sensor Networks in One-D Duct Model

Sensor Scenarios	Concentration Recording Type	Sensors	Number of Measurements	Recordings (g/m^3)
Scenario 1	Alarm sensor	Sensor 1	1	Alarm at 14s
Scenario 2	Alarm sensor	Sensor 1, Sensor 2	2	Sensor 1: alarm at 14s; Sensor 2: alarm at 18s
Scenario 3	Current concentration recording	Sensor 1	1	0.042 g/m^3 at 14s

Scenario 4	Current concentration recording	Sensor 1, Sensor 2	2	Sensor 1: 0.042 g/m^3 at 14s; Sensor 2: 0 g/m^3 at 14s
Scenario 5	Historical concentration recording	Sensor 1	2	0.042 g/m^3 at 14s; 0.99 g/m^3 at 24s
Scenario 6	Historical concentration recording	Sensor 1, Sensor 2	4	Sensor 1: 0.042 g/m^3 at 14s, 0.99 g/m^3 at 24s; Sensor 2: 0 g/m^3 at 14s, 0.019 g/m^3 at 24s
Scenario 7	Historical concentration recording	Sensor 1	3	0.042 g/m^3 at 14s; 0.99 g/m^3 at 24s; 0.97 g/m^3 at 34s
Scenario 8	Historical concentration recording	Sensor 1	4	0.042 g/m^3 at 14s; 0.99 g/m^3 at 24s; 0.97 g/m^3 at 34s; 0.96 g/m^3 at 44s

In the above sensor network table 5-2, the concentration threshold of sensor is 0.009 g/m^3. As we know, once the concentration detected by sensor is higher than 0.009 g/m^3, the alarm sensor will alarm. In the forward model, it's known that after releasing the contaminant source with 14 seconds, the alarm sensor 1 detects a concentration value higher than 0.009 g/m^3 and then alarms. It takes alarm sensor 2 about 18 seconds to detect a concentration higher than 0.009 g/m^3. For the sensor with current concentration recording, it records the contaminant concentration when it alarms. For the sensor with historical concentration recording, the contaminant concentrations in different time are recorded. Sensor with historical concentration recording can provide contaminant

concentration change in historical times. The detected information are then applied to identify contaminant source information.

As described in the thesis, the first-type boundary condition of adjoint equation is still the first-type boundary condition in the forward equation; the second-type boundary condition of adjoint equation becomes the third-type boundary condition in the forward equation; the third-type boundary condition of adjoint equation becomes the second-type boundary condition in the forward equation. According to this guidance, boundary conditions was changed in the inverse model. However, based on the deduced adjoint backward probability equation for the well-mixed zone, there are no special boundary conditions (second type boundary conditions and third type boundary conditions), with only initial condition instead. In the forward model, the boundary conditions associated with the well-mixed zones are airflow rate and pressure. So in the inverse model, airflow path connecting the zones and airflow path connecting the zones and ambient was reversed without changing their absolute values.

For the one dimensional convection-diffusion duct model, this is different since we have to consider the boundary conditions in the duct. In the forward model, contaminant is released at the inlet end of duct. As described above, CONTAM applies Lagrangian model in high velocity airflows and Eulerian finite volume model in low velocity airflows to simulate the contaminant transport in duct. However, the cell at the outlet end of the duct segment will not necessarily have an edge at $x = L$ (the duct length is L) in which case an interpolation is necessary to compute the concentration at $x = L$, which becomes the input concentration to the next duct segment downstream. When two or more duct segments merge at a junction the contaminant concentration at the junction is the flow-weighted average of the concentrations at the end of each incoming duct. The boundary conditions in

the duct is still the first type boundary conditions. Therefore, in the inverse model, the airflow direction in the duct is reversed.

Above all, in the inverse model, all the airflow paths in the CONTAM model are reversed without changing their absolute values. An instantaneous contaminant source with unit mass is released in two sensor locations specifically. In the case of contaminant source location identification, the boundary condition of forward model and backward model are documented in table 5-1 and table 5-3.

Table 5-0-3 Boundary Conditions of Backward Model

Airflow Paths	Airflow Rate	Velocity	Pressure Change	Airflow Direction	
	kg/s	m/s	Pa	From	To
Ventilation Inlet	-1.34	-3.54	-1.16	Terminal 1	Ambient
Exhaust Outlet	-0.5	-1.32	-0.16	Ambient	Terminal 8
Path 1	-0.089	-	-0.93	Ambient	Zone C1
Path 2	-0.089	-	-0.93	Ambient	Zone C1
Path 3	-0.089	-	-0.93	Ambient	Zone B1
Path 4	-0.089	-	-0.93	Ambient	Zone A1
Path 5	-0.089	-	-0.93	Ambient	Zone A1
Path 6	-0.089	-	-0.93	Ambient	Zone A1
Path 7	-0.089	-	-0.93	Ambient	Zone B1
Path 8	-0.089	-	-0.93	Ambient	Zone C1
Path 9	-0.11	-	-0.0033	Zone A1	Zone B1
Path 10	-0.02	-	-0.0001	Zone B1	Zone C1

Note: negative values indicate different airflow and pressure change direction with the forward model. After reversing the airflow field, the ventilation inlet of forward model becomes outlet and the exhaust outlet of forward model becomes inlet, respectively.

According to the flow chart in figure 5-2, the backward location probabilities are calculated for each point under the eight sensing scenarios. The results are sketched in the following figure 5-5. Among the eight points, a point with the highest backward location probabilities may be the actual contaminant source location.

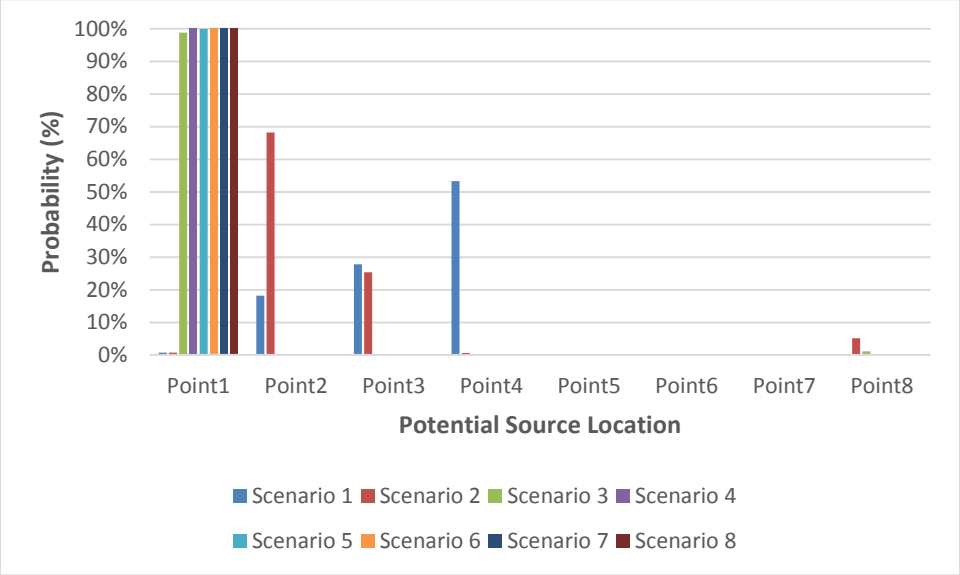

Figure 5-5 Predicted Source Location Probabilities with Given Source Release Time and Source Release Mass

In figure 5-5, except scenario 1 and scenario 2, the remaining scenarios identify source location in point 1 well. Scenario 1 and scenario 2 identify a source location in point 4 and point 2 respectively. The conclusions come to as follows:

(1) Alarm sensor(s) may not identify source location accurately; with alarm-only sensors, it is always predicted that the source location is in a location upstream to it. This is because alarm sensors didn't give much information for the contaminant source identification. In this case of identifying an instantaneous source location, source mass and source release time were given and known. However, in future

research, under the case without knowing any information, alarm sensor network maybe less effective in the identification of contaminant source information.

(2) According to scenario 3, 5, 7, and 8, or scenario 4 and scenario 6, adding more measurements can improve the identification accuracy since more measurements can provide more information.

(3) Based on scenario 3 and scenario 4, or scenario 5 and scenario 6, adding additional sensor can improve the identification accuracy even though sensor can only detect very low concentration. Additional sensors can provide more information for the backward model.

(4) One concentration reading seems sufficient for proper identification of contaminant source location; and more contaminant information will improve the prediction accuracy. In later research, proper sensor locations are studied.

As described above, one dimensional convection-dispersion duct model is adopted to study the contaminant transport mechanic and the contaminant source location identification. Well-mixed zonal duct model is different from one dimensional convection-dispersion duct model. The junction, under the well-mixed assumption, has half the volume of each of the adjacent duct segments. This section documents the comparisons of one-dimensional convection diffusion duct model and well-mixed zonal model.

Same CONTAM model and sensor networks as above model presented in figure 5-1. Boundary conditions are identical with those shown in table 5-1 and table 5-3. An instantaneous contaminant with a mass of 1000 g was released in the fake zone connected t point 1 at 1:00:00AM. The only difference between the two models are that duct in previous model uses one dimensional model while this model applies well-mixed zonal model. Figure

5-4 and figure 5-6 sketch the forward model simulation results of two models. According to figure 5-4 and figure 5-6, differences are as follows:

1) In the one dimensional duct model, there are obvious time delay along the duct.
2) In figure 5-6, contaminant concentration in point 1 increases to maximum slowly while under one dimensional duct model, after releasing the instantaneous source, contaminant concentration in point 1 reaches maximum with one time step (1 second) and then reduces gradually. After releasing the contaminant in source location, contaminant concentration change in point 1 should be like figure 5-4. Additionally, in practical HVAC system, contaminant transport in duct should have time delay. Therefore, it was suggested that using one dimensional duct model to study contaminant source location identification.

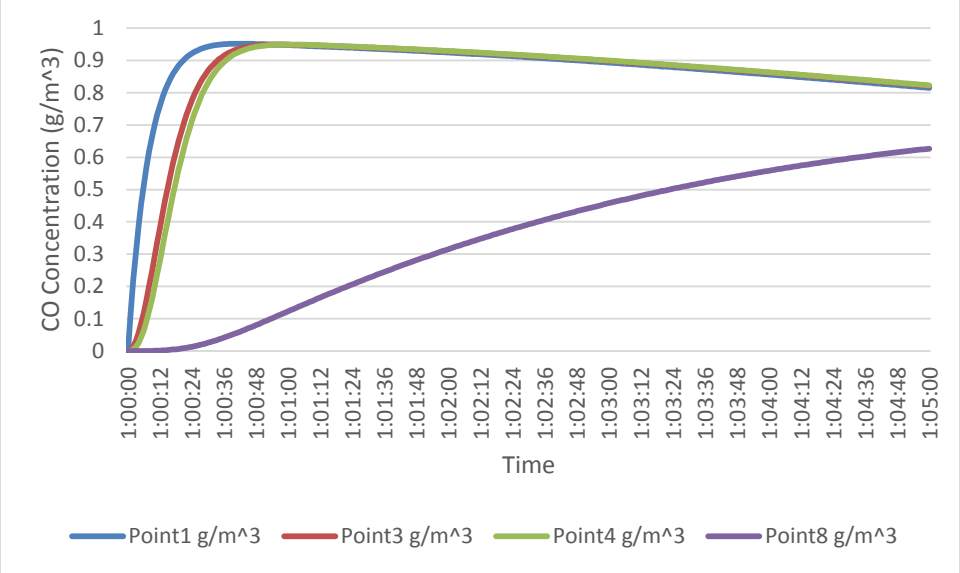

Figure 5-6 Forward Simulation Results under Well-Mixed Zonal Model

Then the airflow field is reversed without changing any absolute values to obtain a backward airflow field and backward model. An instantaneous contaminant source with unit mass is released in two sensor locations respectively. Using adjoint backward

probability equation, equation (3.11), and equation (3.12), probabilities of each scenarios are calculated. According to the forward simulation results, sensor networks of eight scenarios in zonal duct model were presented in following table 5-4. It's similar with table 5-2 with only difference in sensor recordings. Likewise, the sensor threshold is 0.009 g/m^3. Release time and release source mass were known.

Table 5-0-4 Scenario Analysis of Sensor Networks in Well-mixed Zonal Duct Model

Sensor Scenarios	Concentration Recording Type	Sensors	Number of Measurements	Recordings (g/m^3)
Scenario 1	Alarm sensor	Sensor 1	1	Alarm at 3s
Scenario 2	Alarm sensor	Sensor 1, Sensor 2	2	Sensor 1: alarm at 3s; Sensor 2: alarm at 22s
Scenario 3	Current concentration recording	Sensor 1	1	0.0127 g/m^3 at 3s
Scenario 4	Current concentration recording	Sensor 1, Sensor 2	2	Sensor 1: 0.0127 g/m^3 at 3s; Sensor 2: 0 g/m^3 at 3s
Scenario 5	Historical concentration recording	Sensor 1	2	0.0127 g/m^3 at 3s; 0.32 g/m^3 at 13s
Scenario 6	Historical concentration recording	Sensor 1, Sensor 2	4	Sensor 1: 0.0127 g/m^3 at 3s, 0.32 g/m^3 at 13s; Sensor 2: 0 g/m^3 at 3s, 0 g/m^3 at 13s
Scenario 7	Historical concentration recording	Sensor 1	3	0.0127 g/m^3 at 3s; 0.32 g/m^3 at 13s; 0.69 g/m^3 at 23s
Scenario 8	Historical concentration recording	Sensor 1	4	0.0127 g/m^3 at 3s; 0.32 g/m^3 at 13s; 0.69

	g/m^3 at 23s; 0.87 g/m^3 at 33s

Figure 5-5 and figure 5-7 indicates the source location identification analysis of eight scenarios in the one-dimensional duct and well-mixed zonal duct model, respectively. According to figure 5-5, scenario 3, 4, 5, 6, 7, and scenario 8 can identify the source location in point 1 accurately. It's because more measurements and adding extra sensors can improve the identification accuracy largely.

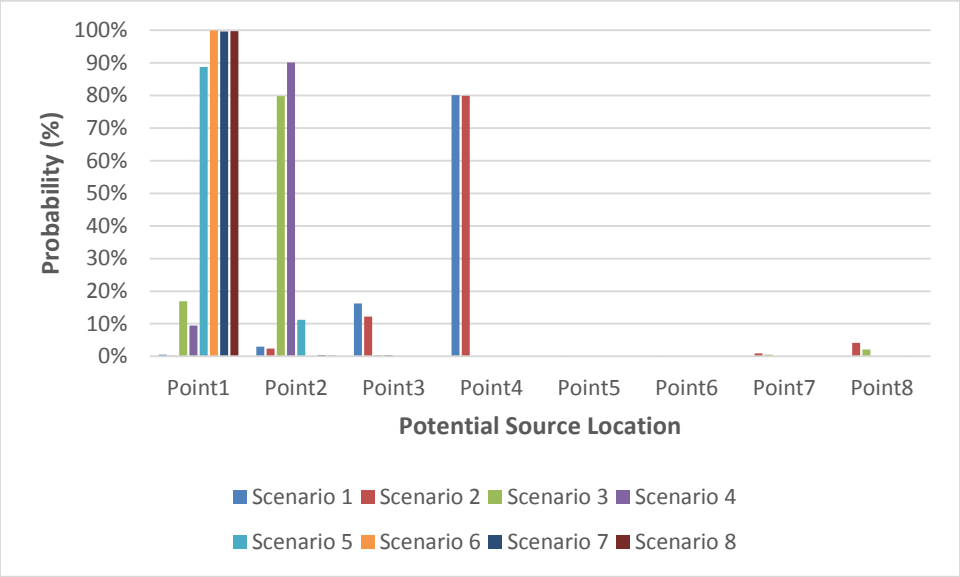

Figure 5-7 Contaminant Source Identification under Well-mixed Zonal Model

According to figure 5-7, only scenario 5, 6, 7, and scenario 8 can identify the contaminant source location in point 1 accurately. Compared to the one dimensional duct model, in well-mixed zonal duct model, scenario 3 and scenario 4 with current concentration recording cannot identify the source location in point 1. It is because in one dimensional duct model, each duct is divided into many cells and the simulated contaminant concentration is more accurate. In well-mixed zonal duct model, each junction

has half the volume of each of the adjacent duct segments, causing that the simulated contaminant concentration is rough. However, in both one-dimensional duct model and well-mixed zonal duct model, adding more sensors and doing more measurements help improve the accuracy of source location identification. Considering sensors are expensive and the demand of fast identification, number of sensors and locations would be researched in later sections.

This section states identification of an instantaneous contaminant source location with given source release time and source release mass using the adjoint probability methodology. Forward model and backward model were built in CONTAM. One-dimensional duct model and well-mixed zonal duct model are applied into the CONTAM model respectively. It's found that adding more sensors and doing more measurements help improve the accuracy of source location identification. Additionally, one-dimensional duct model should be applied instead of well-mixed zonal duct model.

Chapter 6 Sensitivity Analysis of Critical Parameters

Even though HVAC system and other input parameters were designed using standard or code, input parameters may be still different from practical situations. Sensitivity analysis is necessary for these critical parameters. This chapter documents the sensitivity analysis of several critical input parameters, including measurement error, duct velocity, sensor location, and sensor types.

6.1. Sensitivity Analysis of Measurement Error

In numerical simulation, sensor measurement is recorded as exact value. However, as described above, in practical conditions sensor measurement is inexact which has measurement error instead. Measurement error cannot be neglected because it will affect the predicted contaminant source information. This section mainly presents the sensitivity analysis on measurement error using scenario 3 (case with single current concentration recording sensor) in the application of instantaneous source location identification (chapter 5). It will also provide a guidance about how much accurate sensors are helpful in the practical engineering applications.

A same model as the model used in the application of an instantaneous contaminant source location identification (chapter 5) was used to study the sensitivity analysis of measurement error. Boundary conditions were same too. The only difference was sensor measurement error values. The sensor measurement error studied in this research is standard deviation of normal distribution, namely parameter σ in equation (3.13). Eleven

cases with different measurement error values were studied, including cases with different measurement errors of sensors (0.01% error, 0.05% error, 0.1% error, 1% error, 5% error, 10% error, 20% error, 40% error, 60% error, 80% error, and 100% error). The eleven measurement errors (standard deviations σ) were substituted into equation (3.12) to recalculate the backward location probabilities for the eight points respectively. Calculation results were documented in table 6-1 and sketched in figure 6-1. In table 6-1, under each of the eleven measure errors (from 0.01% to 100% error), backward location probabilities were calculated for the eight points. According to above assumption, contaminant source location were assumed in the eight points. Similarly, backward location probabilities in table 6-1 were sketched in figure 6-1 to show the comparison results more clearly.

Table 6-0-1 Backward Location Probabilities of Eight Points under Different Sensor Measurement Errors

Error	Point1	Point2	Point3	Point4	Point5	Point6	Point7	Point8
0.01% σ	100.00%	0%	0%	0%	0%	0%	0%	0%
0.05% σ	100.00%	0%	0%	0%	0%	0%	0%	0%
0.1% σ	100.00%	0%	0%	0%	0%	0%	0%	0%
1% σ	100.00%	0%	0%	0%	0%	0%	0%	0%
5% σ	99.11%	0%	0%	0%	0%	0%	0%	0.89%
10% σ	98.85%	0%	0%	0%	0%	0%	0%	1.15%
20% σ	98.76%	0%	0%	0%	0%	0%	0%	1.22%
40% σ	42.07%	55.89%	1.52%	0%	0%	0%	0%	0.53%
60% σ	10.78%	71.00%	18.08%	0%	0%	0%	0%	0%
80% σ	5.25%	60.46%	33.70%	0.53%	0%	0%	0%	0%
100% σ	3.45%	51.55%	41.29%	3.66%	0%	0%	0%	0%

Note: σ is standard deviation.

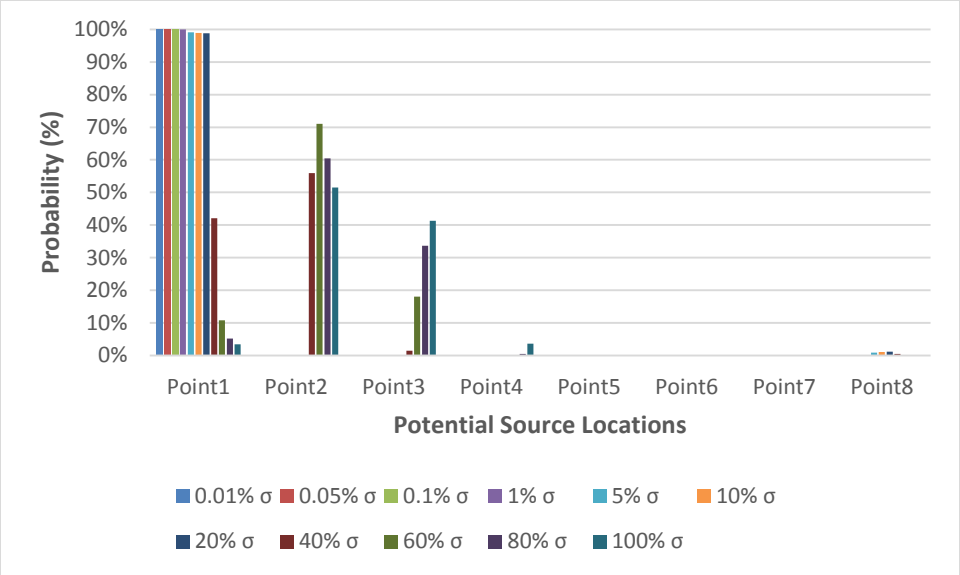

Figure 6-1 Sensitivity Analysis on Measurement Error

According to figure 6-1 and table 6-1, high accuracy sensor can improve the identification accuracy of contaminant source location. As the increase of measurement error, it may not identify the contaminant source location. This makes sense because sensor with large measurement error cannot collect accurate data. When the measurement error is infinitely small, which means that there is no difference between the simulated concentration and the measured value, this algorithm (equation 3.12) is not be able to give any prediction. Therefore, appropriately increasing the measurement error is necessary for the method to give correct prediction. 10% of measurement error will be used for later research.

Additionally, the critical point of sensor measurement error from right to wrong prediction needs to be found out. The following section documents the critical point of sensor measurement error. Same method of data process was conducted as previous analysis. The calculation results were shown in table 6-2 and sketched in figure 6-2.

Table 6-0-2 Critical Point Analysis of Sensor Measurement Error

Error	Point1	Point2	Point3	Point4	Point5	Point6	Point7	Point8
35% σ	63.82%	35.10%	0%	0%	0%	0%	0%	0.80%
37% σ	54.32%	44.39%	0.61%	0%	0%	0%	0%	0.68%
38% σ	49.93%	48.59%	0.85%	0%	0%	0%	0%	0.63%
39% σ	45.84%	52.43%	1.15%	0%	0%	0%	0%	0.58%
40% σ	42.07%	55.89%	1.52%	0%	0%	0%	0%	0.53%

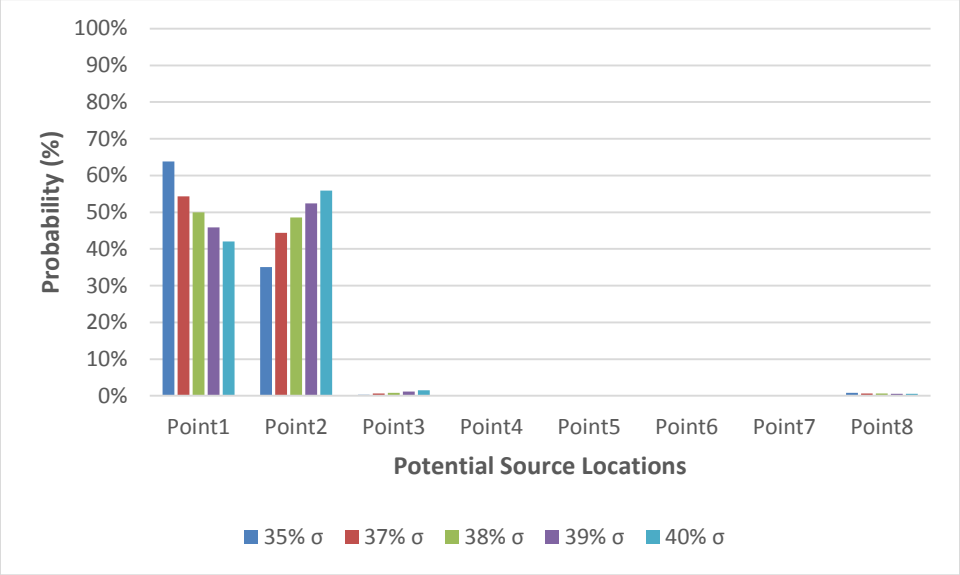

Figure 6-2 Critical Point Analysis of Sensor Measurement Error

In table 6-2 and figure 6-2, it was found that starting from 39% of sensor measurement error (standard deviation), the case with single current concentration recording sensor cannot identify the instantaneous contaminant source location correctly. Therefore, the critical point of sensor measurement error from right to wrong prediction is 38%.

6.2. Sensitivity Analysis of Duct Velocity

This section documents sensitivity analysis on duct velocity under different scenarios, including case with single current concentration recording sensor, case with two current concentration recording sensors, case with single historical concentration recording sensor, and case with two historical concentration recording sensors. In the CONTAM model, duct velocities were calculated based on mechanical system design. However, they may be quite different from the true duct velocity values in practical HVAC system which will cause the predicted source information using the inverse algorithm deviates from the actual source conditions. Therefore, it's necessary to study sensitivity analysis on duct velocity.

Same CONTAM model as the model used in the application of an instantaneous contaminant source location identification was applied. Boundary conditions and sensor networks were same too. 10% of sensor measurement error was used. The only difference was the duct velocity. The change of duct velocity was realized by varying the airflow rate of AHU (air handler unit). Design case (shown in chapter 5) was the base case. Velocities in base case were assumed as V_{0i} (i is duct segment number corresponding to duct number in base case, 1,2,3…). Eight cases with various duct velocities were studied and analyzed (10% V_{0i}, 25% V_{0i}, 50% V_{0i}, 75% V_{0i}, 125% V_{0i}, 150% V_{0i}, 175% V_{0i}, and 200% V_{0i}). Equation (3.12) was applied to calculate backward location probabilities for the eight points in each scenario. In the use of equation (3.12) for sensitivity analysis of duct velocity, same sensor recordings as shown in table 5-2 were applied. In the sensitivity analysis duct velocity, duct velocity affects f_x in equation (3.12) which is backward location probability in the case with single alarm sensor. Therefore, varying duct velocity only changes f_x in equation (3.12).

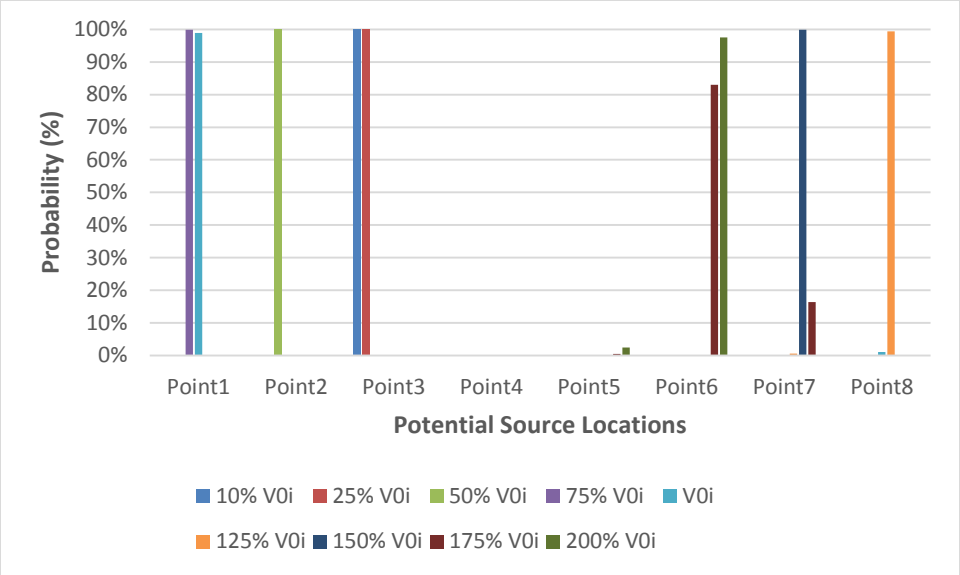

Figure 6-3 Sensitivity Analysis on Duct Velocity for the Case with Single Current Concentration Sensor

Figure 6-3 indicates sensitivity analysis on duct velocity for the case with single current concentration sensor. Only the design case and case with 75% of design case velocity can predict the source location well. Although there is a 25% difference from the design case velocity, it can still predict well the source location. This is because the velocity difference doesn't affect much the inverse contaminant transport.

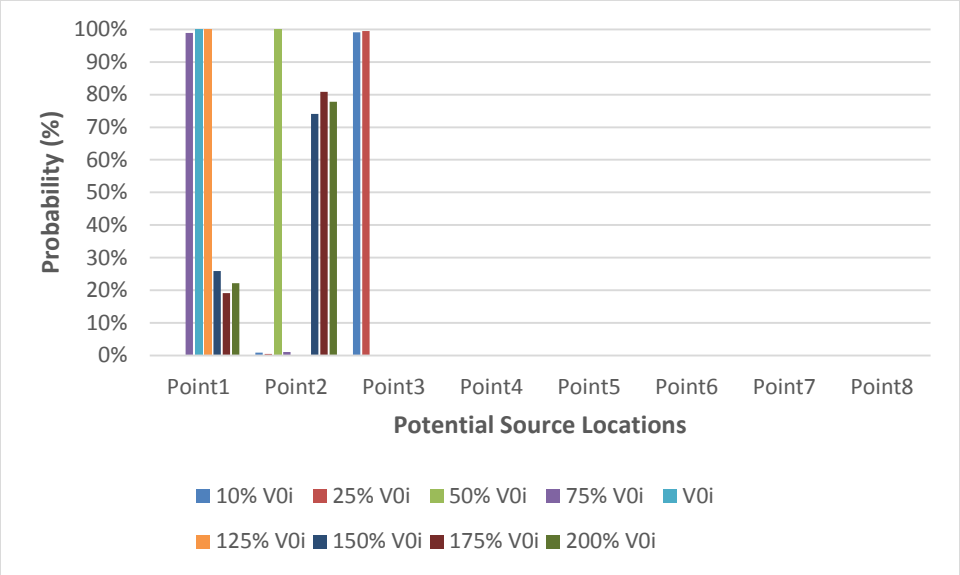

Figure 6-4 Sensitivity Analysis on Duct Velocity under Two Current Concentration Sensors

Compared to figure 6-3, when using two current concentration sensors, the case with 125% of design case velocity can also predict the source location well. Adding another sensor can improve the accuracy of identification.

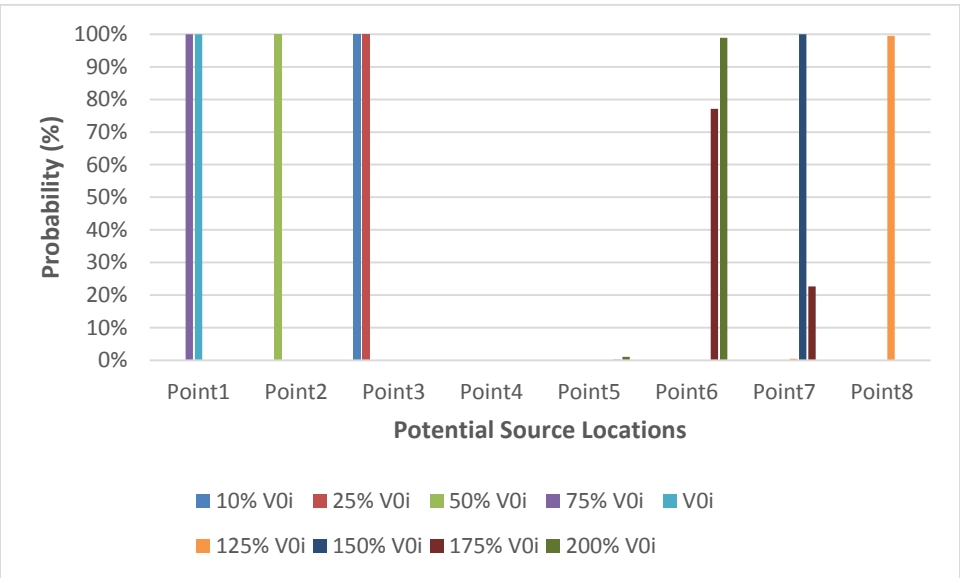

Figure 6-5 Sensitivity Analysis on Duct Velocity under Single Historical Concentration Sensor

In figure 6-5, sensitivity analysis on duct velocity under single historical concentration sensor was documented. Same conclusion with what figure 6-3 indicates, only the design case and the case with 75% of design case velocity can trace back the source location accurately. However, compared to the case with single current concentration sensor, additional measurement improves the accuracy of contaminant source location identification in this case.

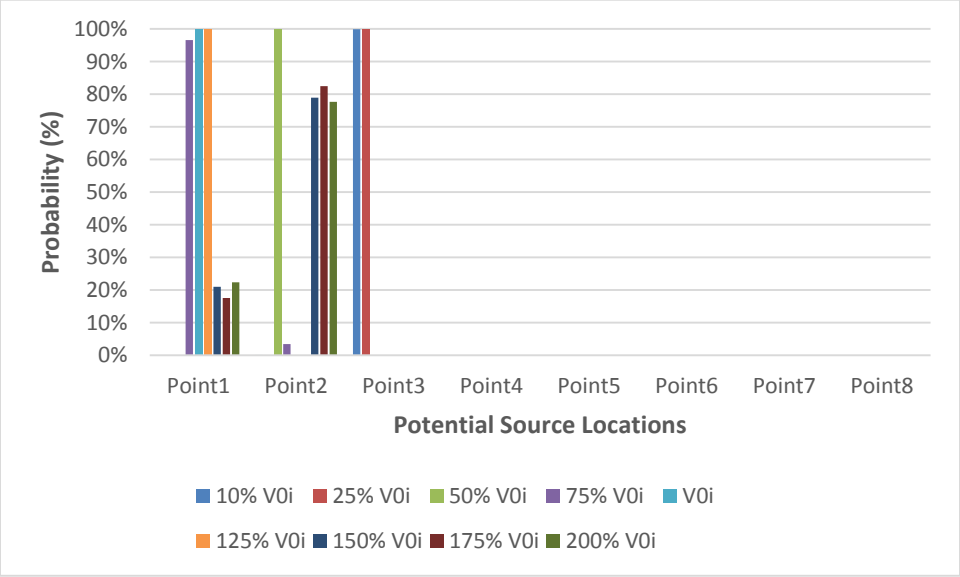

Figure 6-6 Sensitivity Analysis on Duct Velocity under Two Historical Concentration Sensors

According to figure 6-6, three cases can identify source location accurately, including the design case, the case with 75% of design case velocity, and the case with 125% of design case velocity.

Based on above analysis, conclusions about the sensitivity analysis of duct velocity can be summarized as follows:

1) In the case with single current concentration sensor, when the velocity is 75% of design case, it still can identify the source location accurately.
2) In the case with two current concentration sensors, when the velocity is 75% and 1.25 of design case, this scenario still can identify the source location accurately. Adding another sensor can improve the accuracy of source location identification.
3) In the case with single historical concentration sensor, the result is same as that in case with single current concentration sensor.
4) In the case with two historical concentration sensors, the result is same as that in case with two current concentration sensors.

It was found that under case with two sensors, even though the duct velocity has at least 25% of difference, it can still identify the source location accurately. The critical point of velocity difference from right to wrong prediction needs to be identified. Considering that the case with two historical concentration recording sensors can always identify contaminant source location with given source release time and source release mass, this case was used to identify the critical point of velocity difference from right to wrong prediction. When practical duct velocity is smaller than the velocity of base case, backward location probabilities for eight points in each scenario were shown in table 6-3 and sketched in figure 6-7.

Table 6-0-3 Critical Point Analysis when Practical Velocity Less Than That of Base Case

Velocity	Point1	Point2	Point3	Point4	Point5	Point6	Point7	Point8
50% V_{0i}	0%	100.00%	0%	0%	0%	0%	0%	0%
70% V_{0i}	0%	100.00%	0%	0%	0%	0%	0%	0%
72% V_{0i}	0%	99.99%	0%	0%	0%	0%	0%	0%
74% V_{0i}	23.71%	76.29%	0%	0%	0%	0%	0%	0%
75% V_{0i}	99.97%	0%	0%	0%	0%	0%	0%	0%

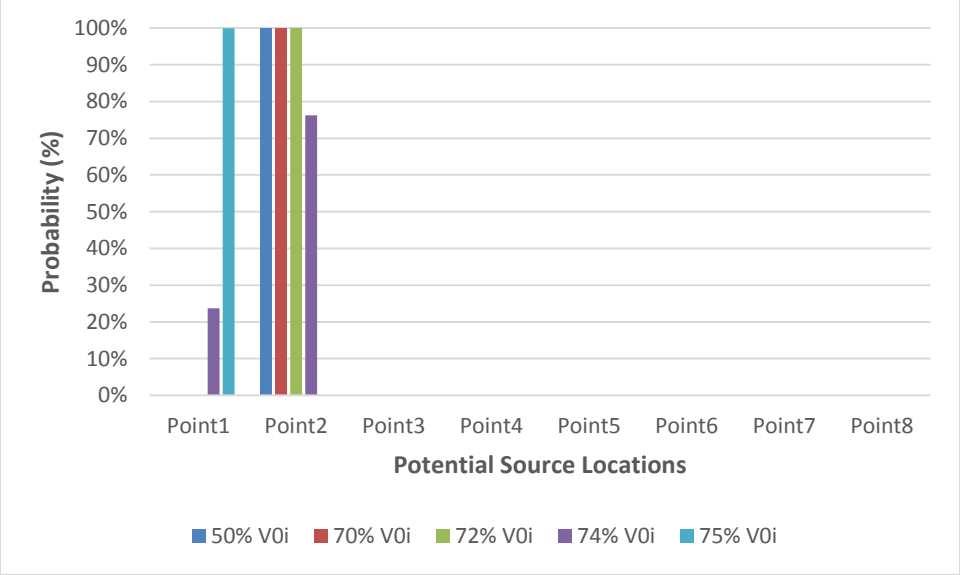

Figure 6-7 Critical Point Analysis when Practical Velocity Less Than That of Base Case

In table 6-3 and figure 6-7, it was found when practical velocity is less than 75% of base case velocity, the identified source location shifts from point 1 to point 2 and then point 3 (shown in figure 6-6). It makes sense because in the sensitivity analysis of duct velocity, velocity only affects fx in equation (3.12), which means velocity only has influence on inverse model. Sensor 1 was put in point 4. When velocity is much smaller than velocity of base case, in the inverse model contaminant doesn't have

chance to transport to point 1 within same time as recorded in base case. Therefore, a much closer location to point 4 can be identified as source location. The conclusions came to as follows:

1) The critical point of velocity from right to wrong prediction is 75% V_{0i}.
2) When the practical velocity is [-25%, 0] different from velocity of base case, contaminant source location still can be identified.

When practical velocity is larger than that of base case, backward location probabilities for eight points in each case were documented in table 6-4 and sketched in figure 6-8.

Table 6-0-4 Critical Point Analysis When Practical Velocity Larger Than That of Base Case

Velocity	Point1	Point2	Point3	Point4	Point5	Point6	Point7	Point8
140% V_{0i}	81.62%	18.38%	0%	0%	0%	0%	0%	0%
143% V_{0i}	57.54%	42.46%	0%	0%	0%	0%	0%	0%
144% V_{0i}	49.58%	50.42%	0%	0%	0%	0%	0%	0%
145% V_{0i}	42.48%	57.52%	0%	0%	0%	0%	0%	0%
150% V_{0i}	21.04%	78.96%	0%	0%	0%	0%	0%	0%

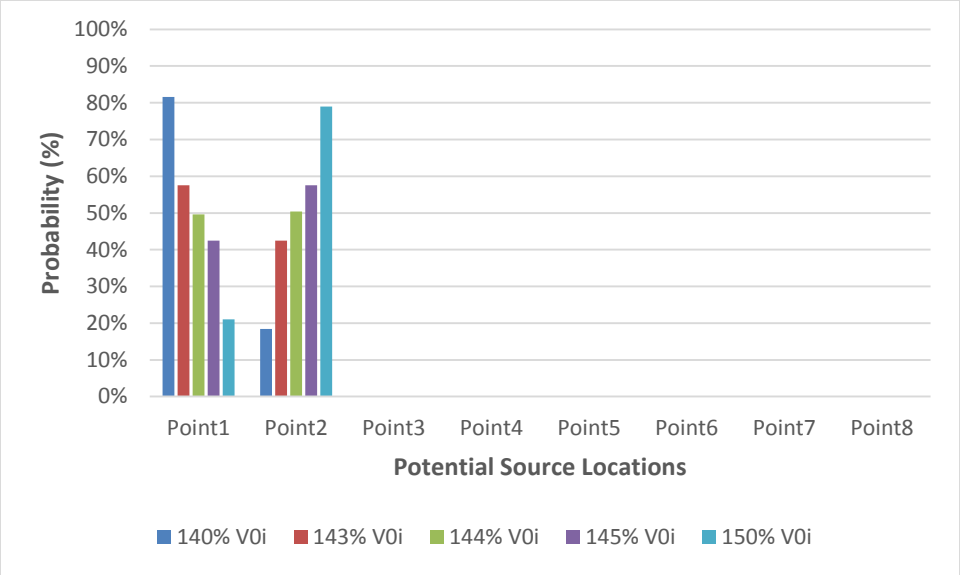

Figure 6-8 Critical Point Analysis When Practical Velocity Larger Than That of Base Case

In table 6-4 and figure 6-8, starting from 144% V_{0i}, point 2 was predicted as the contaminant source location instead of point 1. It makes sense because contaminant with a higher velocity can transport to the whole duct network much more quickly. However, the contaminant source is an instantaneous source released within only one time step (one second). When the velocity is much larger than velocity of base case, contaminant may transport to further point than point 1 within the same time recorded in base case. It will affect the accuracy of instantaneous contaminant source location identification. The conclusions were drawn as follows:

1) The critical point from right to wrong prediction is 143% V_{0i}.
2) When the velocity is [0, 43%] different from velocity of base case, accurate instantaneous contaminant source location still can be identified.

3) Combined with above analysis, when the velocity has a difference of [-25%, 43%] from that of base case, the instantaneous contaminant source location still can be identified properly.

6.3. Sensitivity Analysis of Sensor Locations and Source Locations

This section mainly documents what kind of sensor (alarm sensor, sensor with current concentration recording, or sensor with historical concentration recording) should be used, and where sensor(s) should be placed in the duct network. Same model as the model used in the identification of an instantaneous contaminant source (chapter 5) was adopted. Boundary conditions are same too. The only difference is source location and sensor locations. Based on above assumptions, in this CONTAM model, contaminant source is presumed to be among the eight points. In order to study the sensitivity analysis on sensor location, following steps were conducted:

1) Change the contaminant source location one by one among the eight points (from point 1 to point 8).
2) For each source location, change the sensor location based on sensor networks. If there is a single sensor, totally eight cases are studied. If there are two sensors, the different combinations are analyzed.

An example when the source location assumed in point 1 is shown in following table 6-5 and table 6-6. Table 6-5 indicates the scenarios with single sensor and table 6-6 documents the scenario combinations with two sensors. Under single sensor cases, cases with single current concentration recording sensor and single historical concentration recording sensor were analyzed. Under two-sensor cases, cases with two current

concentration recording sensors and two historical concentration recording sensors were studied.

Table 6-0-5 Cases to be studied with a Single Sensor (Source in Point 1)

Scenarios	Sensor Location
Scenario 1	Point 2
Scenario 2	Point 3
Scenario 3	Point 4
Scenario 4	Point 5
Scenario 5	Point 6
Scenario 6	Point 7
Scenario 7	Point 8

Table 6-0-6 Cases to be studied with Two Sensors (Source in Point 1)

Sensor Locations	Scenarios	Sensor Locations
Located in Supply Duct	Scenario 1	Point 2, Point 3
	Scenario 2	Point 2, Point 4
	Scenario 3	Point 3, Point 4
Located in Return Duct	Scenario 4	Point 5, Point 6
	Scenario 5	Point 5, Point 7
	Scenario 6	Point 5, Point 8
	Scenario 7	Point 6, Point 7
	Scenario 8	Point 6, Point 8
	Scenario 9	Point 7, Point 8
One in Supply Duct and One in Return Duct	Scenario 10	Point 2, Point 5
	Scenario 11	Point 2, Point 6
	Scenario 12	Point 2, Point 7
	Scenario 13	Point 2, Point 8

	Scenario 14	Point 3, Point 5
	Scenario 15	Point 3, Point 6
	Scenario 16	Point 3, Point 7
	Scenario 17	Point 3, Point 8
	Scenario 18	Point 4, Point 5
	Scenario 19	Point 4, Point 6
	Scenario 20	Point 4, Point 7
	Scenario 21	Point 4, Point 8

3) Study the contaminant source location identification for all these cases in order to test the proper sensor types and sensor locations.

There are tons of cases studied for the sensitivity analysis of sensor locations. All the analysis results were presented in detail in the Appendix D. The conclusion came to that two sensors with historical concentration recording are necessary: one sensor should be in point 8 (in the return duct), and the other one should be placed in the supply duct. This conclusion will be used for future research.

Chapter 7 Contaminant Source Location Identification for Single Dynamic Source

7.1. Theoretic Background

The source location identification for single instantaneous contaminant source was studied in the previous chapter 5. Additionally, contaminant source can also release contaminant continuously, such as the Volatile Organic Compound (VOC) from wall, or intermittently, like smoking and fire. These types of contaminant sources are defined as dynamic source compared to the instantaneous source in this research. Volatile Organic Compound (VOC) can also be a kind of potential pollute source in HVAC duct system. This chapter was focused on the contaminant source location identification in HVAC duct work for single dynamic source. A same CONTAM building model as the CONTAM model in the identification of an instantaneous contaminant source location (chapter 5) was still employed. Two dynamic source cases were studied, one is for a single constant release source while the other case is for a decaying source.

The dynamic source is different from instantaneous source in that after a dynamic source is released, the contaminant concentration in each point of the domain would be affected by the released source at each time step. Consequently, the concentration detected by sensors is a combination of concentrations resulted from the dynamic source at each time step. Similarly, the backward location probability equation under single alarm sensor for dynamic sources needs to be derived, which is expressed as $fd_x\left(\overrightarrow{x_0};\tau_0,\overrightarrow{x_{mk}},\tau_{mk}\right)$. It is

defined as the ratio of the resident concentration (volume-averaged) and the initially released mass at first second.

Assume that dynamic contaminant has been released at least eight seconds, which can be considered that the contaminant source was released in each second continuously. The dynamic source can be considered a combination of several instantaneous sources, including an instantaneous source releasing a contaminant mass in the 1st second, an instantaneous source releasing a contaminant mass in the 2nd second, an instantaneous source releasing a contaminant mass in the 3rd second, …, an instantaneous releasing a contaminant mass in the 8th second.

The dynamic source release mass follows the equation as following (Liu, 2008):

$$\frac{dM(t)}{dt} = M_0 \cdot h(t) \tag{7.1}$$

Where, M_0 is the initially released mass in the 1st second; h (t) is the ratio of released source mass after the 1st second and the initially released source mass in 1st second. According to this equation, when a constant contaminant source is released, h (t) should be equal to one.

Figure 7-1 from Dr. Liu's PhD thesis is a good example in below to describe in detail how the dynamic source affect the concentration distribution. Dr. Liu assumed that all the measurement were made at 4s. The released dynamic no later than 4s will add concentration in the measured location at t=4s. According to figure 7-1, an instantaneous source with a mass of $dM(t=1s)$ was released at time t=1s, transported for 3s, and then produced a concentration of $dM(t=1s)\cdot f_x(\overrightarrow{x_0}; t=3s, \overrightarrow{x_m})$ in the measured locations; an

instantaneous source with a mass of $dM\left(t=2s\right)$ was released at time t=2s, transported for 2s, and then produced a concentration of $dM\left(t=2s\right)\cdot f_x\left(\overrightarrow{x_0};t=2s,\overrightarrow{x_m}\right)$ in the measured locations; an instantaneous with a mass of $dM\left(t=3s\right)$ was released at time t=3s, transported for 1s, and then produced a concentration of $dM\left(t=3s\right)\cdot f_x\left(\overrightarrow{x_0};t=1s,\overrightarrow{x_m}\right)$ in the measured locations; an instantaneous with a mass of $dM\left(t=4s\right)$ was released at time t=4s, and then produced a concentration of $dM\left(t=4s\right)\cdot f_x\left(\overrightarrow{x_0};t=0s,\overrightarrow{x_m}\right)$ instantly in the measured locations. Therefore, the measured concentration is a combined influence of dynamic sources in each second no later than the measured time.

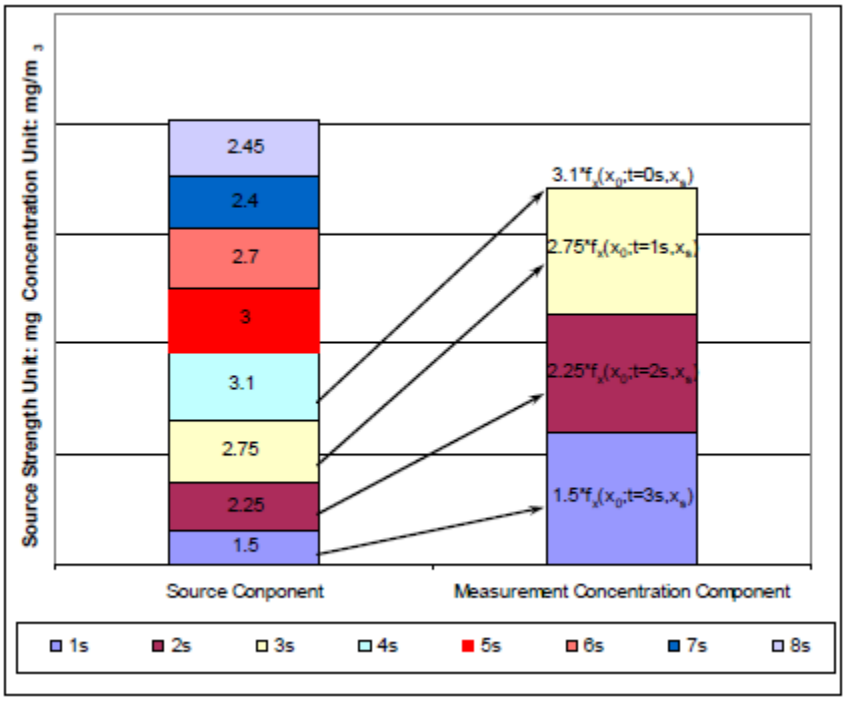

Figure 7-1 Components of Dynamic Source and Measured Concentration (Liu, 2008)

According to the figure 7-1 and above analysis, the relationship between the resident concentration (volume-averaged) and released instantaneous source mass was defined as following (Liu, 2008):

$$dC\left(\overrightarrow{x_1}, t=T\right) = dM\left(t_1\right) \cdot f_x\left(\overrightarrow{x_0}; T-t_1, \overrightarrow{x_m}\right) \tag{7.2}$$

The concentration in the domain after releasing a dynamic contaminant source can be integrated as follows:

$$C\left(\overrightarrow{x_1}, t=T\right) = \int_0^T dC\left(\overrightarrow{x_1}, t=T\right) = \int_0^T M_0 \cdot h(t) \cdot f_x\left(\overrightarrow{x_0}; T-t; \overrightarrow{x_m}\right) dt \tag{7.3}$$

Where, $C\left(\overrightarrow{x_1}, t=T\right)$ is the resident concentration at location $\overrightarrow{x_1}$ after releasing the dynamic source with a time T. The backward probability can be expressed as the ratio of resident concentration and the contaminant source mass released in the 1st second. In order to calculate $fd_x\left(\overrightarrow{x_0}; t=T, \overrightarrow{x_m}\right)$, function h (t) and $f_x\left(\overrightarrow{x_0}; T-t; \overrightarrow{x_m}\right)$ in different time steps need to be calculated in advance.

$$fd_x\left(\overrightarrow{x_0}; t=T, \overrightarrow{x_m}\right) = \frac{C\left(\overrightarrow{x_1}, t=T\right)}{M_0} = \int_0^T h(t) \cdot f_x\left(\overrightarrow{x_0}; T-t; \overrightarrow{x_m}\right) dt \tag{7.4}$$

According to the three types of sensor networks, backward probability equations should be derived. For single alarm sensor in the HVAC duct work, it's only needed to solve the above equation (7.4) to get the backward probability.). $fd_x\left(\overrightarrow{x_0}; \tau_0, \overrightarrow{x_{mk}}, \tau_{mk}\right)$ is a combined contribution of $f_x\left(\overrightarrow{x_0}; T-t; \overrightarrow{x_m}\right)$ and h(t) in time no later than the measured time.

For multiple alarm sensors without concentration recording, the backward probability can be defined as follows (Liu, 2008):

$$fd_x\left(\overrightarrow{x_0};\tau_0,\overrightarrow{x_{m1}},\overrightarrow{x_{m2}},\cdots,\overrightarrow{x_{mN}},\tau_{m1},\tau_{m2},\cdots,\tau_{mN}\right)=\frac{\prod_{k=1}^{N} fd_x\left(\overrightarrow{x_0};\tau_0,\overrightarrow{x_{mk}},\tau_{mk}\right)}{\int_x\prod_{k=1}^{N} fd_x\left(\overrightarrow{x_0};\tau_0,\overrightarrow{x_{mk}},\tau_{mk}\right)dx} \quad (7.5)$$

Where, $fd_x\left(\overrightarrow{x_0};\tau_0,\overrightarrow{x_{mk}},\tau_{mk}\right)$ is the backward location probability in the case of a single alarm sensor for the dynamic source, it can be calculated via equation (7.4).

$fd_x\left(\overrightarrow{x_0};\tau_0,\overrightarrow{x_{mk}},\tau_{mk}\right)$ is a combined contribution of $f_x\left(\overrightarrow{x_0};T-t;\overrightarrow{x_m}\right)$ and h(t) in time no later than the measured time.

According to equation (7.5), the numerator is multiply of backward location probability densities of different inverse case. In each inverse case, an instantaneous contaminant source with a unit mass is released at each sensor location respectively. Number of inverse cases is equal to the number of sensors. Multiple sensors are assumed to be independent. So the multiple inverse cases can also be considered unrelated and independent. According to the probability statistics, the probability of the event that source location is a certain point should be the multiply of probabilities for all independent cases. The integral in the denominator of that equation ensures that the total probability of all the cells is one.

For multiple sensors with concentration recording, the backward probability equation can be expressed as follows (Liu, 2008):

$$fd_x\left(\overrightarrow{x_0} \mid C_{m1}, C_{m2}, \cdots, C_{mN}; \tau_0, \overrightarrow{x_{m1}}, \overrightarrow{x_{m2}}, \cdots, \overrightarrow{x_{mN}}, \tau_{m1}, \tau_{m2}, \cdots, \tau_{mN}\right) = \frac{\int_{M_0} \prod_{k=1}^{N} P\left(C_k \mid M_0, \overrightarrow{x_0}; \tau_0, \overrightarrow{x_{mk}}, \tau_{mk}\right) fd_x\left(\overrightarrow{x_0}; \tau_0, \overrightarrow{x_{mk}}, \tau_{mk}\right) dM_0}{\int_x \int_{M_0} \prod_{k=1}^{N} P\left(C_k \mid M_0, \overrightarrow{x_0}; \tau_0, \overrightarrow{x_{mk}}, \tau_{mk}\right) fd_x\left(\overrightarrow{x_0}; \tau_0, \overrightarrow{x_{mk}}, \tau_{mk}\right) dx dM_0} \quad (7.6)$$

In the above equation, $P\left(C_k \mid M_0, \overrightarrow{x_0}; \tau_0, \overrightarrow{x_{mk}}, \tau_{mk}\right)$ follows a normal distribution, which was shown as following equation:

$$P\left(C_k \mid M_0, \overrightarrow{x_0}; \tau_0, \overrightarrow{x_{mk}}, \tau_{mk}\right) \sim N\left(M_0 \cdot fd_x\left(\overrightarrow{x_0}; \tau_0, \overrightarrow{x_{mk}}, \tau_{mk}\right), \sigma^2\right) \quad (7.7)$$

Equation (7.6) is a little bit different from equation (7.5) because contamination concentrations are recorded in the sampling locations. Sensor information (sensor location, release time and recorded concentration) are used to trace the source location. In practical situations, the sampled contamination concentration contains measurement error. Different from exact detection, measurement error must be considered in practical data tracking process. Based on previous study, the measurement error distribution can be considered as a normal distribution, normally distributed with mean zero and variance σ^2. For a given source location, measured concentration is a normally distributed random variable with mean concentration and variance σ^2. Using Bayes' theorem, the numerator of equation (7.6) is deduced. Likewise, the integral in the denominator of that equation ensures that the total probability of all the cells is one.

According to above analysis, the whole process identifying dynamic contaminant source location with known release time and known release mass were described as follows:

(1) Build simulation model. Based on the building case description, a real building can be idealized and simplified, and then were developed into a CONTAM model.

(2) Sensor networks. A proper sensor network can be built to identify source location. It's necessary to study the effectiveness of sensor network.

(3) Run forward simulation. Forward simulation is run to get a steady state airflow field and forward contaminant concentration distribution.

(4) Obtain the adjoint backward probability in the case of single alarm sensor for an instantaneous contaminant source. In the inverse model, an instantaneous contaminant source with a unit mass is released at each sensor location respectively. The adjoint backward probability equation under a single alarm sensor case for an instantaneous contaminant is solved to get the adjoint backward probability $f_x\left(\overrightarrow{x_0};\tau_0,\overrightarrow{x_{mk}},\tau_{mk}\right)$.

(5) Obtain the backward probability in the case of single alarm sensor for a dynamic source. Based on equation (7.4), the backward probability in the case of single alarm sensor for a dynamic contaminant source can be calculated.

(6) Identify source location based on sensor networks. All of the above five steps are fundamentals to identify dynamic contaminant source information. In this step, based on sensor networks specification, various backward probability equations are applied to calculate the backward probability. If there is only one alarm sensor, the backward location probability acquired in step (5) can be used directly to identify source location. If there are multiple alarm sensors, the backward location probability needs to be calculated using the equation (7.5). If there are multiple sensors with concentration recording, the backward location probability can be obtained using the equation (7.6).

In the following section of this chapter, two cases were studied to identify dynamic source location in different dynamic source types. It was demonstrated that the alarm sensors may not find the source location effectively. Therefore, only sensor networks with sensors reading current concentration and reading historical concentration were applied to identify the constant release source location and the decaying source location.

7.2 Contaminant Source Location Identification for a Single Constant Released Source

This case with a constantly released contaminant source is a special case because h (t) equals to one in equation (7.1). A same building CONTAM model was adopted as previous CONTAM model (chapter 5) shown in figure 5-1. Boundary conditions are same too. The only difference is that a constantly released contaminant source was released in point 1 through the fake zone, instead of an instantaneous contaminant source described in chapter 5. Dynamic contaminant source released in fake zone is 1000g of Carbon Monoxide (CO).In the inverse model, source release time and release mass were known to identify contaminant source location. This is a simple model with known release time and release mass to get started with.

The forward contaminant concentration change in point 4 and point 8 detected by sensor 1 and sensor 2 respectively, was shown in the following figure 7-4. The contaminant increases with time because contaminant source was released constantly. It was found that sensor 1 detected a higher concentration value than sensor 2 because the contaminant

concentration reaches the source concentration. There was a time delay for contaminant transport from point 1 to sensor location at point 4.

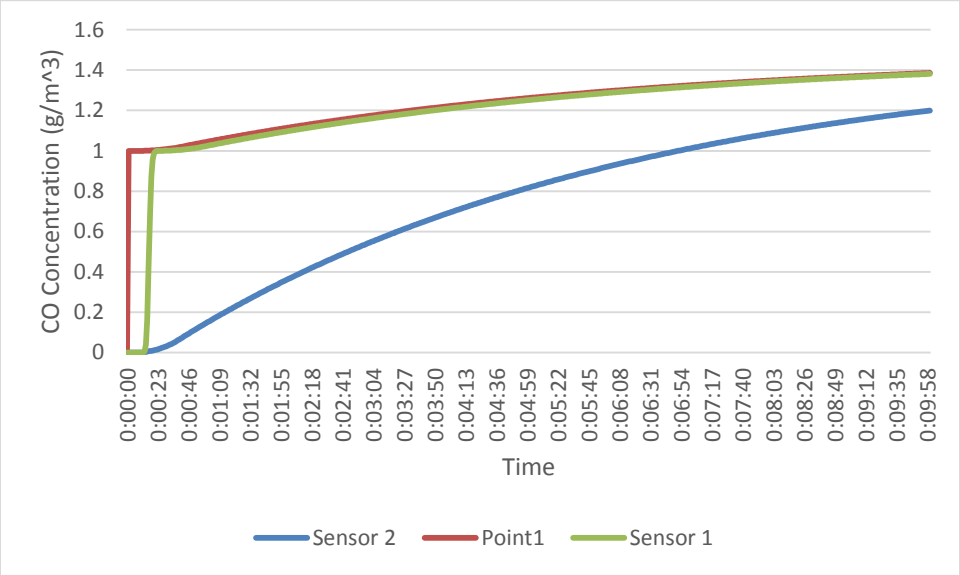

Figure 7-2 Predicted Forward Contaminant Detected by Sensor 1 and Sensor 2

Except the alarm sensor network, six sensing scenarios with concentration recording sensors were shown in table 7-1 in detail. Likewise, assume that the sensor threshold is 0.009 g/m^3.

Table 7-0-1 Six Sensing Scenarios to Identify the Dynamic Source Location

Sensor Cases	Concentration Recording Type	Sensors	Number of Measurements	Recordings (g/m^3)
Scenario 1	Current concentration recording	Sensor 1	1	0.04 g/m^3 at 14s
Scenario 2	Current concentration recording	Sensor 1, Sensor 2	2	Sensor 1: 0.04 g/m^3 at 14s; Sensor 2: 0.01 g/m^3 at 19s
Scenario 3	Historical concentration recording	Sensor 1	2	0.04 g/m^3 at 14s; 0.99 g/m^3 at 24s
Scenario 4	Historical concentration recording	Sensor 1; Sensor 2	4	Sensor 1: 0.04 g/m^3 at 14s, 0.99 g/m^3 at 24s; Sensor 2: 0.01 g/m^3 at 19s, 0.03 g/m^3 at 29s
Scenario 5	Historical concentration recording	Sensor 1	3	0.04 g/m^3 at 14s, 0.99 g/m^3 at 24s, 1.00 g/m^3 at 34s
Scenario 6	Historical concentration recording	Scenario 1	4	0.04 g/m^3 at 14s, 0.99 g/m^3 at 24s, 1.00 g/m^3 at 34s, 1.00 g/m^3 at 44s

According to the above six sensor scenarios, the backward probability of each point in the HVAC duct work under the six sensing scenarios were then calculated using equation (7.6). Calculated results were sketched in following figure 7-3.

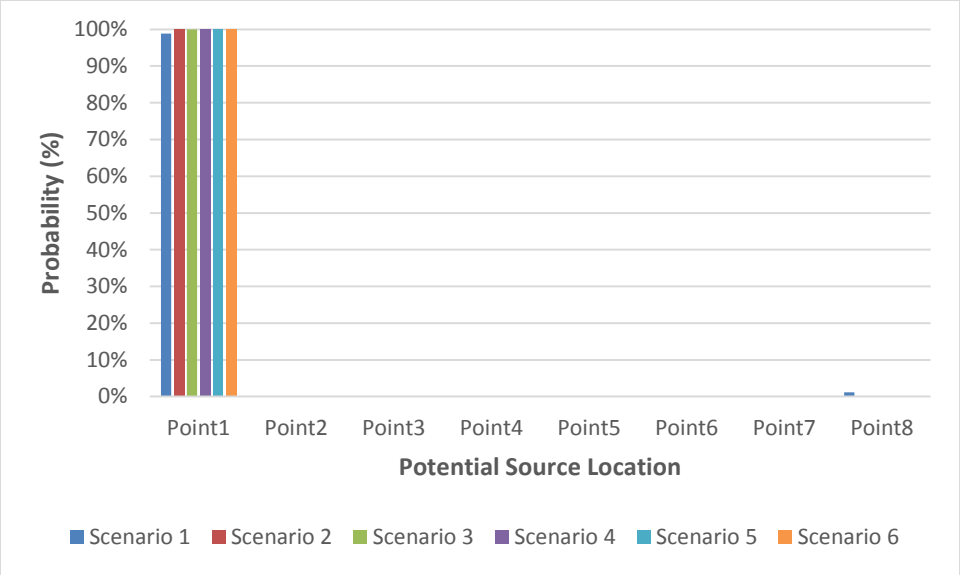

Figure 7-3 Source Location Identification for a Constant Release Source

In figure 7-3, it was found that all of above scenarios can identify the source location in point 1 accurately. The same conclusions can be summarized as above in chapter 5.

(1) Adding more measurements can improve the identification accuracy since more measurements can provide more information. A proper number of measurements are necessary because it's time-consuming and a challenge for sensor memory if too many measurements have to be tracked.

(2) Adding additional sensor can improve the identification accuracy even though sensor can only detect very low concentration. Additional sensors can provide more information for the backward model. But more sensors will be costly since the price of contaminant sensor is high. Study of how many sensors and what kind of sensors are needed is necessary and helpful.

(3) It was found that one concentration reading seems sufficient for proper identification of contaminant source location; and more contaminant information

will improve the prediction accuracy. In the sensitivity analysis of sensor location, it was found two historical concentration recording sensors are necessary for contaminant source identification. This conclusion was also applied for later research.

7.3 Contaminant Source Location Identification for a Single Decaying Source

This section documents the application of contaminant source location identification for a single decaying source. A same building CONTAM model was adopted as previous CONTAM model (chapter 5) shown in figure 5-1. Boundary conditions are same too. The only difference is that a decaying contaminant source was released in point 1 through the fake zone, instead of an instantaneous contaminant source in chapter 5. Like mentioned, walls or furnishings in buildings may release Volatile Organic Components (VOC), which are a threat to people's health. In HVAC system, Volatile Organic Components (VOC) or other decaying contaminant source may be released into HVAC duct work. A decaying contaminant source with a mass described in following equation (7.8) was released in the fake zone. Point 1 connected to the fake zone was assumed the actual decaying contaminant source. In the inverse model, source release time and release mass were known to identify contaminant source location.

$$\frac{dM(t)}{dt} = 100 \cdot e^{-t/9000} \tag{7.8}$$

The unit for the mass is g/s. According to the equation (7.8), the source mass decays along with the time. This decaying source was released into fake zone at time 1:00:00 AM. After being released with some time, the forward predicted contaminant change in point 4

and point 8 detected by sensor 1 and sensor 2, respectively, were shown in following figure 7-4. Figure 7-4 gives contaminant concentration change within 15 minutes after contaminant source was released. It was found that sensor 1 detected a higher concentration value at point 4 than that detected by sensor 2 at point 8, which was already given an explanation in previous chapters. The time delay is not clear to see. It was because the time gap is large.

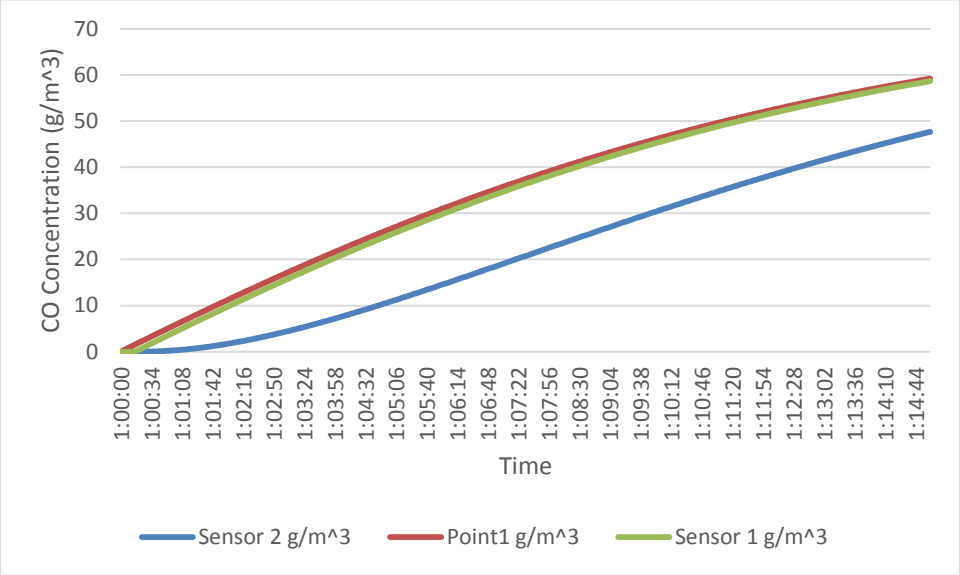

Figure 7-4 Predicted Forward Contaminant Detected by Sensor 1 and Sensor 2

The six sensor scenarios were applied to identify decaying source location with the given release time and given release mass, which were summarized in table 7-2 as following:

Table 7-0-2 Six Sensing Scenarios to Identify the Decaying Source

Sensor Cases	Concentration Recording Type	Sensors	Number of Measurements	Recordings (g/m^3)
Scenario 1	Current concentration recording	Sensor 1	1	0.021 g/m^3 at 15s
Scenario 2	Current concentration recording	Sensor 1, Sensor 2	2	Sensor 1: 0.021 g/m^3 at 15s; Sensor 2: 0 g/m^3 at 15s
Scenario 3	Historical concentration recording	Sensor 1	2	0.021 g/m^3 at 15s; 0.903 g/m^3 at 25s
Scenario 4	Historical concentration recording	Sensor 1; Sensor 2	4	Sensor 1: 0.021 g/m^3 at 15s, 0.903 g/m^3 at 25s; Sensor 2: 0 g/m^3 at 15s, 0.014 g/m^3 at 25s
Scenario 5	Historical concentration recording	Sensor 1	3	0.021 g/m^3 at 15s, 0.903 g/m^3 at 25s, 1.88 g/m^3 at 35s
Scenario 6	Historical concentration recording	Sensor 1	4	0.021 g/m^3 at 15s, 0.903 g/m^3 at 25s, 1.88 g/m^3 at 35s, 2.84 g/m^3 at 45s

According to the sensor networks, the backward probability equation at each point of six sensing scenarios were calculated using equation (7.6) and summarized in the following figure 7-5.

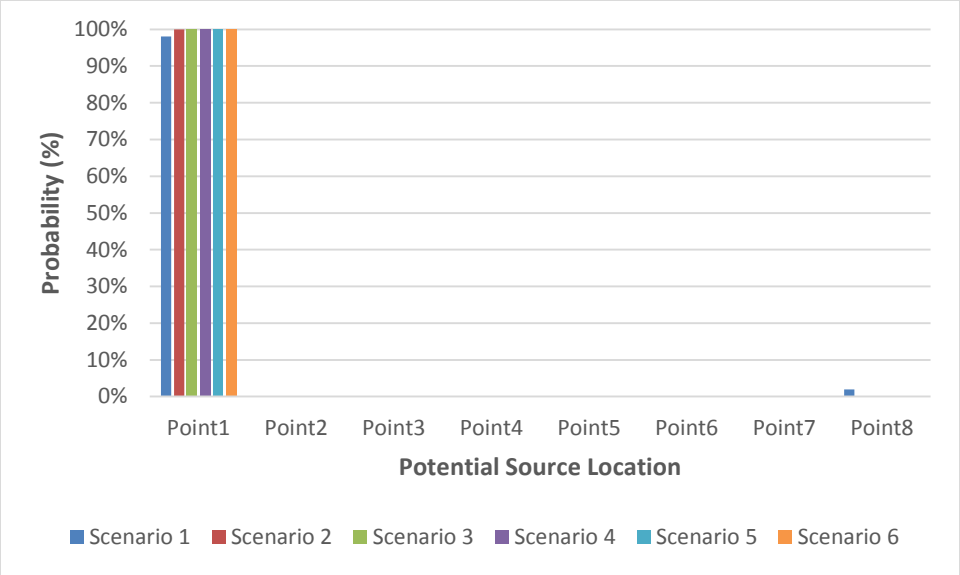

Figure 7-5 Predicted Source Location Probabilities in the Four Scenarios

In the figure 7-5, it was found that all the six sensing scenarios can identify the contaminant source location for a decaying source. All of these sensor networks work well in the identification of decaying source location with given release time and given release mass. Adjoint backward probability is an effective methodology to identify the dynamic source in duct network.

(1) Adding more measurements can improve the identification accuracy since extra measurements can provide more information.

(2) Adding additional sensor can improve the identification accuracy even though sensor can only detect very low concentration. Additional sensors can provide more information for the backward model.

As a sum, this chapter mainly focused on dynamic contaminant source location identification with given release time and given release mass. First, theories on the identification process were described in detail. Second, two types of dynamic contaminant source were studied, including a special case: constant contaminant source, and a decaying contaminant source. Adjoint backward probability can be applied to identify the dynamic source location accurately in HVAC duct system.

In conclusion, it's recommended that two historical concentration recording sensors should be applied, in which, one sensor should be placed in the supply duct, the other one sensor should be set in point 8 (the one point in return duct).

Using the conclusions, the adjoint backward probability method was applied to identify dynamic source location in a two-floor building with known release time and release source mass. The two-floor building was outlined in figure 7-6, in which, above one figure is second floor and below one is first floor. The first floor is same as the model used in previous chapters. Likewise, in the second floor, there are also three zones, zone A2, zone B2, and zone C2 from left to right. Duct network in the two floors are connected by one duct connecting point 3 and point 10 and the other one connecting point 8 and point 15. Air Handler Unit (AHU) is located in first floor and supplies air to the second floor through the duct connecting point 3 and point 10. Airflow in second floor is returned to the AHU through the duct connecting point 8 and point 15. A decaying contaminant source was released in point 9 (located in the second floor) through fake zone. One sensor was placed in point 4 (first floor), the other one sensor was set in point 8 (first floor). In the forward model, sensor 1 and sensor 2 detect contaminant change in point 8 and point 4 respectively after the decaying contaminant source was released. Additionally, it was presumed that

contaminant source was in the 15 points (from point 1 to point 15). Boundary conditions of the forward model were presented in table 7-3. The decaying contaminant source modeling was defined as follows in equation (7.9):

$$\frac{dM(t)}{dt} = 10 \cdot e^{-t/9000} \tag{7.9}$$

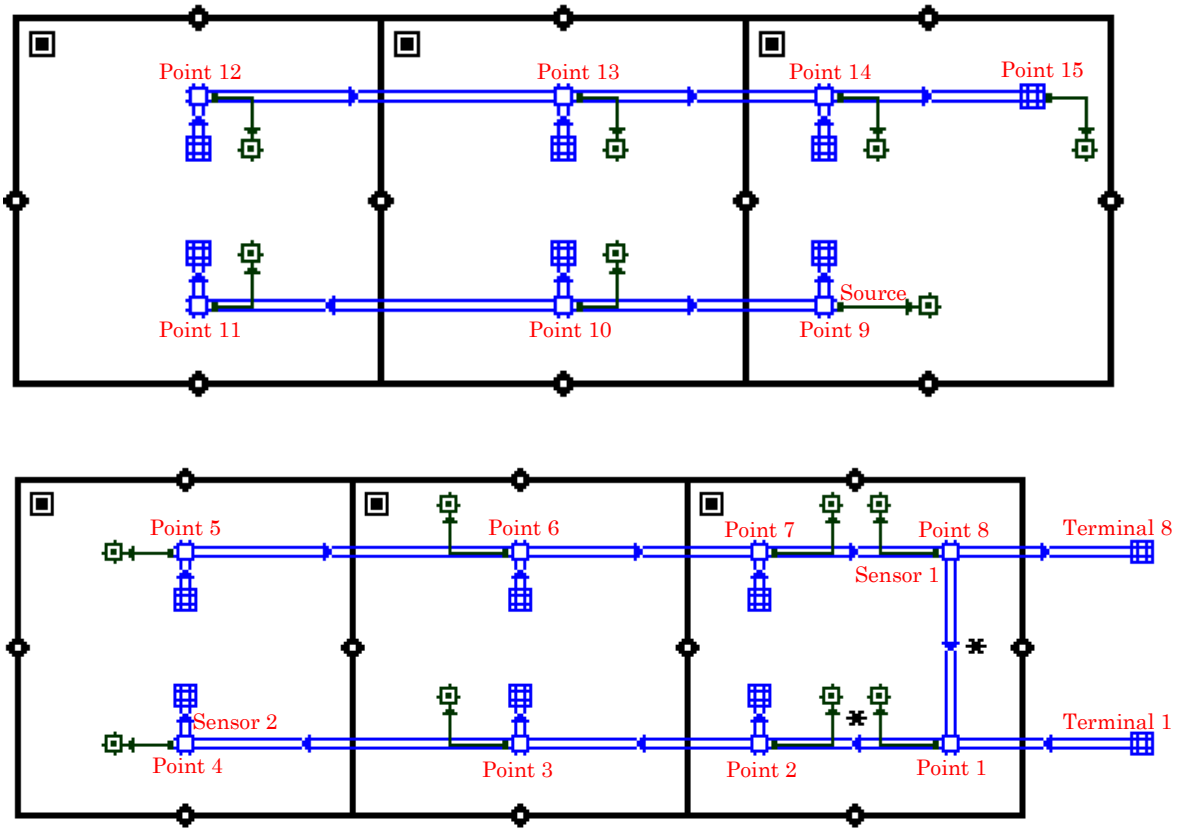

Figure 7-6 Two-floor CONTAM Building Model

Table 7-0-3 Boundary Conditions of Forward Model

Airflow Paths	Airflow Rate	Velocity	Pressure Change	Airflow Direction	
	kg/s	m/s	Pa	From	to
Ventilation Inlet	0.73	1.93	1.76	Ambient	Terminal 1
Exhaust Duct	0.5	1.32	0.16	Terminal 8	Ambient
Path 1	0.0126	-	0.018	Zone C1	Ambient
Path 2	0.0126	-	0.018	Zone C1	Ambient
Path 3	0.0126	-	0.018	Zone C1	Ambient
Path 4	0.013	-	0.019	Zone B1	Ambient
Path 5	0.007	-	0.006	Zone A1	Ambient
Path 6	0.007	-	0.006	Zone A1	Ambient
Path 7	0.007	-	0.006	Zone A1	Ambient
Path 8	0.013	-	0.019	Zone B1	Ambient
Path 9	0.215	-	0.013	Zone B1	Zone A1
Path 10	0.06	-	0.001	Zone B1	Zone C1
Path 11	0.015	-	0.025	Ambient	Zone C2
Path 12	0.015	-	0.025	Ambient	Zone C2
Path 13	0.015	-	0.025	Ambient	Zone C2
Path 14	0.0129	-	0.019	Ambient	Zone B2
Path 15	0.015	-	0.026	Ambient	Zone A2
Path 16	0.015	-	0.026	Ambient	Zone A2
Path 17	0.015	-	0.026	Ambient	Zone A2
Path 18	0.0129	-	0.019	Ambient	Zone B2
Path 19	0.158	-	0.007	Zone B2	Zone A2
Path 20	0.141	-	0.006	Zone B2	Zone C2

Sensor 1 and sensor 2 recorded contaminant concentration change in point 8 and point 4 respectively after decaying source was released in point 9 (second floor) through the

fake zone, which was shown in figure 7-7. In the figure 7-7, concentration values of point 4 and point 8 were small compared to that of contaminant source. Time delays can be found when contaminant transports from source location to point 4 and point 8.

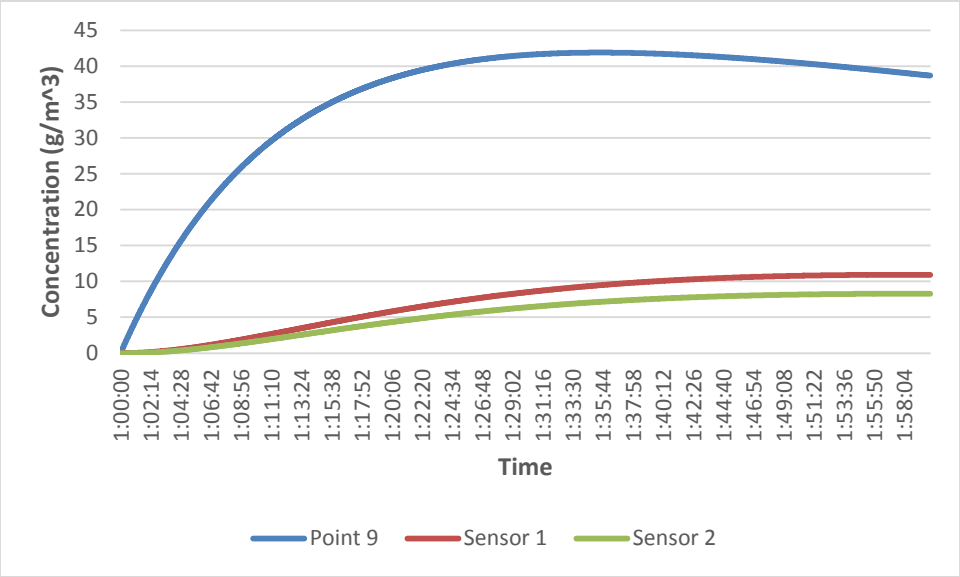

Figure 7-7 Contaminant Concentration Detected by Sensor 1 and Sensor 2

According to the information detected by sensors, sensor networks were outlined in table 7-4. Six scenarios were compared and analyzed. Assume that sensor threshold is 0.009 g/m^3.

Table 7-0-4 Six Scenarios to Identify Source Location

Sensor Cases	Concentration Recording Type	Sensors	Number of Measurements	Recordings (g/m^3)
Scenario 1	Current concentration recording	Sensor 1	1	0.0095 g/m^3 at 40s
Scenario 2	Current concentration recording	Sensor 1, Sensor 2	2	Sensor 1: 0.0095 g/m^3 at 40s; Sensor 2: 0 g/m^3 at 40s
Scenario 3	Historical concentration recording	Sensor 1	2	0.0095 g/m^3 at 40s; 0.017 g/m^3 at 50s
Scenario 4	Historical concentration recording	Sensor 1; Sensor 2	4	Sensor 1: 0.0095 g/m^3 at 40s, 0.017 g/m^3 at 50s; Sensor 2: 0 g/m^3 at 40s, 0 g/m^3 at 50s
Scenario 5	Historical concentration recording	Sensor 1	3	0.0095 g/m^3 at 40s, 0.017 g/m^3 at 50s, 0.0257 g/m^3 at 60s
Scenario 6	Historical concentration recording	Sensor 1	4	0.0095 g/m^3 at 40s, 0.017 g/m^3 at 50s, 0.0257 g/m^3 at 60s, 0.0365 g/m^3 at 70s

In the inverse model, the airflow field was reversed without changing absolute values. The boundary conditions of backward model was documented in table 7-5. The negative values indicate reverse airflow directions compared to that in forward model.

Table 7-0-5 Boundary Conditions of Backward Model

Airflow Paths	Airflow Rate	Velocity	Pressure Change	Airflow Direction	
	kg/s	m/s	Pa	From	to
Ventilation Inlet	-0.73	-1.93	-1.76	Ambient	Terminal 1
Exhaust Duct	-0.5	-1.32	-0.16	Terminal 8	Ambient
Path 1	-0.0126	-	-0.018	Zone C1	Ambient
Path 2	-0.0126	-	-0.018	Zone C1	Ambient
Path 3	-0.0126	-	-0.018	Zone C1	Ambient
Path 4	-0.013	-	-0.019	Zone B1	Ambient
Path 5	-0.007	-	-0.006	Zone A1	Ambient
Path 6	-0.007	-	-0.006	Zone A1	Ambient
Path 7	-0.007	-	-0.006	Zone A1	Ambient
Path 8	-0.013	-	-0.019	Zone B1	Ambient
Path 9	-0.215	-	-0.013	Zone B1	Zone A1
Path 10	-0.06	-	-0.001	Zone B1	Zone C1
Path 11	-0.015	-	-0.025	Ambient	Zone C2
Path 12	-0.015	-	-0.025	Ambient	Zone C2
Path 13	-0.015	-	-0.025	Ambient	Zone C2
Path 14	-0.0129	-	-0.019	Ambient	Zone B2
Path 15	-0.015	-	-0.026	Ambient	Zone A2
Path 16	-0.015	-	-0.026	Ambient	Zone A2
Path 17	-0.015	-	-0.026	Ambient	Zone A2
Path 18	-0.0129	-	-0.019	Ambient	Zone B2
Path 19	-0.158	-	-0.007	Zone B2	Zone A2
Path 20	-0.141	-	-0.006	Zone B2	Zone C2

Note: negative values indicate different airflow and pressure change direction with the forward model. After reversing the airflow field, the ventilation inlet of forward model becomes outlet and the exhaust outlet of forward model becomes inlet, respectively.

In the inverse model, an instantaneous contaminant source with a unit mass was then released in two sensor locations respectively. The adjoint backward probability methodology was used to study the dynamic contaminant source identification in two-floor building. Equation (7.6) was applied to calculate the backward location probabilities for the fifteen points under the case with two sensors recording historical concentrations. The results were sketched in figure 7-8.

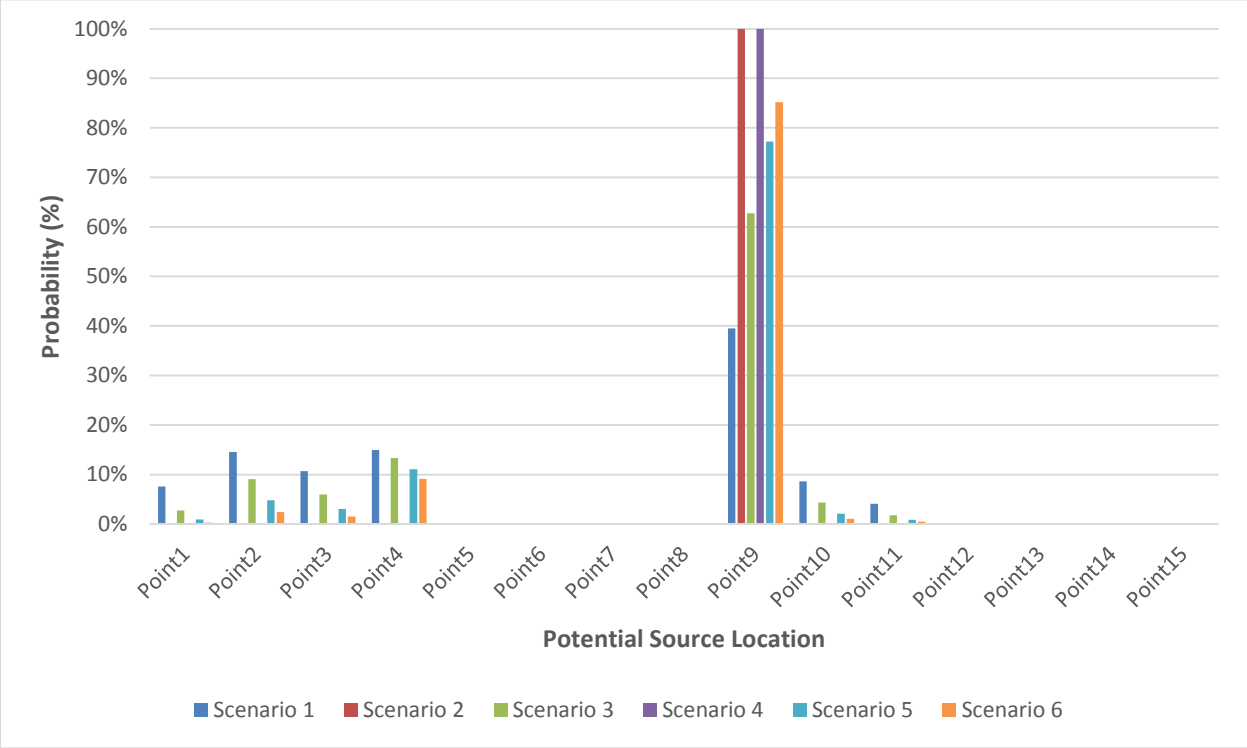

Figure 7-8 Scenarios Analysis under the Two-floor Building Case

According to figure 7-8, same conclusions can be summarized as previous chapter. It was found that adjoint backward probability methodology is effective for the application of dynamic contaminant source identification. Adding more measurements can improve the identification accuracy because extra measurements can provide more information of

contaminant transport in different times. Additionally, adding additional sensor can improve the identification accuracy even though sensor can only detect very low concentration. It seems that additional sensors can provide more information for identification than adding more measurements using only single sensor. It's because extra sensors can provide more information of contaminant transport in the duct work and different times.

Chapter 8 Simultaneous Identification of a Decaying Contaminant Source Release Time and Source Location

In above chapters, contaminant source locations were identified with known release time and release mass. However, source release time maybe unknown in the practical situations. This section focused on identifying both the source release time and source release mass. Using previous conclusions, two historical concentration recording sensors were applied to identify both release time and source location of a decaying contaminant source with given source release mass.

According to previous work done by Liu (2008), the backward probability equations were defined as follows. For the case identifying an instantaneous contaminant source release time with known source location, the backward probability was expressed as follows:

$$f_\tau\left(\tau_0 \mid C_{m1}, C_{m2}, \cdots, C_{mN}; \overrightarrow{x_{m1}}, \overrightarrow{x_{m2}}, \cdots, \overrightarrow{x_{mN}}, \tau_{m1}, \tau_{m2}, \cdots, \tau_{mN}\right) = \frac{\int_x \int_{M_0} \prod_{k=1}^{N} P\left(C_k \mid M_0, \overrightarrow{x_0}; \tau, \overrightarrow{x_{mk}}, \tau_{mk}\right) f_x\left(\overrightarrow{x_0}; \tau, \overrightarrow{x_{mk}}, \tau_{mk}\right) dM_0 dx}{\int_\tau \int_x \int_{M_0} \prod_{k=1}^{N} P\left(C_k \mid M_0, \overrightarrow{x_0}; \tau, \overrightarrow{x_{mk}}, \tau_{mk}\right) f_x\left(\overrightarrow{x_0}; \tau, \overrightarrow{x_{mk}}, \tau_{mk}\right) dx dM_0 d\tau} \tag{8.1}$$

Where, $f_x\left(\overrightarrow{x_0}; \tau, \overrightarrow{x_{mk}}, \tau_{mk}\right)$ is the adjoint backward location probability under a single alarm sensor case. $P\left(C_k \mid M_0, \overrightarrow{x_0}; \tau, \overrightarrow{x_{mk}}, \tau_{mk}\right)$ follows a normal distribution which was shown as following:

$$P\left(C_k \mid M_0, \overrightarrow{x_0}; \tau, \overrightarrow{x_{mk}}, \tau_{mk}\right) \sim N\left(M_0 \cdot f_x\left(\overrightarrow{x_0}; \tau, \overrightarrow{x_{mk}}, \tau_{mk}\right), \sigma_s^2\right) \tag{8.2}$$

According to equation (8.1), the numerator is integrating the multiply of backward release time probability densities of different inverse models. In each inverse model, an instantaneous contaminant source with a unit mass is released at each sensor location respectively. Number of inverse cases is equal to the number of sensors. Multiple sensors are assumed to be independent because they don't influence mutually. The multiple inverse cases can also be considered unrelated and independent. According to the probability statistics, the probability of the event that source location is a certain point should be the multiply of probabilities for all independent cases. The integral in the denominator of equation (7.1) ensures that the total probability of all the cells is one.

For the case identifying both release time and source location of an instantaneous contaminant source, the backward probability was defined as follows:

$$f_{x,\tau}\left(x_0, \tau_0 \mid C_{m1}, C_{m2}, \cdots, C_{mN}; \overrightarrow{x_{m1}}, \overrightarrow{x_{m2}}, \cdots, \overrightarrow{x_{mN}}, \tau_{m1}, \tau_{m2}, \cdots, \tau_{mN}\right) = \frac{\int_{M_0} \prod_{k=1}^{N} P\left(C_k \mid M_0, \overrightarrow{x_0}; \tau, \overrightarrow{x_{mk}}, \tau_{mk}\right) f_x\left(\overrightarrow{x_0}; \tau, \overrightarrow{x_{mk}}, \tau_{mk}\right) dM_0}{\int_{\tau}\int_{x}\int_{M_0} \prod_{k=1}^{N} P\left(C_k \mid M_0, \overrightarrow{x_0}; \tau, \overrightarrow{x_{mk}}, \tau_{mk}\right) f_x\left(\overrightarrow{x_0}; \tau, \overrightarrow{x_{mk}}, \tau_{mk}\right) dx dM_0 d\tau} \tag{8.3}$$

Equation (8.3) is applied to calculate the backward probabilities in the application of identifying both release time and source location. The difference between equation (8.1) and equation (8.2) is equation (8.1) is integrating of equation (8.3). Likewise, the integral in the denominator of that equation ensures that the total probability of all the cells is one.

Equation (8.3) was deduced to identify both release time and source location of an instantaneous pollute source. Dynamic contaminant source is more common than an instantaneous source in the indoor air quality issues. In this chapter, simultaneous identification of source release time and source location were studied for a decaying contaminant source. Above equations were changed to be applicable for a dynamic contaminant source.

For the case identifying a decaying contaminant source release time with known source location, the backward probability was defined as follows:

$$fd_{\tau}\left(\tau_0 \mid C_{m1}, C_{m2}, \cdots, C_{mN}; \overrightarrow{x_{m1}}, \overrightarrow{x_{m2}}, \cdots, \overrightarrow{x_{mN}}, \tau_{m1}, \tau_{m2}, \cdots, \tau_{mN}\right) = \frac{\int_x \int_{M_0} \prod_{k=1}^{N} P\left(C_k \mid M_0, \overrightarrow{x_0}; \tau, \overrightarrow{x_{mk}}, \tau_{mk}\right) fd_x\left(\overrightarrow{x_0}; \tau, \overrightarrow{x_{mk}}, \tau_{mk}\right) dM_0 dx}{\int_{\tau} \int_x \int_{M_0} \prod_{k=1}^{N} P\left(C_k \mid M_0, \overrightarrow{x_0}; \tau, \overrightarrow{x_{mk}}, \tau_{mk}\right) fd_x\left(\overrightarrow{x_0}; \tau, \overrightarrow{x_{mk}}, \tau_{mk}\right) dx dM_0 d\tau} \tag{8.4}$$

Where, $fd_x\left(\overrightarrow{x_0}; \tau_0, \overrightarrow{x_{mk}}, \tau_{mk}\right)$ is the adjoint backward location probability under a single alarm sensor case. $P\left(C_k \mid M_0, \overrightarrow{x_0}; \tau_0, \overrightarrow{x_{mk}}, \tau_{mk}\right)$ follows a normal distribution which was shown as following:

$$P\left(C_k \mid M_0, \overrightarrow{x_0}; \tau, \overrightarrow{x_{mk}}, \tau_{mk}\right) \sim N\left(M_0 \cdot fd_x\left(\overrightarrow{x_0}; \tau, \overrightarrow{x_{mk}}, \tau_{mk}\right), \sigma_s^2\right) \tag{8.5}$$

For the case identifying both release time and source location of an instantaneous contaminant source, the backward probability was expressed as follows:

$$fd_{x,\tau}\left(x_0,\tau_0 \mid C_{m1},C_{m2},\cdots,C_{mN};\overrightarrow{x_{m1}},\overrightarrow{x_{m2}},\cdots,\overrightarrow{x_{mN}},\tau_{m1},\tau_{m2},\cdots,\tau_{mN}\right)=$$

$$\frac{\int_{M_0}\prod_{k=1}^{N}P\left(C_k \mid M_0,\overrightarrow{x_0};\tau,\overrightarrow{x_{mk}},\tau_{mk}\right)fd_x\left(\overrightarrow{x_0};\tau,\overrightarrow{x_{mk}},\tau_{mk}\right)dM_0}{\int_{\tau}\int_{x}\int_{M_0}\prod_{k=1}^{N}P\left(C_k \mid M_0,\overrightarrow{x_0};\tau,\overrightarrow{x_{mk}},\tau_{mk}\right)fd_x\left(\overrightarrow{x_0};\tau,\overrightarrow{x_{mk}},\tau_{mk}\right)dxdM_0d\tau} \tag{8.6}$$

A same CONTAM building model as that model used in identification of an instantaneous contaminant source (chapter 5) was employed in this chapter. Boundary conditions are same too. The only difference is a decaying contaminant source was released in point 1 through fake zone at 1:00:00AM, instead of an instantaneous contaminant source. Equation (7.8) in chapter 7 expresses the decaying contaminant source used in this case. Two historical concentration recording sensors were applied in the sensor network. Assume that the sensor threshold is still 0.009 g/m^3. Boundary conditions of the forward model and backward model were shown in table 5-1 and table 5-3. Sensor 1 and sensor 2 recorded contaminant change in point 4 and point 8 respectively, which was shown in figure 7-4 (chapter 7). Sensor network with recording information was presented in table 8-1. In the inverse model, an instantaneous contaminant source with unit mass was released in the two sensor locations respectively to acquire the adjoint backward probability $f_x\left(\overrightarrow{x_0};\tau,\overrightarrow{x_{mk}},\tau_{mk}\right)$.

Table 8-0-1 Sensor Network to Identify Both Release Time and Source Location

Sensor Cases	Concentration Recording Type	Sensors	Number of Measurements	Recordings (g/m^3)
Scenario 1	Historical concentration recording	Sensor 1; Sensor 2	4	Sensor 1: 0.021 g/m^3; 10 seconds later, 0.903 g/m^3 at 25s Sensor 2: 0 g/m^3; 10 seconds later, 0.014 g/m^3 at 25s

Considering the CONTAM model is simple, contaminant can be transported to the whole duct network in 60 seconds, and high sensitivity of sensors, first 60 seconds of contaminant transport was analyzed. It was assumed that contaminant source location can be identified through recoding the first 60 seconds of contaminant. $fd_x\left(\overrightarrow{x_0};\tau,\overrightarrow{x_{mk}},\tau_{mk}\right)$ was calculated for all the points using equation (7.4). For the sensor network of two historical concentration recording sensors, equation (8.6) was used to solve the backward probabilities of the eight points. The analysis results were documented in figure 8-1. The time difference between two readings in figure 8-1 is one second.

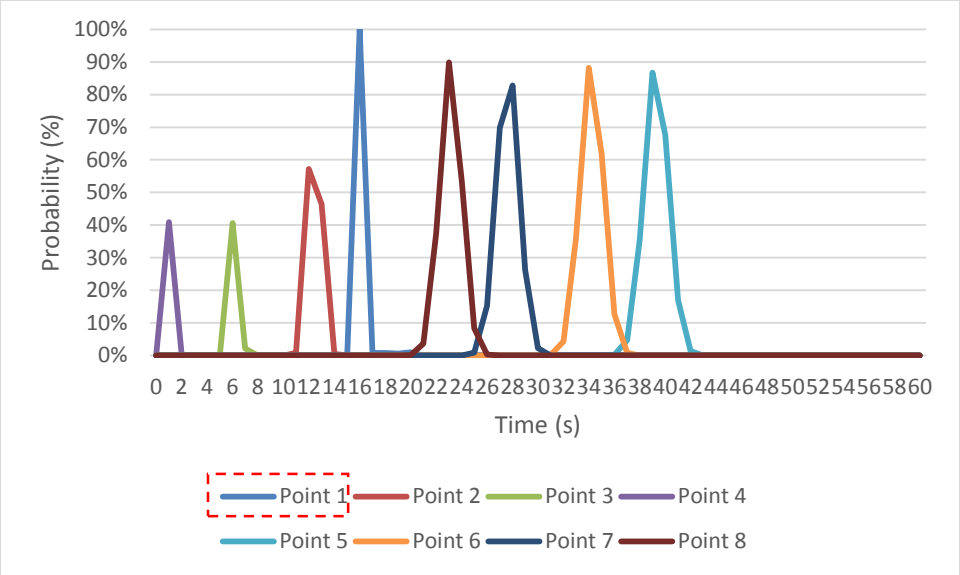

Figure 8-1 Backward Probabilities (%) to Identify Both Release Time and Source Location

According to figure 8-1, it was found that the largest probability is in point 1 and at 16s. This means that contaminant source location was identified accurately since the decaying contaminant source was released in point 1 in the forward model. In the numerical experiment of forward model, it can be extracted that forward release time is 15 seconds, with only 1 second difference compared to the identified source release time. Considering the measurement error in practical conditions, 1 second doesn't matter much. Therefore, both release time and source location were identified accurately. The results tell that both adjoint backward probability methodology and two historical concentration recording sensors are effective to identify source release time and source location simultaneously.

The time difference between two readings in figure 8-1 is one second. It's necessary to study sensitivity analysis of time difference between two readings. Except the above case with one second of time difference, 2s, 4s, and 8s of time difference were analyzed again.

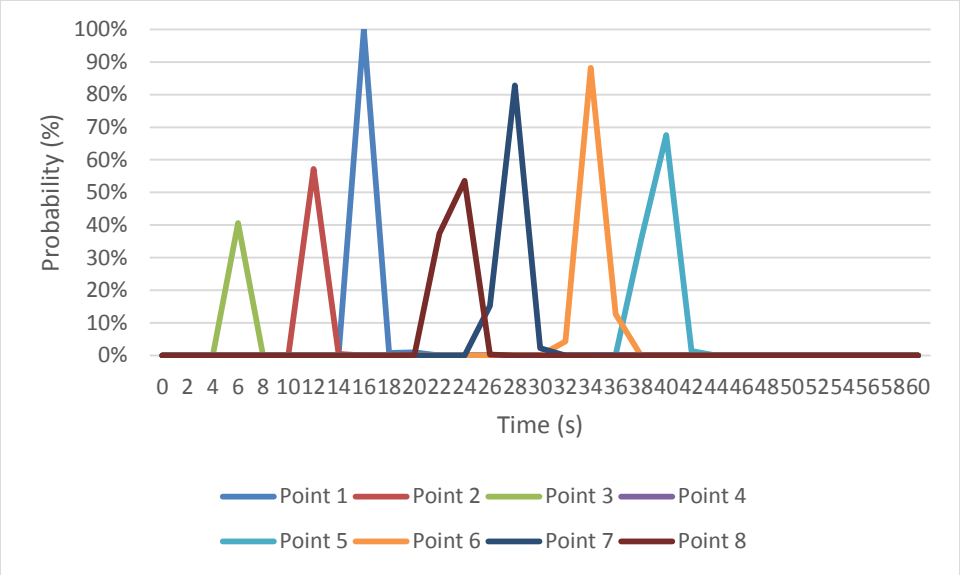

Figure 8-2 2s of Time Difference between Two Readings

According to figure 8-2, in the case with 2s of time difference, point 1 and 16s were identified as the contaminant source location and release time respectively. The lines are sharp which means the backward location probabilities change sharply.

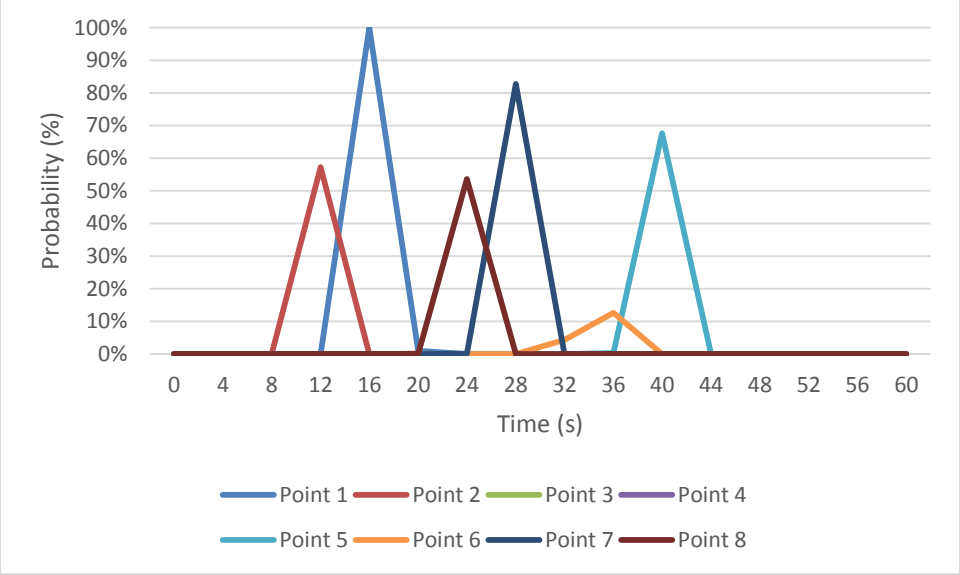

Figure 8-3 4s of Time Difference between Two Readings

According to figure 8-3, in the case with 2s of time difference, point 1 and 16s were identified as the contaminant source location and release time respectively. The lines are much sharper than those in figure 8-2.

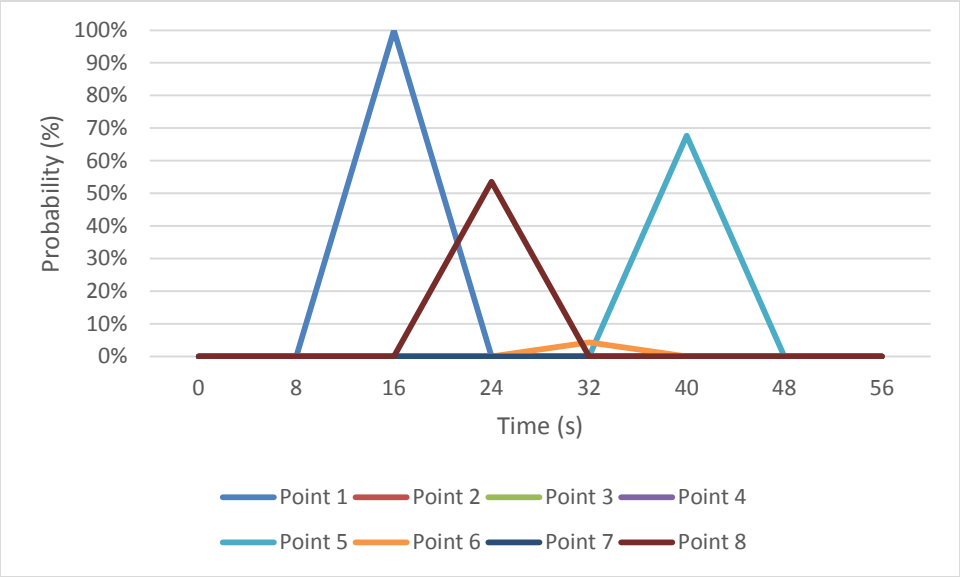

Figure 8-4 8s of Time Difference between Two Readings

According to figure 8-4, in the case with 2s of time difference, point 1 and 16s were identified as the contaminant source location and release time respectively. The lines are changing much more sharply than those in figure 8-3. The identified backward location probabilities change sharply.

Through figure 8-2, 8-3, and 8-4, although release time and source location were identified accurately, a much smaller time difference will help identify correct results. Large time difference may neglect actual results.

As a summary, in this chapter, the task of identifying both the source location and source release time of a decaying contaminant source was analyzed and discussed. Previous

conclusions were applied to this study. It was concluded that two historical concentration recordings sensors are helpful in the identification of source release time and source location simultaneously. Adjoint backward probability methodology is a good method to identify contaminant source location and source release time.

Chapter 9 Conclusions

This thesis studies the application of adjoint backward probability model in identification of contaminant source in Building HVAC system. In order to identify contaminant source, four kinds of information must be recovered, including contaminant source release strength or release mass, source release time, source location, and number of contaminant sources. The adjoint backward probability method has already been evidenced a good alternative to identify the four kinds of contamination source information.

In order to identify contaminant source information, proper sensor networks must be studied and applied in the HVAC systems. Sensors are used to detect contaminant concentration change in certain sampling locations of HVAC ductwork. Using sensor detection information, we can trace back and find the source information. CONTAM is a multi-zone indoor air quality and ventilation analysis computer program used to determine the contaminant concentration distribution in buildings and HVAC systems. CONTAM has many successful applications in building indoor air quality (IAQ) research. In this research it is used to provide a steady state airflow field. A simple building model with three zones and detailed duct work is built. This model is applied into later research in identification of contaminant source in HVAC system.

Different cases are analyzed in the research to study the application of adjoint backward probability method. Four kinds of information are complex to be recovered simultaneously. In order to show how the adjoint backward probability method works, simplified cases with part of known source information are studied. The first case is identifying an instantaneous contaminant source location with known source release time

and source release mass. The second case is identifying the location of a dynamic contaminant source with known release time and known release mass. The third case is identifying source release time and release location simultaneously for a decaying contaminant source with known source release mass. The fourth case is identifying the location of a dynamic contaminant source in a two-floor building with known release time and known release mass. The conclusions come to that a sensor network with two sensors reading historical concentrations can identify source information accurately. Further, in future research, contaminant source information will be recovered without knowing any source information in advance.

In a sum, the goal of the thesis is to study the application of adjoint backward probability method in contaminant source identification in building HVAC system. This may provide an efficient approach to identify and remove the emission source in HVAC system.

Chapter 10 Further Research on Contaminant Source Identification

This thesis focuses on contaminant source identification in building HVAC system. Four kinds of information need to be recovered, including contaminant source location, source release time, source release mass, and number of sources. Identifying the four source information simultaneously is difficult. Instead, several simplified cases were studied in this research: 1) instantaneous source location identification with known source release time and known source release mass; 3) source location identification with given release time for a dynamic source; 2) simultaneous source location identification and source release time identification with known source mass for a decaying contaminant source; 4) source location identification in HVAC system of two-floor building with given source release time and given release mass for a decaying contaminant source. Therefore, I only identified contaminant source location and source release time with known number of source and source release mass in this research. Adjoint probability method was evidenced as a solid methodology to identify contaminant source in HVAC system. However, in practical engineering practices, none of the four types of source information could be known in advance. All the four contaminant source information, including source location, source release time, source release mass, and number of sources, should be identified simultaneously. This is the most complex application case. But fundamentals of this research are still solid foundation for a more complex case study.

Considering the assumptions of this research and goals of contaminant source identification, the research work could be improved in future as follows:

(1) Seek an additional tool which can put contaminant source in the duct directly and record contaminant concentration in the whole duct network. I was told by the CONTAM developer that these two functions will be applicable to future CONTAM versions. In such case, the two assumptions would be removed and a more decent research can be conducted.

(2) Using the fundamentals of this research, a practical building can be used to verify the adjoint probability methodology. If it is possible, an experiment can be conducted in the practical building and verify the simulation model.

(3) According to the fundamentals of this research, four kinds of contaminant source information can be identified simultaneously. This is not a tough topic but requires tons of calculations. A proper data process tool will be much more helpful. In this research, CONTAM tool was used. COTNAM is not like CFD tool which has powerful data process function. In this research, I mainly applied excel spreadsheet process tons of data, which is greatly time-consuming and needs much attention in QC (quality control) process.

Appendix A: Adjoint Equation Deducing Process for the One Dimensional Convection Dispersion Duct

General forward contaminant transport equation for one-dimensional convection-dispersion duct in the CONTAM model was shown in below equation:

$$\begin{aligned}
&\frac{\partial(C)}{\partial t}+\frac{\partial(\mathrm{uC})}{\partial x}=\frac{\partial}{\partial x}\left(\beta\frac{\partial C}{\partial x}\right)+Q_{\text{source}}\\
&C\left(\vec{x},0\right)=C_0\left(\vec{x}\right)\\
&C\left(\vec{x},\ \mathrm{t}\right)=g_1(t)\\
&\beta\frac{\partial C}{\partial x}=g_2(t)\\
&\mathrm{uC}-\beta\frac{\partial \mathrm{C}}{\partial x}=g_3(t)
\end{aligned}\qquad (A.1)$$

Where, $\frac{\partial C}{\partial t}$ is the transient term; $\frac{\partial(uC)}{\partial x}$ is convection term; $\frac{\partial}{\partial x}\left(\beta\frac{\partial C}{\partial x}\right)$ is the dispersion term; Q_{source} is the source term. C is the contaminant concentration (volume-averaged); u is the velocity of airflow; ß is the dispersion coefficient; $g_1(t), g_2(t), g_3(t)$ are three types of boundaries. Initial condition and boundary conditions are required to solve the governing contaminant transport equation.

It was proved that the backward probability equation is adjoint of the forward contaminant transport equation. According to the forward transport equation, the general adjoint backward probability equation for one dimensional convection dispersion duct is deduced as following. Referring to previous research work by Dr. Neupauer (2000) and Dr. Liu (2008), the adjoint equation was derived in following steps.

As you know, the adjoint method is commonly used in sensitivity analysis. Sensitivity analysis is used to determine the sensitivity of the state of the system parameters (model output parameters) to changes in parameter values (model input parameters). The direct method of performing a sensitivity analysis is to change the input parameter gradually, and then determine the effect on the model output, which requires one simulation for each parameter change. So it's time-consuming in this analysis process. Instead, the adjoint method can provide a more efficient approach in which the adjoint equation is solved once, and then the result is used to directly compute the sensitivity of the state of the system to all parameters (Liu, 2008).

In sensitivity analysis, a performance measure is defined to quantity the state sensitivity of the system, which is to determine the marginal sensitivity of this performance measure to small changes in parameter values.

First, assume a performance measure P that quantities the state of the system as following:

$$P = \iint_{x,t} h(\alpha, C) dx dt \tag{A.2}$$

Where, $h(\alpha, C)$ is a function of the state sensitivity of the system; α is a vector of system parameters, (e.g $\alpha = [u, \beta, M]$). The sensitivity analysis in terms of these parameters (u, ß, M) can be analyzed

The integration is over the entire space domain and time domain. For one dimensional duct, the space domain is one dimensional. The marginal sensitivity of this

performance measure with respect to one parameter, α is obtained by differentiating with respect to α, shown as following:

$$\frac{dP}{d\alpha} = \iint_{x,t} \left[\frac{\partial h(\alpha, C)}{\partial \alpha} + \frac{\partial h(\alpha, C)}{\partial C} \psi \right] dxdt \tag{A.3}$$

Where, $\frac{dP}{d\alpha}$ is the marginal sensitivity; $\psi = \frac{\partial C}{\partial \alpha}$ is defined as the state sensitivity, a measure of the change in system state, C, due to a small change in one of the parameters, α (e.g., $\alpha = [u, \beta, M]$), while holding constant location x, time t, and other parameters in α.

In this equation, although the state sensitivity is unknown, adjoint theory can be used to eliminate it from the previous equation. This can be done by first differentiating the convection-dispersion equation (including initial and boundary conditions) with respect to the parameter, α, in order to obtain a form of the convection-dispersion equation in terms of the state sensitivity, ψ.

Differentiating the one dimensional convection-dispersion equation with its boundary and initial conditions with respect to α, yields,

Deducing process,

$$\frac{\partial}{\partial \alpha}\left(\frac{\partial C}{\partial t}\right) = \frac{\partial}{\partial t}\left(\frac{\partial C}{\partial \alpha}\right) = \frac{\partial \psi}{\partial t} \tag{A.4}$$

$$\frac{\partial}{\partial\alpha}\left(\frac{\partial uC}{\partial x}\right)=\frac{\partial}{\partial\alpha}\left(u\frac{\partial C}{\partial x}+C\frac{\partial u}{\partial x}\right)=\frac{\partial}{\partial\alpha}\left(u\frac{\partial C}{\partial x}\right)+\frac{\partial}{\partial\alpha}\left(C\frac{\partial u}{\partial x}\right)=\frac{\partial}{\partial x}(u\psi)+\frac{\partial}{\partial x}\left(C\frac{\partial u}{\partial\alpha}\right) \quad (A.5)$$

$$\frac{\partial}{\partial\alpha}\left(\frac{\partial}{\partial x}\left(\beta\frac{\partial C}{\partial x}\right)\right)=\frac{\partial}{\partial x}\left(\frac{\partial}{\partial\alpha}\left(\beta\frac{\partial C}{\partial x}\right)\right)=\frac{\partial}{\partial x}\left(\beta\frac{\partial}{\partial\alpha}\left(\frac{\partial C}{\partial x}\right)+\frac{\partial\beta}{\partial\alpha}\frac{\partial C}{\partial x}\right)=\frac{\partial}{\partial x}\left(\beta\frac{\partial\psi}{\partial x}+\frac{\partial\beta}{\partial\alpha}\frac{\partial C}{\partial x}\right)$$
$$=\frac{\partial}{\partial x}\left(\beta\frac{\partial\psi}{\partial x}\right)+\frac{\partial}{\partial x}\left(\frac{\partial\beta}{\partial\alpha}\frac{\partial C}{\partial x}\right) \quad (A.6)$$

$$\frac{\partial}{\partial\alpha}\left(Q_{source}\right)=\frac{\partial Q_{source}}{\partial\alpha} \quad (A.7)$$

Combine above four equations together, yields,

$$\frac{\partial\psi}{\partial t}+\frac{\partial}{\partial x}(u\psi)+\frac{\partial}{\partial x}\left(C\frac{\partial u}{\partial\alpha}\right)=\frac{\partial}{\partial x}\left(\beta\frac{\partial\psi}{\partial x}\right)+\frac{\partial}{\partial x}\left(\frac{\partial\beta}{\partial\alpha}\frac{\partial C}{\partial x}\right)+\frac{\partial Q_{source}}{\partial\alpha} \quad (A.8)$$

For the boundary conditions and initial condition:

$$\frac{\partial C(\vec{x},0)}{\partial\alpha}=\frac{\partial C_0}{\partial\alpha}\rightarrow\psi(\vec{x},0)=\frac{\partial C_0}{\partial\alpha} \quad (A.9)$$

$$\frac{\partial C(\vec{x},t)}{\partial\alpha}=\frac{\partial g_1(t)}{\partial\alpha}\rightarrow\psi(\vec{x},t)=0 \quad (A.10)$$

$$\frac{\partial}{\partial\alpha}\left(\beta\frac{\partial C}{\partial x}\right)=\frac{\partial\beta}{\partial\alpha}\frac{\partial C}{\partial x}+\beta\frac{\partial}{\partial\alpha}\left(\frac{\partial C}{\partial x}\right)=\frac{\partial\beta}{\partial\alpha}\frac{\partial C}{\partial x}+\beta\frac{\partial\psi}{\partial x}=\frac{\partial g_2(t)}{\partial\alpha}\rightarrow\frac{\partial\beta}{\partial\alpha}\frac{\partial C}{\partial x}+\beta\frac{\partial\psi}{\partial x}=0 \quad (A.11)$$

$$\frac{\partial}{\partial\alpha}\left(uC-\beta\frac{\partial C}{\partial x}\right)=\frac{\partial}{\partial\alpha}(uC)-\frac{\partial}{\partial\alpha}\left(\beta\frac{\partial C}{\partial x}\right)=\frac{\partial u}{\partial\alpha}C+\frac{\partial C}{\partial\alpha}u-\frac{\partial\beta}{\partial\alpha}\frac{\partial C}{\partial x}-\beta\frac{\partial}{\partial\alpha}\left(\frac{\partial C}{\partial x}\right)$$
$$\rightarrow\frac{\partial u}{\partial\alpha}C+\psi u-\frac{\partial\beta}{\partial\alpha}\frac{\partial C}{\partial x}-\beta\frac{\partial\psi}{\partial x}=0 \quad (A.12)$$

Above all, the equations are:

$$\begin{aligned}
&\frac{\partial \psi}{\partial t}+\frac{\partial}{\partial x}(u\psi)+\frac{\partial}{\partial x}\left(C\frac{\partial u}{\partial \alpha}\right)=\frac{\partial}{\partial x}\left(\beta\frac{\partial \psi}{\partial x}\right)+\frac{\partial}{\partial x}\left(\frac{\partial \beta}{\partial \alpha}\frac{\partial C}{\partial x}\right)+\frac{\partial Q_{source}}{\partial \alpha}\\
&\psi(\vec{x},0)=\frac{\partial C_0}{\partial \alpha}\\
&\psi(\vec{x},t)=0\\
&\frac{\partial \beta}{\partial \alpha}\frac{\partial C}{\partial x}+\beta\frac{\partial \psi}{\partial x}=0\\
&\frac{\partial u}{\partial \alpha}C+\psi u-\frac{\partial \beta}{\partial \alpha}\frac{\partial C}{\partial x}-\beta\frac{\partial \psi}{\partial x}=0
\end{aligned} \tag{A.13}$$

The next step is to obtain a similar form of the convection-dispersion equation in terms of the adjoint state, ψ^*, which, at this stage, is just an arbitrary function. Defining an inner product of two functions, we multiply ψ^* to the two sides of above convection-dispersion equation.

$$\int_0^T\int_{x_1}^{x_2}\left[\begin{aligned}
&-\psi^*\frac{\partial \psi}{\partial t}-\psi^*\frac{\partial}{\partial x}(u\psi)-\psi^*\frac{\partial}{\partial x}\left(C\frac{\partial u}{\partial \alpha}\right)+\psi^*\frac{\partial}{\partial x}\left(\beta\frac{\partial \psi}{\partial x}\right)\\
&+\psi^*\frac{\partial}{\partial x}\left(\frac{\partial \beta}{\partial \alpha}\frac{\partial C}{\partial x}\right)+\psi^*\frac{\partial Q_{source}}{\partial \alpha}
\end{aligned}\right]dxdt=0 \tag{A.14}$$

Change the equation type:

$$\int_0^T\int_{x_1}^{x_2}\left[-\psi^*\frac{\partial \psi}{\partial t}\right]dxdt=\int_0^T\int_{x_1}^{x_2}\left[-\frac{\partial(\psi\psi^*)}{\partial t}+\psi\frac{\partial \psi^*}{\partial t}\right]dxdt \tag{A.15}$$

$$\int_0^T\int_{x_1}^{x_2}\left[\psi^*\frac{\partial}{\partial x}\left(\beta\frac{\partial\psi}{\partial x}\right)\right]dxdt$$
$$=\int_0^T\int_{x_1}^{x_2}\left[\frac{\partial}{\partial x}\left(\beta\psi^*\frac{\partial\psi}{\partial x}\right)-\beta\frac{\partial}{\partial x}\left(\psi^*\frac{\partial\psi}{\partial x}\right)\right]dxdt \tag{A.16}$$
$$=\int_0^T\int_{x_1}^{x_2}\left[\frac{\partial}{\partial x}\left(\beta\psi^*\frac{\partial\psi}{\partial x}\right)-\frac{\partial}{\partial x}\left(\beta\psi\frac{\partial\psi^*}{\partial x}\right)+\psi\frac{\partial}{\partial x}\left(\beta\frac{\partial\psi^*}{\partial x}\right)\right]dxdt$$

$$\int_0^T\int_{x_1}^{x_2}\left[-\psi^*\frac{\partial}{\partial x}(u\psi)\right]dxdt=\int_0^T\int_{x_1}^{x_2}\left[-\frac{\partial}{\partial x}\left(u\psi\psi^*\right)+u\psi\frac{\partial}{\partial x}\left(\psi^*\right)\right]dxdt \tag{A.17}$$

Substituting the above three equations into the CDE and rearranging the different terms, yields,

$$\int_0^T\int_{x_1}^{x_2}\left\{\begin{array}{l}\psi\left[\frac{\partial\psi^*}{\partial t}+\frac{\partial}{\partial x}\left(\beta\frac{\partial\psi^*}{\partial x}\right)+u\frac{\partial}{\partial x}\left(\psi^*\right)\right]+\psi^*\frac{\partial}{\partial x}\left(\frac{\partial\beta}{\partial\alpha}\frac{\partial C}{\partial x}\right)-\psi^*\frac{\partial}{\partial x}\left(C\frac{\partial u}{\partial\alpha}\right)+\psi^*\frac{\partial Q_{source}}{\partial\alpha}\\ +\frac{\partial}{\partial x}\left(\beta\psi^*\frac{\partial\psi}{\partial x}-\beta\psi\frac{\partial\psi^*}{\partial x}-u\psi\psi^*\right)-\frac{\partial\left(\psi\psi^*\right)}{\partial t}\end{array}\right\}dxdt=0 \tag{A.18}$$

Since the left-hand side of this equation is equal to zero, it can be added to the right-hand side of the marginal sensitivity equation. Gives:

$$\frac{dP}{d\alpha}=\int_0^T\int_{x_1}^{x_2}\left\{\begin{array}{l}\dfrac{\partial h(\alpha,C)}{\partial\alpha}+\psi\left[\dfrac{\partial h(\alpha,C)}{\partial C}+\dfrac{\partial\psi^*}{\partial t}+\dfrac{\partial}{\partial x}\left(\beta\dfrac{\partial\psi^*}{\partial x}\right)+u\dfrac{\partial}{\partial x}\left(\psi^*\right)\right]+\psi^*\dfrac{\partial}{\partial x}\left(\dfrac{\partial\beta}{\partial\alpha}\dfrac{\partial C}{\partial x}\right)\\ -\psi^*\dfrac{\partial}{\partial x}\left(C\dfrac{\partial u}{\partial\alpha}\right)+\psi^*\dfrac{\partial Q_{source}}{\partial\alpha}+\dfrac{\partial}{\partial x}\left(\beta\psi^*\dfrac{\partial\psi}{\partial x}-\beta\psi\dfrac{\partial\psi^*}{\partial x}-u\psi\psi^*\right)-\dfrac{\partial\left(\psi\psi^*\right)}{\partial t}\end{array}\right\}dxdt$$

(A.19)

The last two terms in this equation are divergence terms, which, after integration, are evaluated at the boundary conditions. Thus these terms can be simplified as following:

$$\int_0^T\int_{x_1}^{x_2}\left[\frac{\partial}{\partial x}\left(\beta\psi^*\frac{\partial\psi}{\partial x}-\beta\psi\frac{\partial\psi^*}{\partial x}-u\psi\psi^*\right)\right]dxdt=\int_0^T\left[\beta\psi^*\frac{\partial\psi}{\partial x}-\beta\psi\frac{\partial\psi^*}{\partial x}-u\psi\psi^*\right]_{x=x1,x=x2}dt \quad \text{(A.20)}$$

$$\int_0^T\int_{x_1}^{x_2}\left[-\frac{\partial\left(\psi\psi^*\right)}{\partial t}\right]dxdt=\int_{x1}^{x2}\left[-\frac{\partial\left(\psi\psi^*\right)}{\partial t}\right]_{t=0,t=T}dt \quad \text{(A.21)}$$

As we know, the goal of this process is to eliminate the unknown state sensitivity, ψ .And ψ^* is still an arbitrary function. Thus the adjoint state, ψ^* can be defined in such a way as to eliminate the state sensitivity, ψ . From these considerations, the governing equation for the adjoint state is:

$$\frac{\partial h(\alpha,C)}{\partial C}+\frac{\partial\psi^*}{\partial t}+\frac{\partial}{\partial x}\left(\beta\frac{\partial\psi^*}{\partial x}\right)+u\frac{\partial}{\partial x}\left(\psi^*\right)=0 \quad \text{(A.22)}$$

$$\left[\beta\psi^* \frac{\partial \psi}{\partial x} - \beta\psi \frac{\partial \psi^*}{\partial x} - u\psi\psi^* \right]_{x=x1, x=x2} = 0 \tag{A.23}$$

$$\left[-\frac{\partial \left(\psi\psi^* \right)}{\partial t} \right]_{t=0, t=T} = 0 \tag{A.24}$$

According to the above initial conditions and boundary conditions,

$$\begin{aligned} &\psi\left(\vec{x}, 0\right) = \frac{\partial C_0}{\partial \alpha} \\ &\psi\left(\vec{x}, t\right) = 0 \\ &\frac{\partial \beta}{\partial \alpha}\frac{\partial C}{\partial x} + \beta\frac{\partial \psi}{\partial x} = 0 \\ &\frac{\partial u}{\partial \alpha} C + \psi u - \frac{\partial \beta}{\partial \alpha}\frac{\partial C}{\partial x} - \beta\frac{\partial \psi}{\partial x} = 0 \end{aligned} \tag{A.25}$$

We can get the initial condition and boundary conditions for ψ^*, which are shown as following:

$$\begin{aligned} &\psi^*\left(T\right) = 0 \\ &\psi^* = 0 \\ &\beta\frac{\partial \psi^*}{\partial x} + u\psi^* = 0 \\ &\beta\frac{\partial \psi^*}{\partial x} = 0 \end{aligned} \tag{A.26}$$

In order to solve ψ^*, we define a new time variable, the backward time, $\tau = \mathrm{T} - \mathrm{t}$. Then the initial condition of ψ^* in backward time is $\psi^*(\tau = 0) = 0$.

Therefore, the complete adjoint equation in terms of backward time with defined initial and boundary conditions, is:

$$\begin{aligned}
&\frac{\partial \psi^*}{\partial t} = \frac{\partial}{\partial x}\left(\beta \frac{\partial \psi^*}{\partial x}\right) + u\frac{\partial}{\partial x}\left(\psi^*\right) + \frac{\partial h}{\partial C} \\
&\psi^*(\vec{x}, 0) = 0 \\
&\psi^*(\vec{x}, \tau) = 0 \\
&\beta \frac{\partial \psi^*}{\partial x} + u\psi^* = 0 \\
&\beta \frac{\partial \psi^*}{\partial x} = 0 \\
&\frac{\partial h}{\partial C} = \delta(\vec{x} - \vec{x}_w) \bullet \delta(\tau)
\end{aligned} \tag{A.27}$$

Where, $\frac{\partial h}{\partial C}$ can be defined as the load term (Neupauer, 2000); ψ^* is the adjoint probability; τ is the backward time; $\vec{x}_m$ is the measurement locations. In the inverse model, the load term can be considered as a unit source. Other parameters are same with those of forward transport equation.

Appendix B: Adjoint Backward Probability Equation Deriving Process for Well-mixed Zones

Multi-zone models represent a building as a network of well-mixed spaces, or zones, connected by flow elements, or links. The multi-zone model calculates air flow rate and contaminant concentration in each zone based on the mass balance. Empirical nonlinear mathematical models are usually used, which is the relationship between the flow and the pressure difference across a crack or opening in the building envelope.

$$\mathrm{F} = \mathrm{C}\left(\Delta P\right)^{n} \tag{B.1}$$

Where, F is the air flow rate in zone, [kg/s]; P is the pressure, [Pa].

For each zone,

$$\begin{aligned} \frac{\partial \mathrm{m}}{\partial \mathrm{t}} &= \sum F \\ \frac{\partial \left(\mathrm{mC}\right)}{\partial \mathrm{t}} &= \sum \left(FC\right) \end{aligned} \tag{B.2}$$

The mass of contaminant k in interior zone i is:

$$\begin{aligned} m_{k,i} &= Q_i \cdot C_{k,i} \\ \frac{\mathrm{d}m_{k,i}}{\mathrm{dt}} &= Q_i \frac{dC_{k,i}}{dt} \end{aligned} \tag{B.3}$$

Q_i is the zone volume. The mass of contaminant k in zone i will vary due to several process:

(1) Outward airflows from zone i at the rate of $\sum_{j=0,\neq i}^{n} F_{i,j} \cdot C_{k,i}$

$F_{i,j}$ is the air flow rate from zone i to adjacent zone j;

(2) Inward airflows to zone i at the rate of $\sum_{j=0,\neq i}^{n}(1-\eta_{k,j,i})F_{j,i}\cdot C_{k,j}$ where $\eta_{k,j,i}$ is the filter efficiency in the path from zone j to zone i;

(3) Removal at the rate of $C_{k,i}\cdot R_{k,i}$ where $R_{k,i}$ is a removal coefficient;

(4) Generation at the rate of $G_{k,i}$;

(5) First order chemical reactions with other contaminants $C_{l,i}$ at the rate of $Q_i\sum_l k_{k,l}\cdot C_{l,i}$ where $K_{k,l}$ is the kinetic reaction coefficient in zone i between species k and l (positive $K_{k,l}$ for generation and negative $K_{k,l}$ for removal)

Therefore, according to the mass balance:

$$\frac{\mathrm{d}m_{k,i}}{\mathrm{dt}}=Q_i\frac{dC_{k,i}}{dt}=\sum_{j=0,\neq i}^{n}\left(1-\eta_{k,j,i}\right)F_{j,i}\cdot C_{k,j}+G_{k,i}+Q_i\sum_l k_{k,l}\cdot C_{l,i}-\sum_{j=0,\neq i}^{n}F_{i,j}\cdot C_{k,i}-C_{k,i}\cdot R_{k,i}$$
$$=\left[\sum_{j=0,\neq i}^{n}\left(1-\eta_{k,j,i}\right)F_{j,i}\cdot C_{k,j}--\sum_{j=0,\neq i}^{n}F_{i,j}\cdot C_{k,i}\right]+\left[Q_i\sum_l k_{k,l}\cdot C_{l,i}+G_{k,i}-C_{k,i}\cdot R_{k,i}\right] \quad \text{(B.4)}$$

$$\frac{dC_{k,i}}{dt}=\left[\sum_{j=0,\neq i}^{n}\frac{\left(1-\eta_{k,j,i}\right)F_{j,i}}{Q_i}\cdot C_{k,j}--\sum_{j=0,\neq i}^{n}\frac{F_{i,j}}{Q_i}\cdot C_{k,i}\right]+\left[\sum_l k_{k,l}\cdot C_{l,i}+\frac{G_{k,i}}{Q_i}-C_{k,i}\cdot\frac{R_{k,i}}{Q_i}\right]$$
$$=\sum_{m=1}^{n}A_{k,i,m}\cdot C_{k,m}+B_{k,i} \quad \text{(B.5)}$$
$$C_{k,i}(0)=C_{k,initial}$$

The coefficients in above equation:

$$A_{k,i,m}=\begin{cases}\dfrac{-R_{m,i}-\sum_{j=0,\neq i}^{n}F_{i,j}}{Q_i}, & (m=i,m\neq 0)\\ \dfrac{F_{m,i}\left(1-\eta_{k,m,i}\right)}{Q_i}, & (m\neq i,m\neq 0)\end{cases} \quad \text{(B.6)}$$

For a building with n interior zones, Ck,i distribution in the entire building can be expressed with a concentration vector $\overline{C_k} = \left(C_{k,1}, C_{k,2} \cdots C_{k,n}\right)^T$, which is a function of time t. The contaminant concentration transport equation for a whole building with n interior zones can thus be written in a matrix equation format like this:

$$\begin{aligned} &\frac{d\overline{C_k}}{dt} = A \cdot \overline{C_k} + B \\ &\overline{C_k}(0) = \overline{C_{k,initial}} \end{aligned} \tag{B.7}$$

Where,

$$\begin{aligned} A &= \begin{bmatrix} A_{k,1,1} & A_{k,1,2} & A_{k,1,3} & \cdots & A_{k,1,n} \\ \vdots & & & \ddots & \vdots \\ A_{k,n,1} & A_{k,n,2} & A_{k,n,3} & \cdots & A_{k,n,n} \end{bmatrix} \\ B &= \left(B_{k,1}\, B_{k,2}\, B_{k,3} \cdots B_{k,n}\right)^T \end{aligned} \tag{B.8}$$

Following same procedures as deducing one-D convection-diffusion equation, the adjoint equation for equation can be obtained as following:

$$\begin{aligned} &\frac{\partial \psi^*}{\partial \tau} = A^T \cdot \psi^* + \frac{\partial h}{\partial C} \\ &\psi^*\left(\vec{x}, \tau = 0\right) = 0 \end{aligned} \tag{B.9}$$

Where, $\frac{\partial h}{\partial C}$ can be defined as the load term, which can be considered as a unit source; ψ^* is the adjoint probability; τ is the backward time; A^T is the transpose matrix of A. Other parameters are same with those of forward transport equation.

Appendix C: Analytical Solution of 1 Dimensional Convection Dispersion Equation without Source Term

General governing contaminant transport equation is defined as following equation (convection-dispersion equation):

$$\frac{\partial(\rho C)}{\partial t}+\frac{\partial(\rho u C)}{\partial x}=\frac{\partial}{\partial x}\left(\tau\frac{\partial C}{\partial x}\right)+q_{source} \tag{C.1}$$

Where, $\frac{\partial(\rho C)}{\partial t}$ is the transient term; $\frac{\partial(\rho u C)}{\partial x}$ is the convection term; $\frac{\partial}{\partial x}\left(\tau\frac{\partial C}{\partial x}\right)$ is the dispersion term; q_{source} is the source term. In this equation, C is the contaminant resident concentration; ρis the density of air; u is the velocity of air flow; τ is the dispersion coefficient.

In this research, ρ, u, and τ are constant, there is no source term. The Convection-Diffusion Equation (ADE) was simplified into the following equation according to above analysis:

$$\begin{aligned}&\frac{\partial(C)}{\partial t}+u\frac{\partial(C)}{\partial x}=E\frac{\partial}{\partial x}\left(\frac{\partial C}{\partial x}\right)\\&C(x,0)=0\\&C(0,t)=C_0\\&\left.\frac{\partial C}{\partial x}\right|_{x=L}=0\end{aligned} \tag{C.2}$$

Where, E is the dispersion coefficient [m^2/s]. Initial Condition is $C(x,0)=0$;

Boundary Conditions are $C(0,t)=C_0$; assume a continuous input point source, $\left.\frac{\partial \mathrm{C}}{\partial \mathrm{x}}\right|_{x=L}=0$

The problem is to characterize the contaminant concentration as a function of x and t.

Solution:

To reduce above Advection-Diffusion Equation to a more familiar form (remove the advection term), assume

$$\mathrm{C}(\mathrm{x},\mathrm{t})=\mathrm{K}(\mathrm{x},\mathrm{t})\exp\left(\frac{ux}{2E}-\frac{u^2t}{4E}\right) \tag{C.3}$$

$$\frac{\partial \mathrm{C}}{\partial \mathrm{t}}=\frac{\partial \mathrm{K}}{\partial \mathrm{t}}\exp\left(\frac{\mathrm{ux}}{2\mathrm{E}}-\frac{\mathrm{u}^2\mathrm{t}}{4\mathrm{E}}\right)+\mathrm{K}(\mathrm{x},\mathrm{t})\left(-\frac{\mathrm{u}^2}{4\mathrm{E}}\right)\exp\left(\frac{\mathrm{ux}}{2\mathrm{E}}-\frac{\mathrm{u}^2\mathrm{t}}{4\mathrm{E}}\right) \tag{C.4}$$

$$\frac{\partial \mathrm{C}}{\partial \mathrm{x}}=\frac{\partial \mathrm{K}}{\partial \mathrm{x}}\exp\left(\frac{\mathrm{ux}}{2\mathrm{E}}-\frac{\mathrm{u}^2\mathrm{t}}{4\mathrm{E}}\right)+\mathrm{K}(\mathrm{x},\mathrm{t})\left(\frac{\mathrm{u}}{2\mathrm{E}}\right)\exp\left(\frac{\mathrm{ux}}{2\mathrm{E}}-\frac{\mathrm{u}^2\mathrm{t}}{4\mathrm{E}}\right) \tag{C.5}$$

$$\begin{aligned}\frac{\partial}{\partial \mathrm{x}}\left(\frac{\partial \mathrm{C}}{\partial \mathrm{x}}\right)&=\frac{\partial}{\partial \mathrm{x}}\left(\frac{\partial \mathrm{K}}{\partial \mathrm{x}}\right)\exp\left(\frac{\mathrm{ux}}{2\mathrm{E}}-\frac{\mathrm{u}^2\mathrm{t}}{4\mathrm{E}}\right)+\frac{\partial \mathrm{K}}{\partial \mathrm{x}}\left(\frac{\mathrm{u}}{2\mathrm{E}}\right)\exp\left(\frac{\mathrm{ux}}{2\mathrm{E}}-\frac{\mathrm{u}^2\mathrm{t}}{4\mathrm{E}}\right)\\&+\frac{\partial \mathrm{K}}{\partial \mathrm{x}}\left(\frac{\mathrm{u}}{2\mathrm{E}}\right)\exp\left(\frac{\mathrm{ux}}{2\mathrm{E}}-\frac{\mathrm{u}^2\mathrm{t}}{4\mathrm{E}}\right)+\mathrm{K}(\mathrm{x},\mathrm{t})\left(\frac{\mathrm{u}}{2\mathrm{E}}\right)\left(\frac{\mathrm{u}}{2\mathrm{E}}\right)\exp\left(\frac{\mathrm{ux}}{2\mathrm{E}}-\frac{\mathrm{u}^2\mathrm{t}}{4\mathrm{E}}\right)\end{aligned} \tag{C.6}$$

$$\begin{aligned}\frac{\partial}{\partial \mathrm{x}}\left(\frac{\partial C}{\partial x}\right)&=\frac{\partial}{\partial \mathrm{x}}\left(\frac{\partial K}{\partial x}\right)\exp\left(\frac{ux}{2E}-\frac{u^2t}{4E}\right)+\frac{\partial \mathrm{K}}{\partial \mathrm{x}}\left(\frac{u}{E}\right)\exp\left(\frac{ux}{2E}-\frac{u^2t}{4E}\right)\\&+K(x,t)\left(\frac{u}{2E}\right)^2\exp\left(\frac{ux}{2E}-\frac{u^2t}{4E}\right)\end{aligned} \tag{C.7}$$

Substitute above three equations, $\frac{\partial \mathrm{C}}{\partial \mathrm{t}}$, $\frac{\partial \mathrm{C}}{\partial \mathrm{x}}$, $\frac{\partial}{\partial \mathrm{x}}\left(\frac{\partial C}{\partial x}\right)$ into the convection dispersion equation, get

$$\frac{\partial \mathrm{K}}{\partial \mathrm{t}} = \mathrm{E}\frac{\partial}{\partial \mathrm{x}}\left(\frac{\partial \mathrm{K}}{\partial \mathrm{x}}\right) \tag{C.8}$$

The convection term is vanish with transient term and diffusion term left. This equation belongs to parabolic type PDE equation. So this equation can be solved easily.

New Initial Condition and Boundary Conditions are employed:

$$\begin{aligned} &\mathrm{C}(x,0) = K(x,0)\exp\left(\frac{ux}{2E}\right) = 0 \\ &K(x,0) = 0 \end{aligned} \tag{C.9}$$

$$\begin{aligned} &\mathrm{C}(0,\mathrm{t}) = \mathrm{K}(0,\mathrm{t})\exp\left(-\frac{u^2 t}{4E}\right) = C_0 \\ &\mathrm{K}(0,\mathrm{t}) = C_0\exp\left(\frac{u^2 t}{4E}\right) \end{aligned} \tag{C.10}$$

$$\begin{aligned} &\left.\frac{\partial C}{\partial x}\right|_{x=L} = \left[\frac{\partial \mathrm{K}}{\partial \mathrm{x}}\exp\left(\frac{ux}{2E}-\frac{u^2 t}{4E}\right) + K(x,t)\left(\frac{u}{2E}\right)\exp\left(\frac{ux}{2E}-\frac{u^2 t}{4E}\right)\right]\Bigg|_{x=L} = 0 \\ &\left[\frac{\partial \mathrm{K}}{\partial \mathrm{x}} + K(x,t)\left(\frac{u}{2E}\right)\right]\Bigg|_{x=L} = 0 \end{aligned} \tag{C.11}$$

Above all, new convection dispersion equation and its initial condition and boundary conditions were given as following:

$$\frac{\partial \mathrm{K}}{\partial \mathrm{t}} = \mathrm{E}\frac{\partial}{\partial \mathrm{x}}\left(\frac{\partial K}{\partial x}\right)$$
$$K\left(x,0\right) = 0$$
$$\mathrm{K}\left(0,\mathrm{t}\right) = C_0 \exp\left(\frac{u^2 t}{4E}\right) \tag{C.12}$$
$$\left[\frac{\partial \mathrm{K}}{\partial \mathrm{x}} + K\left(x,t\right)\left(\frac{u}{2E}\right)\right]\Bigg|_{x=L} = 0$$

Applying **Laplace Transformation** above initial and boundary conditions reduced to an ordinary second order boundary value problem, which comprises of the following three equations:

Laplace Transformation Method:

$$\bar{K} = \int_0^\infty K\left(x,t\right)e^{-st}dt \tag{C.13}$$

$\frac{\partial \mathrm{K}}{\partial \mathrm{t}} = \mathrm{E}\frac{\partial}{\partial \mathrm{x}}\left(\frac{\partial K}{\partial x}\right)$ is multiplied by e^{-st} and integrated term by term, it is reduced to an ordinary differential equation:

$$\frac{\mathrm{d}}{\mathrm{dx}}\left(\frac{d\bar{K}}{dx}\right) - \frac{s}{E}\bar{K} = 0 \tag{C.14}$$

Deducing process for the above equation:

$$\begin{aligned}\int_0^\infty \frac{\partial K}{\partial t}e^{-st}dt = \int_0^\infty \left[\frac{\partial\left(Ke^{-st}\right)}{\partial t} + Ke^{-st}s\right]dt &= \int_0^\infty \frac{\partial\left(Ke^{-st}\right)}{\partial t}dt + \int_0^\infty Ke^{-st}sdt \\ &= \left[Ke^{-st}\right]_0^\infty + s\bar{K} = 0 - \left[Ke^{-st}\right]_0 + s\bar{K} = s\bar{K}\end{aligned} \tag{C.15}$$

$$\int_0^\infty E\frac{\partial^2 K}{\partial x^2}e^{-st}dt = E\int_0^\infty \frac{\partial^2 K}{\partial x^2}e^{-st}dt = E\frac{\partial^2}{\partial x^2}\int_0^\infty Ke^{-st}dt = E\frac{\partial^2 \bar{K}}{\partial x^2} \tag{C.16}$$

Thus,

$$\frac{\partial^2 \overline{K}}{\partial x^2} - \frac{s}{E}\overline{K} = 0 \tag{C.17}$$

Boundary Conditions:

$$\begin{aligned}\int_0^\infty K(0,t)e^{-st}dt = \int_0^\infty C_0 \exp\left(\frac{u^2 t}{4E}\right)e^{-st}dt = C_0\int_0^\infty \exp\left(a^2 t\right)e^{-st}dt \\ = \frac{C_0}{a^2 - s}\left[e^{-\left(s-a^2\right)t}\right]_0^\infty = \frac{C_0}{s-a^2}\end{aligned} \tag{C.18}$$

$$\overline{K}(0,s) = \frac{C_0}{s-a^2}, \tag{C.19}$$

Where, $a^2 = u^2 / 4E$

$$\begin{aligned}\int_0^\infty \left(\frac{\partial K}{\partial x} + K\frac{u}{2E}\right)e^{-st}dt = \int_0^\infty \frac{\partial K}{\partial x}e^{-st}dt + \int_0^\infty K\frac{u}{2E}e^{-st}dt \\ = \frac{\partial}{\partial x}\int_0^\infty Ke^{-st}dt + \frac{u}{2E}\int_0^\infty Ke^{-st}dt = \frac{\partial \overline{K}}{\partial x} + \frac{u}{2E}\overline{K}\end{aligned} \tag{C.20}$$

$$\left[\frac{\mathrm{d}\overline{K}}{\mathrm{dx}} + \frac{u}{2E}\overline{K}\right]_{x=L} = 0 \tag{C.21}$$

The solution of above governing equation is shown as following:

$$\overline{K} = \mathrm{A}e^{-qx} + Be^{qx} \tag{C.22}$$

Where, $\mathrm{q} = \sqrt{s/E}$

According to the boundary conditions,

As x=0, $\mathrm{A} + \mathrm{B} = \frac{C_0}{s-a^2}$

As x=L, $\left(-q+\frac{u}{2E}\right)Ae^{-qx}+\left(q+\frac{u}{2E}\right)Be^{qx}=0$

Based on the two equations:

B=0; $A=\frac{C_0}{s-a^2}$; $q=\frac{u}{2E}$

So the particular solution of this boundary value problem is obtained as:

$$\bar{K}(x,s)=\frac{C_0}{s-a^2}\exp\left(\left(-\sqrt{s/E}\right)x\right) \tag{C.23}$$

Employing inverse Laplace Transformation on it, using the appropriate tables (Van Genuchten and Alves, 1982) and using the necessary transformations, we may get the desired solution as:

$$K(t)=\frac{C_0}{2E}\left[\exp\left(\frac{u^2}{4E^2}t-\frac{u}{2E}x\right)erfc\left(\frac{x}{2\sqrt{t}}-\frac{u}{2E}\sqrt{t}\right)+\exp\left(\frac{u^2}{4E^2}t+\frac{u}{2E}x\right)erfc\left(\frac{x}{2\sqrt{t}}+\frac{u}{2E}\sqrt{t}\right)\right] \tag{C.24}$$

Deducing process for the above equation:

According to the Laplace Transformation table,

$$
\begin{aligned}
&f(s):\frac{e^{-x\sqrt{s}}}{s-a^2}\\
&F(t):\frac{1}{2}(C+D)\\
&C=\exp\left(a^2t-ax\right)erfc\left(\frac{x}{2\sqrt{t}}-a\sqrt{t}\right)\\
&D=\exp\left(a^2t+ax\right)erfc\left(\frac{x}{2\sqrt{t}}+a\sqrt{t}\right)
\end{aligned}
\tag{C.25}
$$

$$
\bar{K}(x,s)=\frac{C_0}{s-a^2}\exp\left(\left(-\sqrt{s/E}\right)x\right) \tag{C.26}
$$

Assume

$$
\begin{aligned}
&S_1=\frac{S}{E}\\
&S=S_1E\\
&a_1^2=\frac{a^2}{E}=\frac{a^2}{4E^2}
\end{aligned}
\tag{C.27}
$$

$$
\bar{K}(x,s)=\frac{C_0}{s-a^2}\exp\left(\left(-\sqrt{s/E}\right)x\right)=\frac{C_0}{ES_1-a^2}\exp\left(-\sqrt{S_1}x\right)=\frac{C_0}{E}\frac{1}{S_1-a_1^2}\exp\left(-\sqrt{S_1}x\right) \tag{C.28}
$$

$$
K(t)=\frac{C_0}{2E}\left[\exp\left(a_1^2t-a_1x\right)erfc\left(\frac{x}{2\sqrt{t}}-a_1\sqrt{t}\right)+\exp\left(a_1^2t+a_1x\right)erfc\left(\frac{x}{2\sqrt{t}}+a_1\sqrt{t}\right)\right] \tag{C.29}
$$

$$
K(t)=\frac{C_0}{2E}\left[\exp\left(\frac{u^2}{4E^2}t-\frac{u}{2E}x\right)erfc\left(\frac{x}{2\sqrt{t}}-\frac{u}{2E}\sqrt{t}\right)+\exp\left(\frac{u^2}{4E^2}t+\frac{u}{2E}x\right)erfc\left(\frac{x}{2\sqrt{t}}+\frac{u}{2E}\sqrt{t}\right)\right] \tag{C.30}
$$

According to the assumption,

$$
\mathrm{C}(\mathrm{x},\mathrm{t})=\mathrm{K}(\mathrm{x},\mathrm{t})\exp\left(\frac{ux}{2E}-\frac{u^2t}{4E}\right)
$$

Then we may get the analytical solution of the contaminant concentration as following:

$$C(x,t)=\frac{C_0}{2E}\left[\begin{array}{l}\exp\left(\frac{u^2}{4E^2}t-\frac{u}{2E}x\right)erfc\left(\frac{x}{2\sqrt{t}}-\frac{u}{2E}\sqrt{t}\right)+\\ \exp\left(\frac{u^2}{4E^2}t+\frac{u}{2E}x\right)erfc\left(\frac{x}{2\sqrt{t}}+\frac{u}{2E}\sqrt{t}\right)\end{array}\right]\bullet\exp\left(\frac{ux}{2E}-\frac{u^2}{4E}t\right) \qquad (C.31)$$

Where erfc is the complementary error function, is defined as:

$$\mathrm{erfc}(x)=1-\mathrm{erf}(x)=\frac{2}{\sqrt{\pi}}\int_x^{\infty}e^{-t^2}dt$$

erf(x) is the error function, as called the Gauss error function

$$\mathrm{erf}(x)=\frac{2}{\sqrt{\pi}}\int_0^{x}e^{-t^2}dt$$

In our equation:

$$erfc\left(\frac{x-ut}{2\sqrt{Et}}\right)=\frac{2}{\sqrt{\pi}}\int_{\frac{x-ut}{2\sqrt{Et}}}^{\infty}e^{-t^2}dt$$

$$erfc\left(\frac{x+ut}{2\sqrt{Et}}\right)=\frac{2}{\sqrt{\pi}}\int_{\frac{x+ut}{2\sqrt{Et}}}^{\infty}e^{-t^2}dt$$

Another method applied solving the one dimensional convection dispersion equation was directly from Van Genuchten M.Th. and Alves W. J., which was shown in following:

$$C(x,t) = C_0 * A(x,t)$$

$$A(x,t) = 0.5 * erfc\left[\frac{x-ut}{2\sqrt{Et}}\right] + 0.5 * \exp\left(\frac{ux}{E}\right) erfc\left(\frac{x+ut}{2\sqrt{Et}}\right) + 0.5 * \left[2 + \frac{u(2L-x)}{E} + \frac{u^2 t}{E}\right] \quad \text{(C.32)}$$

$$\exp\left(\frac{uL}{E}\right) erfc\left(\frac{2L-x+ut}{2\sqrt{Et}}\right) - \sqrt{\frac{u^2 t}{\pi E}} \exp\left[\frac{uL}{E} - \frac{1}{4Et}(2L-x+ut)^2\right]$$

This equation was adopted in this research to calculate the one dimensional convection dispersion equation.

Appendix D Sensitivity Analysis of Sensor Locations

The section documents the sensitivity analysis of sensor locations. It's presumed that source location is among the eight points in CONTAM model of figure 5-1. Based on the description of sensitivity analysis in section 6.3, results were shown as following.

Under the cases of only single current concentration recording sensor:

Source in Point 1		Source in Point 2		Source in Point 3		Source in Point 4	
Scenarios	Sensor Location	Scenarios	Sensor Location	Scenarios	Sensor Location	Scenarios	Sensor Location
Scenario 1	Point 2	Scenario 1	Point 1	Scenario 1	Point 1	Scenario 1	Point 1
Scenario 2	Point 3	Scenario 2	Point 3	Scenario 2	Point 2	Scenario 2	Point 2
Scenario 3	Point 4	Scenario 3	Point 4	Scenario 3	Point 4	Scenario 3	Point 3
Scenario 4	Point 5	Scenario 4	Point 5	Scenario 4	Point 5	Scenario 4	Point 5
Scenario 5	Point 6	Scenario 5	Point 6	Scenario 5	Point 6	Scenario 5	Point 6
Scenario 6	Point 7	Scenario 6	Point 7	Scenario 6	Point 7	Scenario 6	Point 7
Scenario 7	Point 8	Scenario 7	Point 8	Scenario 7	Point 8	Scenario 7	Point 8
Source in Point 5		**Source in Point 6**		**Source in Point 7**		**Source in Point 8**	
Scenarios	Sensor Location	Scenarios	Sensor Location	Scenarios	Sensor Location	Scenarios	Sensor Location
Scenario 1	Point 1	Scenario 1	Point 1	Scenario 1	Point 1	Scenario 1	Point 1
Scenario 2	Point 2	Scenario 2	Point 2	Scenario 2	Point 2	Scenario 2	Point 2
Scenario 3	Point 3	Scenario 3	Point 3	Scenario 3	Point 3	Scenario 3	Point 3
Scenario 4	Point 4	Scenario 4	Point 4	Scenario 4	Point 4	Scenario 4	Point 4
Scenario 5	Point 6	Scenario 5	Point 5	Scenario 5	Point 5	Scenario 5	Point 5
Scenario 6	Point 7	Scenario 6	Point 7	Scenario 6	Point 6	Scenario 6	Point 6
Scenario 7	Point 8	Scenario 7	Point 8	Scenario 7	Point 8	Scenario 7	Point 7

Note: scenarios highlighted with red characters indicate the scenarios identify source location accurately.

Under the cases of only single historical concentration recording sensor:

Source in Point 1		Source in Point 2		Source in Point 3		Source in Point 4	
Scenarios	Sensor Location	Scenarios	Sensor Location	Scenarios	Sensor Location	Scenarios	Sensor Location
Scenario 1	Point 2	Scenario 1	Point 1	Scenario 1	Point 1	Scenario 1	Point 1
Scenario 2	Point 3	Scenario 2	Point 3	Scenario 2	Point 2	Scenario 2	Point 2
Scenario 3	Point 4	Scenario 3	Point 4	Scenario 3	Point 4	Scenario 3	Point 3
Scenario 4	Point 5	Scenario 4	Point 5	Scenario 4	Point 5	Scenario 4	Point 5
Scenario 5	Point 6	Scenario 5	Point 6	Scenario 5	Point 6	Scenario 5	Point 6
Scenario 6	Point 7	Scenario 6	Point 7	Scenario 6	Point 7	Scenario 6	Point 7
Scenario 7	Point 8	Scenario 7	Point 8	Scenario 7	Point 8	Scenario 7	Point 8
Source in Point 5		**Source in Point 6**		**Source in Point 7**		**Source in Point 8**	
Scenarios	Sensor Location	Scenarios	Sensor Location	Scenarios	Sensor Location	Scenarios	Sensor Location
Scenario 1	Point 1	Scenario 1	Point 1	Scenario 1	Point 1	Scenario 1	Point 1
Scenario 2	Point 2	Scenario 2	Point 2	Scenario 2	Point 2	Scenario 2	Point 2
Scenario 3	Point 3	Scenario 3	Point 3	Scenario 3	Point 3	Scenario 3	Point 3
Scenario 4	Point 4	Scenario 4	Point 4	Scenario 4	Point 4	Scenario 4	Point 4
Scenario 5	Point 6	Scenario 5	Point 5	Scenario 5	Point 5	Scenario 5	Point 5
Scenario 6	Point 7	Scenario 6	Point 7	Scenario 6	Point 6	Scenario 6	Point 6
Scenario 7	Point 8	Scenario 7	Point 8	Scenario 7	Point 8	Scenario 7	Point 7

Note: scenarios highlighted with red characters indicate the scenarios identify source location accurately.

Under the cases of two current concentration recording sensors:

Source in Point 1			Source in Point 2		
	Scenarios	Sensor Locations		Scenarios	Sensor Locations
Supply	Scenario 1	Point 2, Point 3	Supply	Scenario 1	Point 1, Point 3
	Scenario 2	Point 2, Point 4		Scenario 2	Point 1, Point 4
	Scenario 3	Point 3, Point 4		Scenario 3	Point 3, Point 4
Return	Scenario 4	Point 5, Point 6	Return	Scenario 4	Point 5, Point 6
	Scenario 5	Point 5, Point 7		Scenario 5	Point 5, Point 7
	Scenario 6	Point 5, Point 8		Scenario 6	Point 5, Point 8
	Scenario 7	Point 6, Point 7		Scenario 7	Point 6, Point 7
	Scenario 8	Point 6, Point 8		Scenario 8	Point 6, Point 8
	Scenario 9	Point 7, Point 8		Scenario 9	Point 7, Point 8
Supply/Retrun	Scenario 10	Point 2, Point 5	Supply/Retrun	Scenario 10	Point 1, Point 5
	Scenario 11	Point 2, Point 6		Scenario 11	Point 1, Point 6
	Scenario 12	Point 2, Point 7		Scenario 12	Point 1, Point 7
	Scenario 13	Point 2, Point 8		Scenario 13	Point 1, Point 8
	Scenario 14	Point 3, Point 5		Scenario 14	Point 3, Point 5
	Scenario 15	Point 3, Point 6		Scenario 15	Point 3, Point 6
	Scenario 16	Point 3, Point 7		Scenario 16	Point 3, Point 7
	Scenario 17	Point 3, Point 8		Scenario 17	Point 3, Point 8
	Scenario 18	Point 4, Point 5		Scenario 18	Point 4, Point 5
	Scenario 19	Point 4, Point 6		Scenario 19	Point 4, Point 6
	Scenario 20	Point 4, Point 7		Scenario 20	Point 4, Point 7
	Scenario 21	Point 4, Point 8		Scenario 21	Point 4, Point 8

Note: scenarios highlighted with red characters indicate the scenarios identify source location accurately.

Source in Point 3			Source_Point 4		
	Scenarios	Sensor Locations		Scenarios	Sensor Locations

Supply	Scenario 1	Point 1, Point 2	Supply	Scenario 1	Point 1, Point 2
	Scenario 2	Point 1, Point 4		Scenario 2	Point 1, Point 3
	Scenario 3	Point 2, Point 4		Scenario 3	Point 2, Point 3
Return	Scenario 4	Point 5, Point 6	Return	Scenario 4	Point 5, Point 6
	Scenario 5	Point 5, Point 7		Scenario 5	Point 5, Point 7
	Scenario 6	Point 5, Point 8		Scenario 6	Point 5, Point 8
	Scenario 7	Point 6, Point 7		Scenario 7	Point 6, Point 7
	Scenario 8	Point 6, Point 8		Scenario 8	Point 6, Point 8
	Scenario 9	Point 7, Point 8		Scenario 9	Point 7, Point 8
Supply/Retrun	Scenario 10	Point 1, Point 5	Supply/Retrun	Scenario 10	Point 1, Point 5
	Scenario 11	Point 1, Point 6		Scenario 11	Point 1, Point 6
	Scenario 12	Point 1, Point 7		Scenario 12	Point 1, Point 7
	Scenario 13	Point 1, Point 8		Scenario 13	Point 1, Point 8
	Scenario 14	Point 2, Point 5		Scenario 14	Point 2, Point 5
	Scenario 15	Point 2, Point 6		Scenario 15	Point 2, Point 6
	Scenario 16	Point 2, Point 7		Scenario 16	Point 2, Point 7
	Scenario 17	Point 2, Point 8		Scenario 17	Point 2, Point 8
	Scenario 18	Point 4, Point 5		Scenario 18	Point 3, Point 5
	Scenario 19	Point 4, Point 6		Scenario 19	Point 3, Point 6
	Scenario 20	Point 4, Point 7		Scenario 20	Point 3, Point 7
	Scenario 21	Point 4, Point 8		Scenario 21	Point 3, Point 8

Note: scenarios highlighted with red characters indicate the scenarios identify source location accurately.

Source in Point 5			Source in Point 6		
	Scenarios	Sensor Locations		Scenarios	Sensor Locations
Supply	Scenario 1	Point 1, Point 2	Supply	Scenario 1	Point 1, Point 2
	Scenario 2	Point 1, Point 3		Scenario 2	Point 1, Point 3
	Scenario 3	Point 1, Point 4		Scenario 3	Point 1, Point 4
	Scenario 4	Point 2, Point 3		Scenario 4	Point 2, Point 3

	Scenario 5	Point 2, Point 4		Scenario 5	Point 2, Point 4
	Scenario 6	Point 3, Point 4		Scenario 6	Point 3, Point 4
Return	Scenario 7	Point 6, Point 7	Return	Scenario 7	Point 5, Point 7
	Scenario 8	Point 6, Point 8		Scenario 8	Point 5, Point 8
	Scenario 9	Point 7, Point 8		Scenario 9	Point 7, Point 8
Supply/Retrun	Scenario 10	Point 1, Point 6	Supply/Retrun	Scenario 10	Point 1, Point 5
	Scenario 11	Point 1, Point 7		Scenario 11	Point 1, Point 7
	Scenario 12	Point 1, Point 8		Scenario 12	Point 1, Point 8
	Scenario 13	Point 2, Point 6		Scenario 13	Point 2, Point 5
	Scenario 14	Point 2, Point 7		Scenario 14	Point 2, Point 7
	Scenario 15	Point 2, Point 8		Scenario 15	Point 2, Point 8
	Scenario 16	Point 3, Point 6		Scenario 16	Point 3, Point 5
	Scenario 17	Point 3, Point 7		Scenario 17	Point 3, Point 7
	Scenario 18	Point 3, Point 8		Scenario 18	Point 3, Point 8
	Scenario 19	Point 4, Point 6		Scenario 19	Point 4, Point 5
	Scenario 20	Point 4, Point 7		Scenario 20	Point 4, Point 7
	Scenario 21	Point 4, Point 8		Scenario 21	Point 4, Point 8

Note: scenarios highlighted with red characters indicate the scenarios identify source location accurately.

Source in Point 7			Source in Point 8		
	Scenarios	Sensor Locations		Scenarios	Sensor Locations
Supply	Scenario 1	Point 1, Point 2	Supply	Scenario 1	Point 1, Point 2
	Scenario 2	Point 1, Point 3		Scenario 2	Point 1, Point 3
	Scenario 3	Point 1, Point 4		Scenario 3	Point 1, Point 4
	Scenario 4	Point 2, Point 3		Scenario 4	Point 2, Point 3
	Scenario 5	Point 2, Point 4		Scenario 5	Point 2, Point 4
	Scenario 6	Point 3, Point 4		Scenario 6	Point 3, Point 4
Return	Scenario 7	Point 5, Point 6	Return	Scenario 7	Point 5, Point 6
	Scenario 8	Point 5, Point 8		Scenario 8	Point 5, Point 7

	Scenario 9	Point 6, Point 8		Scenario 9	Point 6, Point 7
Supply/Retrun	Scenario 10	Point 1, Point 5	Supply/Retrun	Scenario 10	Point 1, Point 5
	Scenario 11	Point 1, Point 6		Scenario 11	Point 1, Point 6
	Scenario 12	Point 1, Point 8		Scenario 12	Point 1, Point 7
	Scenario 13	Point 2, Point 5		Scenario 13	Point 2, Point 5
	Scenario 14	Point 2, Point 6		Scenario 14	Point 2, Point 6
	Scenario 15	Point 2, Point 8		Scenario 15	Point 2, Point 7
	Scenario 16	Point 3, Point 5		Scenario 16	Point 3, Point 5
	Scenario 17	Point 3, Point 6		Scenario 17	Point 3, Point 6
	Scenario 18	Point 3, Point 8		Scenario 18	Point 3, Point 7
	Scenario 19	Point 4, Point 5		Scenario 19	Point 4, Point 5
	Scenario 20	Point 4, Point 6		Scenario 20	Point 4, Point 6
	Scenario 21	Point 4, Point 8		Scenario 21	Point 4, Point 7

Note: scenarios highlighted with red characters indicate the scenarios identify source location accurately.

Under the cases of two historical concentration recording sensors:

Source in Point 1			Source in Point 2		
	Scenarios	Sensor Locations		Scenarios	Sensor Locations
Supply	Scenario 1	Point 2, Point 3	Supply	Scenario 1	Point 1, Point 3
	Scenario 2	Point 2, Point 4		Scenario 2	Point 1, Point 4
	Scenario 3	Point 3, Point 4		Scenario 3	Point 3, Point 4
Return	Scenario 4	Point 5, Point 6	Return	Scenario 4	Point 5, Point 6
	Scenario 5	Point 5, Point 7		Scenario 5	Point 5, Point 7
	Scenario 6	Point 5, Point 8		Scenario 6	Point 5, Point 8
	Scenario 7	Point 6, Point 7		Scenario 7	Point 6, Point 7
	Scenario 8	Point 6, Point 8		Scenario 8	Point 6, Point 8
	Scenario 9	Point 7, Point 8		Scenario 9	Point 7, Point 8
Supply/Retrun	Scenario 10	Point 2, Point 5	Supply/Retrun	Scenario 10	Point 1, Point 5
	Scenario 11	Point 2, Point 6		Scenario 11	Point 1, Point 6

	Scenario 12	Point 2, Point 7		Scenario 12	Point 1, Point 7
	Scenario 13	Point 2, Point 8		Scenario 13	Point 1, Point 8
	Scenario 14	Point 3, Point 5		Scenario 14	Point 3, Point 5
	Scenario 15	Point 3, Point 6		Scenario 15	Point 3, Point 6
	Scenario 16	Point 3, Point 7		Scenario 16	Point 3, Point 7
	Scenario 17	Point 3, Point 8		Scenario 17	Point 3, Point 8
	Scenario 18	Point 4, Point 5		Scenario 18	Point 4, Point 5
	Scenario 19	Point 4, Point 6		Scenario 19	Point 4, Point 6
	Scenario 20	Point 4, Point 7		Scenario 20	Point 4, Point 7
	Scenario 21	Point 4, Point 8		Scenario 21	Point 4, Point 8

Note: scenarios highlighted with red characters indicate the scenarios identify source location accurately.

Source in Point 3			Source in Point 4		
	Scenarios	Sensor Locations		Scenarios	Sensor Locations
Supply	Scenario 1	Point 1, Point 2	Supply	Scenario 1	Point 1, Point 2
	Scenario 2	Point 1, Point 4		Scenario 2	Point 1, Point 3
	Scenario 3	Point 2, Point 4		Scenario 3	Point 2, Point 3
Return	Scenario 4	Point 5, Point 6	Return	Scenario 4	Point 5, Point 6
	Scenario 5	Point 5, Point 7		Scenario 5	Point 5, Point 7
	Scenario 6	Point 5, Point 8		Scenario 6	Point 5, Point 8
	Scenario 7	Point 6, Point 7		Scenario 7	Point 6, Point 7
	Scenario 8	Point 6, Point 8		Scenario 8	Point 6, Point 8
	Scenario 9	Point 7, Point 8		Scenario 9	Point 7, Point 8
Supply/Retrun	Scenario 10	Point 1, Point 5	Supply/Retrun	Scenario 10	Point 1, Point 5
	Scenario 11	Point 1, Point 6		Scenario 11	Point 1, Point 6
	Scenario 12	Point 1, Point 7		Scenario 12	Point 1, Point 7
	Scenario 13	Point 1, Point 8		Scenario 13	Point 1, Point 8
	Scenario 14	Point 2, Point 5		Scenario 14	Point 2, Point 5
	Scenario 15	Point 2, Point 6		Scenario 15	Point 2, Point 6

	Scenario 16	Point 2, Point 7		Scenario 16	Point 2, Point 7
	Scenario 17	Point 2, Point 8		Scenario 17	Point 2, Point 8
	Scenario 18	Point 4, Point 5		Scenario 18	Point 3, Point 5
	Scenario 19	Point 4, Point 6		Scenario 19	Point 3, Point 6
	Scenario 20	Point 4, Point 7		Scenario 20	Point 3, Point 7
	Scenario 21	Point 4, Point 8		Scenario 21	Point 3, Point 8

Note: scenarios highlighted with red characters indicate the scenarios identify source location accurately.

Source in Point 5			Source in Point 6		
	Scenarios	Sensor Locations		Scenarios	Sensor Locations
Supply	Scenario 1	Point 1, Point 2	Supply	Scenario 1	Point 1, Point 2
	Scenario 2	Point 1, Point 3		Scenario 2	Point 1, Point 3
	Scenario 3	Point 1, Point 4		Scenario 3	Point 1, Point 4
	Scenario 4	Point 2, Point 3		Scenario 4	Point 2, Point 3
	Scenario 5	Point 2, Point 4		Scenario 5	Point 2, Point 4
	Scenario 6	Point 3, Point 4		Scenario 6	Point 3, Point 4
Return	Scenario 7	Point 6, Point 7	Return	Scenario 7	Point 5, Point 7
	Scenario 8	Point 6, Point 8		Scenario 8	Point 5, Point 8
	Scenario 9	Point 7, Point 8		Scenario 9	Point 7, Point 8
Supply/Retrun	Scenario 10	Point 1, Point 6	Supply/Retrun	Scenario 10	Point 1, Point 5
	Scenario 11	Point 1, Point 7		Scenario 11	Point 1, Point 7
	Scenario 12	Point 1, Point 8		Scenario 12	Point 1, Point 8
	Scenario 13	Point 2, Point 6		Scenario 13	Point 2, Point 5
	Scenario 14	Point 2, Point 7		Scenario 14	Point 2, Point 7
	Scenario 15	Point 2, Point 8		Scenario 15	Point 2, Point 8
	Scenario 16	Point 3, Point 6		Scenario 16	Point 3, Point 5
	Scenario 17	Point 3, Point 7		Scenario 17	Point 3, Point 7
	Scenario 18	Point 3, Point 8		Scenario 18	Point 3, Point 8
	Scenario 19	Point 4, Point 6		Scenario 19	Point 4, Point 5

	Scenario 20	Point 4, Point 7		Scenario 20	Point 4, Point 7
	Scenario 21	Point 4, Point 8		Scenario 21	Point 4, Point 8

Note: scenarios highlighted with red characters indicate the scenarios identify source location accurately.

Source in Point 7			Source in Point 8		
	Scenarios	Sensor Locations		Scenarios	Sensor Locations
Supply	Scenario 1	Point 1, Point 2	Supply	Scenario 1	Point 1, Point 2
	Scenario 2	Point 1, Point 3		Scenario 2	Point 1, Point 3
	Scenario 3	Point 1, Point 4		Scenario 3	Point 1, Point 4
	Scenario 4	Point 2, Point 3		Scenario 4	Point 2, Point 3
	Scenario 5	Point 2, Point 4		Scenario 5	Point 2, Point 4
	Scenario 6	Point 3, Point 4		Scenario 6	Point 3, Point 4
Return	Scenario 7	Point 5, Point 6	Return	Scenario 7	Point 5, Point 6
	Scenario 8	Point 5, Point 8		Scenario 8	Point 5, Point 7
	Scenario 9	Point 6, Point 8		Scenario 9	Point 6, Point 7
Supply/Retrun	Scenario 10	Point 1, Point 5	Supply/Retrun	Scenario 10	Point 1, Point 5
	Scenario 11	Point 1, Point 6		Scenario 11	Point 1, Point 6
	Scenario 12	Point 1, Point 8		Scenario 12	Point 1, Point 7
	Scenario 13	Point 2, Point 5		Scenario 13	Point 2, Point 5
	Scenario 14	Point 2, Point 6		Scenario 14	Point 2, Point 6
	Scenario 15	Point 2, Point 8		Scenario 15	Point 2, Point 7
	Scenario 16	Point 3, Point 5		Scenario 16	Point 3, Point 5
	Scenario 17	Point 3, Point 6		Scenario 17	Point 3, Point 6
	Scenario 18	Point 3, Point 8		Scenario 18	Point 3, Point 7
	Scenario 19	Point 4, Point 5		Scenario 19	Point 4, Point 5
	Scenario 20	Point 4, Point 6		Scenario 20	Point 4, Point 6
	Scenario 21	Point 4, Point 8		Scenario 21	Point 4, Point 7

Note: scenarios highlighted with red characters indicate the scenarios identify source location accurately.

References

[1] Abramowitz M. and Stegun A.I. 1972. Handbook of Mathematical Functions with Formulas, Graphs, and Mathematical Tables. Library of Congress Card Number: 64-60036.

[2] Allen C.T., Haupt S.E., and Young G.S. 2007. Source Characterization with a Genetic Algorithm-Coupled Dispersion-Backward Model Incorporating SCIPUFF. American Meteorological Society.

[3] Annunzio A.J., Young G.S., and Haupt S.E. Utilizing state estimation to determine the source location for a contaminant. Atmos Environ 2012; 46(0):580-9.

[4] Atmadja J. and Bagtzoglou A.C. 2000. "Groundwater pollution source identification using the backward beam equation method. In: Computational Methods for Subsurface Flow and Transport," 397-404. Rotterdam, the Netherlands, A.A. Balkema.

[5] ASHRAE, 2009a. Position Document on Airborne Infectious Diseases. Atlanta, GA: American Society of Heating, Refrigerating, and Air-Conditioning Engineers, Inc.

[6] ASHRAE, 2009b. Fundamentals Handbook, Indoor Environmental Health, Chapter 10. Atlanta, GA: American Society of Heating, Refrigerating, and Air-Conditioning Engineers, Inc.

[7] Atmadja J. and Bagtzoglou A.C. State of the art report on mathematical methods for groundwater pollution source identification. Environ Forensics 2001; 2(3): 205-14.

[8] Bagtzoglou, A.C., D.E. Dougherty, and A.F.B. Thompson. Application of Particle Methods to Reliable Identification of Groundwater Pollution Sources. Water Resources Management, 6, 15-23, 1992.

[9] Bastani A., Haghighat F., and Kozinski J. Contaminant source identification within a building: Toward design of immune buildings. Building and Environment 51 (2012) 320-329.

[10] Burge S., Hedge A., Wilson S., Bass J.H., and Robertson A. 1987. Sick building syndrome: A study of 4373 office workers. Ann. Occup. Hyg. 31: 493-504.

[11] Cai H., Li X., Chen Z., and Kong L. Fast identification of multiple indoor constant contaminant sources by ideal sensors: a theoretical model and numerical validation. Indoor Built Environ 2012; 22(6):897-909.

[12] Cai H., Li X., Chen Z., and Wang M. Rapid identification of multiple constantly-released contaminant sources in indoor environments with unknown release time. Building and Environment 81 (2014) 7-19.

[13] Cornacchiulo D., Bagtzoglou A.C., and Atmadja J. 2002, "Hydrologic inversion using marching-jury backward beam equation and quasi-reversibility methods," 15th ASCE Engineering Mechanics Conference, June 2-5, Columbia University, New York, NY.

[14] Dols W.S. and Persity A.K. A software tool for analyzing building airflow and airborne CBR agent concentrations. 2008 EP&R and R&RS Topical Meeting, Albuquerque, New Mexico, March 9-12, 2008.

[15] Dorgan C.B., Dorgan C.E., Kanarek M.S., and Willman A.J. 1998. "Health and productivity benefits of improved indoor air quality," ASHRAE Transactions, 104(1): 4161.

[16] Draper N.R., and Smith H. 1966. "Applied regression analysis," John Wiley, New York.

[17] Fanger P.O., Lauridsen J., Bluyssen P., and Clausen P.G. 1988. Air pollution sources in offices and assembly halls quantified by the olf unit. Energy and Buildings 12: 7-19.

[18] Feustel, H.E., and V.M. Kendon. 1985. Infiltration Models for Multicellular Structures – A Literature Review. Energy and Buildings, 8, 123-136.

[19] Feustel, H.E., and J. Dieris. 1992. A Survey of Airflow Models for Multi-zone Structures. Energy and Buildings, 18, 79-100.

[20] Fisk W.J. 2000. "Health and productivity gains from better indoor environments and their relationship with energy efficiency," Annual Review of Energy and the Environment, 25: 537-566.

[21] Friedr J.B. 1978. "Stable solution – inverse problems," Vieweg & Sohn Verlagsgesellschaft mbH, Braunschweig.

[22] Gorelick S.M., Evans B.E., and Remson I. 1983. "Identifying sources of groundwater pollution: an optimization approach," Water Resour. Res. 19, 779-790. No. 3.

[23] Huang C. and Wang S. A three-dimensional inverse heat conduction problem in estimating surface heat flux by conjugate gradient method. International Journal Heat Mass Transfer 1999; 42(18):3387-403.

[24] Jones A.P. Indoor air quality and health. Atmospheric Environment 33 (1999) 4535-4564.

[25] Lai A.C.K. and Cheng Y.C. 2007. Study of expiratory droplet dispersion and transport using a new Eulerian modeling approach. Atmospheric Environment 41, 7473-7484.

[26] Lin R. 2003. Identification of groundwater contamination sources using probabilities conditioned on measured concentrations. M.S. thesis, Dept. of Civil Eng., University of Virginia, Charlottesville, Virginia.

[27] Liu X. PhD dissertation: Identification of Indoor Airborne Contaminant Sources with Probability-Based Inverse Modeling Methods. Department of Civil, Environmental and Architectural Engineering at University of Colorado Boulder. 2008.

[28] Liu X. and Zhai Z. Inverse modeling methods for indoor airborne pollutant tracking: literature review and fundamentals. Indoor Air 2007; 17(6):419-38.

[29] Liu X. and Zhai Z. Location identification for indoor instantaneous point contaminant source by probability-based inverse computational fluid dynamics modeling. Indoor Air 2008; 18(10):2-11.

[30] Liu X. and Zhai Z. Prompt tracking of indoor airborne contaminant source location with probability-based inverse multi-zone modeling. Build Environ 2009; 44(6):1135-43.

[31] Liu X. and Zhai Z. Protecting a whole building from critical indoor contamination with optimal sensor network design and source identification methods. Building and Environment 44 (2009) 2276–2283.

[32] Mahar P.S. and Datta B. 1997. "Optimal monitoring network and ground-water pollution source 235 identification," J.Water Res. Pl. 123, 199-207.

[33] MathWorks. Complementary Error Function, erfc(x). http://www.mathworks.com/help/matlab/ref/erfc.html.

[34] Molhave, L. and Thorsen M. 1991. A model for investigations of ventilation systems as sources for volatile organic compounds in indoor climates. Atmos. Environ. 25A (2): 241-249.

[35] Neupauer R.M. 2000. "Receptor based modeling of groundwater contamination," Ph.D. dissertation, New Mexico Institute of Mining and Technology, Socorro, New Mexico.

[36] Neupauer R.M. and Wilson J.L. 1999. "Adjoint method for obtaining backward-in-time location and travel time probabilities of a conservative groundwater contaminant," Water Resour. Res. 35, 3389-398. No. 11.

[37] Neupauer R.M. and Wilson J.L. Backward probabilistic model of groundwater contamination in non-uniform and transient flow. Adv Water Resour 2002; 25:733-46.

[38] Neupauer R.M. and Wilson J.L. Backward location and travel time probabilities for a decaying contaminant in an aquifer. J Contam Hydrol 2003; 66:39-58.

[39] Pelletret R.Y. and Keilholz W.P. 1997. "COMIS 3.0 – a new simulation environment for multi-zone air flow and pollutant transport modeling," Building Simulation'97 – fifth international IBPSA Conference, Prague, IBPSA.

[40] Shaelin A., Dorer V. et al. 1993. "Improvement of multi-zone model predictions by detailed flow path values from CFD calculation," ASHRAE Transactions, 93-7-4, pp. 709-720.

[41] Skaggs T.H. and Kabala Z.J. 1995. "Recovering the history of a groundwater contaminant plume: Method of quasi-reversibility," Water Resour. Res. 31, 2669-2673. No. 11.

[42] Sohn M.D., Reynolds P., Gadgil A.J., and Sextro R.G. 2002 "Rapidly locating sources and predicting contaminant dispersion in buildings", Proceedings: Indoor Air.

[43] Sohn M.D., Sextro R.G., Gadgil A.J., and Daisey J.M. 2003 "Responding to sudden pollutant release in office buildings: 1. Framework and analysis tools," Indoor Air, 13, 267-276.

[44] Sohn M.D., Reynolds P., Singh N., and Gadgil A.J. 2002. Rapidly locating and characterizing pollutant releases in buildings. Journal of the Air Waste Management Association, 52, 1422–1432.

[45] Taylor L.D. Estimation by minimizing the sum of absolute errors, in Frontiers in Econometrics, edited by P. Zarembka, pp. 169-190, Academic Press, New York, 1974.

[46] United States Environmental Protection Agency. Buildings and Their Impact on the Environment: A Statistical Summary. Revised on April 22, 2009.

[47] Van Genuchten M.Th. and Alves W. J. Analytical Solutions of the One Dimensional Convective-Dispersive Solute Transport Equation. US Department of Agriculture, Technical Bulletin, No. 1661, 1982.

[48] Vukovic V. and Srebric J. 2007. Application of neural networks trained with multizone Models for fast detection of contaminant source position in buildings. ASHRAE Transaction, volume 113, part 2.

[49] Vukovic V., Tabares-Velasco P., and Srebric J. 2010. Real-time identification of indoor pollutant source positions based on neural network locator of contaminant sources and optimized sensor networks. Journal of the air & waste management association, 60:9, 1034-1048.

[50] Wagner B.J. 1992. “Simultaneously parameter estimation and contaminant source characterization for coupled groundwater flow and contaminant transport modeling,” J. Hydrol. 135, 275-303.

[51] Walton G.N. and Dols W.S. NISTIR 7251: CONTAM User Guide and Program Documentation. U.S. National Institute of Standards and Technology. 2013.

[52] Wang, J.; Zhang, J.S.; Shaw, C.Y.; Reardon, J.T.; Su, J.Z. Comparisons of Multi-zone Airflow/Contaminant Dispersal Models. NRC Publications Archive. May 1998.

[53] Wang X., Tao W., Lu Y., and Wang F. A method to identify the point source of indoor gaseous contaminant based on limited on-site steady concentration measurements. Build Simul 2013; 6(4):395-402.

[54] Wilson, J.L. and J. Liu. Backward Tracking to Find the Source of Pollution, in Waste-management: From Risk to Remediation, edited by R. Bhada et al., ECM Press, Albuquerque, NM, 181-199, 1994.

[55] Wilson, J.L. and J. Liu. Field Validation of the Backward-in-time Advection Dispersion Theory. Proceedings of the 1996 HSRC/WERC Joint Conference on the Environment, Great Plains-Rocky Mountain Hazardous Substance Center, Manhattan, Kansas. 1997.

[56] Woodbury A.D., Sudicky E., Ulrych T.J., and Ludwig R. 1998. "Three-dimensional plume source reconstruction using minimum relative entropy inversion," J. Contam. Hydrol. 32, 131-158.

[57] Woodbury A.D. and Ulrych T.J. 1996. "Minimum relative entropy inversion: theory and application to recovering the release history of groundwater contaminant," Water Resour. Res. 32, 2671-2681. No. 9.

[58] Zhang T. and Chen Q. 2007a. Identification of contaminant sources in enclosed environments by inverse CFD modeling. Indoor Air 17, 167-177.

[59] Zhang T. and Chen Q. 2007b. Identification of contaminant sources in enclosed spaces by a single sensor. Indoor Air 17, 439-449.

[60] Zhang T., Li H. and Wang S. 2012. Inversely tracking indoor airborne particles to locate their release sources.

[61] Zhang C., Wu L., Luo Y., Zhang H., and Christie P. Identifying sources of soil inorganic pollutants on a regional scale using a multivariate statistical approach: role of pollutant migration and soil physicochemical properties. Environmental Pollution 2008; 151(3):470-6.

[62] Zhao B. and Wu J. Modeling particle deposition onto rough walls in ventilation duct. Atmospheric Environment 40 (2006) 6918-6927.